

**The effects of added mass on the dynamic motions of the head and trunk during  
running and walking**

A Thesis

Submitted to the Faculty

of

Drexel University

by

James W. N. Green

in partial fulfillment of the

requirements for the degree

of

Master of Science in Mechanical Engineering

September 2009



## Acknowledgements

Thank you to my fiancé Priya for all her love and support throughout this long and trying process, I could not have done this without you. When we first met you had no idea this is the path I would take and you have taken the long nights and stressful times better than anyone could have and next time you can be the one to pursue your dreams with me supporting you all the way.

Thank you to my advisor, Dr. James Tangorra, for the opportunities you have provided for me. You took a chance bringing me in to this lab and it has been one of the greatest learning experiences of my life.

Thank you to my parents for all of your support over the years. None of this would have been possible without the drive you instilled in me to be the best I can be.

Last but not least, thank you to all of my labmates in the LBSA; Jonah Gottlieb, Christopher Esposito, Christopher Phelan, Venkat Palgat, and Mary Milone. I have learned a huge amount from all of you and you have helped keep me sane with tea breaks, card breaks, and by providing humor at all of the most stressful times!

## Table of Contents

<b>List of Tables</b> .....	v
<b>List of Figures</b> .....	vi
<b>Abstract</b> .....	xii
<b>CHAPTER 1: INTRODUCTION</b> .....	1
<b>1.1 Specific Aims</b> .....	1
<b>1.2 Background and Significance</b> .....	2
<b>1.2.1 Literature Review</b> .....	2
<b>CHAPTER 2: METHODS</b> .....	5
<b>2.1 Testing Protocol</b> .....	5
<b>2.2 Development of the Testing Protocol</b> .....	7
<b>2.2.1 Preliminary Studies</b> .....	7
<b>2.2.2 Acceptable Mass</b> .....	12
<b>2.3 Testing Equipment</b> .....	14
<b>2.3.1 Treadmill</b> .....	14
<b>2.3.2 Helmets and Added Mass</b> .....	14
<b>2.3.3 Sensor System</b> .....	18
<b>2.4 Data Acquisition</b> .....	21
<b>2.5 Subjects</b> .....	24
<b>2.6 Data Processing</b> .....	25
<b>CHAPTER 3: RESULTS</b> .....	27
<b>3.1 Control Condition</b> .....	27

3.2 Pitch Motion .....	38
3.3 Yaw Motion .....	54
3.4 Roll Motion .....	62
3.5 Z-Direction Motion .....	71
<b>CHAPTER 4: DISCUSSION .....</b>	<b>80</b>
4.1 Limitations and Assumptions .....	84
<b>CHAPTER 5: CONCLUSIONS AND FUTURE WORK .....</b>	<b>85</b>
5.1 Future Work .....	86
5.1.1 Changes to the Sensor System .....	86
5.1.2 Changes to the Testing Protocol .....	87
List of References .....	89
Appendix A: Torque and Moment of Inertia Calculations .....	92
Appendix B: Data Processing Algorithms .....	94
B.1 Low Pass Filter .....	95
Appendix C: Equipment Specification Sheets .....	96
C.1 ADIS16350 .....	97
C.2 Optotrak 3020 .....	99
Appendix D: Raw Statistical Data .....	100
D. 1 Pitch .....	101
D. 2 Yaw .....	105
D. 2 Yaw .....	105
D.4 Z-Direction .....	109

**List of Tables**

Table 1: Testing Conditions.....6

## List of Figures

Figure 1: Sensors Coordinate System .....	7
Figure 2: Probability Distribution Function of Head Acceleration in x, y, and z.....	9
Figure 3: Probability Distribution Function of Head Position Relative to Trunk.....	11
Figure 4: Petzel Ecrin Roc Climbing Helmet .....	15
Figure 5: Riddell Revolution IQ Football Helmet .....	16
Figure 6: Additional Mass Mounting System (Side View) .....	17
Figure 7: Additional Mass Mounting System (Top View).....	17
Figure 8: ADIS16350 with Mounting Plate.....	18
Figure 9: ADIS16350 Mounted on Helmet (Side View).....	19
Figure 10: ADIS16350 Mounted on Helmet (Top View).....	19
Figure 11: ADIS16250 Torso Mounting Box.....	20
Figure 12: Strain Gauge LabView DAQ Program Front .....	22
Figure 13: ADIS16350 LabView DAQ Program Front.....	23
Figure 14: ADIS16350 LabView DAQ Raw Data Conversion.....	24
Figure 15: Subject running with mass and counterbalance .....	27
Figure 16: Representative Head Pitch Rotation plots over A) Complete Trial, B) Five Second Window, and C) Moving average showing mean head position over a two second window.....	29
Figure 17: Representative Frequency Content of Pitch Rotations while A) Walking and B) Running.....	29

Figure 18: Representative Head Pitch Velocity plots over A) Complete Trial and B) Five-second window.....	29
Figure 19: Representative Head and Trunk Pitch Rotation while A) Walking and B) Running. Frequency Analysis of Head and Trunk Pitch Rotation while C) Walking and D) Running.....	30
Figure 20: Representative Pitch Rotational Velocity A) Walking B) Running. Frequency Spectrum A) Walking B) Running .....	31
Figure 21: Representative Head Yaw Rotation plots over A) Complete Trial and B) Five-second window.....	32
Figure 22: Representative Frequency Content of Yaw Rotations while A) Walking and B) Running.....	32
Figure 23: Head and Trunk Yaw Rotation while A) Walking and B) Running. Frequency Analysis of Head and Trunk Yaw Rotation while C) Walking and D) Running. ....	33
Figure 24: Representative Head Roll Rotation plots while walking over A) Complete Trial and B) Five-second window.....	34
Figure 25: Representative Frequency Content of Roll Rotations while A) Walking and B) Running.....	35
Figure 26: Representative Head Roll Rotation plots while running .....	35
Figure 27: Head and Trunk Roll Rotation while A) Walking and B) Running. Frequency Analysis of Head and Trunk Roll Rotation while C) Walking and D) Running. ....	36
Figure 28: Representative Head Z-direction position plots while walking .....	37



Figure 29: Representative Frequency Content of Z-direction motions while A) Walking and B) Running .....	37
Figure 30: Head and Trunk Z-Position while A) Walking and B) Running. Frequency Analysis of Head and Trunk Motion while C) Walking and D) Running.....	38
Figure 31: Mean Walking Head Pitch Rotation around Moving Average with Standard Deviation for A) Increasing Mass, B) Increasing Moment of Inertia, and C) Increasing Torque Applied .....	42
Figure 32: Mean Running Head Pitch Rotation around Moving Average with Standard Deviation for A) Increasing Mass, B) Increasing Moment of Inertia, and C) Increasing Torque Applied .....	43
Figure 33: Representative Probability Distribution Function of Head Pitch Rotation around moving average A) Walking B) Running .....	44
Figure 34: Representative Normalized Power Spectrum Density of Head Pitch Rotation A) Walking B) Running.....	44
Figure 35: Mean Walking Head Pitch Rotational Velocity with Root Mean Square for A) Increasing Mass, B) Increasing Moment of Inertia, and C) Increasing Torque Applied.....	45
Figure 36: Mean Running Head Pitch Rotational Velocity with Root Mean Square for A) Increasing Mass, B) Increasing Moment of Inertia, and C) Increasing Torque Applied.....	46
Figure 37: Mean Walking Head Pitch Rotation with Standard Deviation for A) Increasing Mass, B) Increasing Moment of Inertia, and C) Increasing Torque Applied .....	47
Figure 38: Mean Running Head Pitch Rotation with Standard Deviation for A) Increasing Mass, B) Increasing Moment of Inertia, and C) Increasing Torque Applied .....	48

Figure 39: An example of significant changes in moving average during a run .....	49
Figure 40: Mean Running Trunk Pitch Rotation around Moving Average with Standard Deviation.....	50
Figure 41: Mean Running Trunk Pitch Rotational Velocity with Root Mean Square.....	51
Figure 42: Mean Running Trunk Pitch Rotation with Standard Deviation .....	52
Figure 43: Walking Pitch Rotation with Moving Average Removed A) Trunk Conditions 1, 2, 6; B) Trunk Conditions 3, 4, 5; C) Head Conditions 1, 2, 6 D) Head Conditions 3, 4, 5. The plots are all zero mean but offset for comparison purposes. ....	53
Figure 44: Running Pitch Rotation with Moving Average Removed A) Trunk Conditions 1, 2, 6; B) Trunk Conditions 3, 4, 5; C) Head Conditions 1, 2, 6 D) Head Conditions 3, 4, 5. The plots are all zero mean but offset for comparison purposes. ....	53
Figure 45: Pitch Position A) Walking B) Running. Frequency Analysis C) Walking D) Running.....	54
Figure 46: Mean Walking and Running Head Yaw Rotation with Standard Deviation.....	56
Figure 47: Mean Walking and Running Head Yaw Rotational Velocity with Root Mean Square .....	57
Figure 48: Representative Probability Distribution Function of Head Yaw Rotation around moving average A) Walking B) Running.....	58
Figure 49: Representative Normalized Power Spectrum Density of Head Yaw Rotation A) Walking B) Running.....	58
Figure 50: Mean Walking and Running Trunk Yaw Rotation with Standard Deviation .....	59

Figure 51: Mean Walking and Running Yaw Trunk Rotational Velocity with Root Mean Square .....	60
Figure 52: Walking Yaw Rotation with Moving Average Removed A) Trunk Conditions 1, 2, 6; B) Trunk Conditions 3, 4, 5; C) Head Conditions 1, 2, 6 D) Head Conditions 3, 4, 5. The plots are all zero mean but offset for comparison purposes. ....	61
Figure 53: Running Yaw Rotation with Moving Average Removed A) Trunk Conditions 1, 2, 6; B) Trunk Conditions 3, 4, 5; C) Head Conditions 1, 2, 6 D) Head Conditions 3, 4, 5. The plots are all zero mean but offset for comparison purposes. ....	61
Figure 54: Yaw Position A) Walking B) Running. Frequency Analysis C) Walking D) Running.....	62
Figure 55: Mean Walking and Running Head Roll Rotation with Standard Deviation .....	64
Figure 56: Mean Walking and Running Roll Head Rotational Velocity with Root Mean Square .....	65
Figure 57: Representative Normalized Power Spectrum Density of Head Roll Rotation A) Walking B) Running.....	66
Figure 58: Representative Probability Distribution Function of Head Roll Rotation around moving average A) Walking B) Running .....	67
Figure 59: Mean Walking and Running Trunk Roll Rotation with Standard Deviation .....	68
Figure 60: Mean Walking and Running Roll Trunk Rotational Velocity with Root Mean Square .....	69

Figure 61: Walking Roll Rotation with Moving Average Removed A) Trunk Conditions 1, 2, 6; B) Trunk Conditions 3, 4, 5; C) Head Conditions 1, 2, 6 D) Head Conditions 3, 4, 5. The plots are all zero mean but offset for comparison purposes. ....	70
Figure 62: Running Roll Rotation with Moving Average Removed A) Trunk Conditions 1, 2, 6; B) Trunk Conditions 3, 4, 5; C) Head Conditions 1, 2, 6 D) Head Conditions 3, 4, 5. The plots are all zero mean but offset for comparison purposes. ....	70
Figure 63: Roll Position A) Walking B) Running. Frequency Analysis C) Walking D) Running.....	71
Figure 64: Walking and Running Head Z-Position Standard Deviation .....	73
Figure 65: Mean Walking and Running Head Z-Acceleration with Root Mean Square.....	74
Figure 66: Zero-Mean walking Z-direction position A) Trunk Conditions 1, 2, 6; B) Trunk Conditions 3, 4, 5; C) Head Conditions 1, 2, 6 D) Head Conditions 3, 4, 5. The plots are all zero mean but offset for comparison purposes.....	75
Figure 67: Zero-Mean running Z-direction position A) Trunk Conditions 1, 2, 6; B) Trunk Conditions 3, 4, 5; C) Head Conditions 1, 2, 6 D) Head Conditions 3, 4, 5. The plots are all zero mean but offset for comparison purposes.....	75
Figure 68: Power Spectral Density of Head Z-Position while A) Walking and B) Running .....	76
Figure 69: Walking and Running Trunk Z-Position Standard Deviation .....	77
Figure 70: Mean Walking and Running Trunk Z-Acceleration with Root Mean Square .....	78
Figure 71: Z-position A) Walking B) Running. Frequency Analysis C) Walking D) Running.....	79
Figure 72: Pitch Position and Moving Average for A) Trunk and B) Head.....	81

## **Abstract**

The effects of added mass on the dynamic motions of the head and trunk during running and walking

James W. N. Green  
James L. Tangorra, Ph.D.

The addition of mass to the head has applications from the design of football helmets to the placement of loads on head mounted displays. Determining the effects of mass placed on the head ensures that the design of these systems can be optimized to reduce the effects on the user and to reduce the change of injury occurring.

A testing protocol was developed to determine the effect of mass added to the head which causes changes to total mass, moment of inertia, and torque applied. This testing protocol asked subjects to walk and run on a treadmill with different helmets and masses attached to their heads which changed the moment of inertia and torque applied.

Position, velocity, and acceleration sensors were attached to the head and trunk in order to determine how the positioning and dynamic motions of the head and trunk were affected.

The results showed that the addition of mass to the head had very little effect on the positioning and dynamic motions of the head and trunk and there was no correlation between mass, moment of inertia, or torque applied and the positioning and dynamic motions exhibited by the subjects.



## CHAPTER 1: INTRODUCTION

### 1.1 Specific Aims

The objective of this research is to quantify the effects of added mass on the dynamic motions of the head and trunk during walking and running.

Based on the literature and preliminary data collected, the following hypotheses were made and tested experimentally:

**H1:** The addition of mass to the head, which can apply a torque to the head and change the head's center of gravity and moment of inertia, will result in changes to the dynamic motions of the head and trunk during locomotion.

**H2:** The muscular control system will stabilize the head against the added mass through muscle activation and by altering how the head and trunk are positioned to support the mass. This active compensation will result in lower changes to dynamic motions of the head than would be predicted for a purely passive system.

These hypotheses were tested by measuring head and trunk positions, velocities, and accelerations during trials where subjects walked and ran while wearing helmets with and without additional mass.

## **1.2 Background and Significance**

### **1.2.1 Literature Review**

In order to design systems such as helmets, head mounted displays (HMD), and night vision devices (NVD) properly, a designer should have an understanding of how the mass of these devices affects the user. The effects of placing mass on the head can be seen through changes in the dynamic motions of the head and trunk and in the fatigue of the muscles in the neck.

There is evidence available regarding the effect that mass added to the head has on the dynamic motions of the head and trunk and on fatigue of the neck muscles. Studies have been conducted considering the effect of mass on neck fatigue and head movements during high accelerations (1, 3, 8, 16, 19, 24); the effect of mass on neck fatigue during active rotations of the head (13, 14, 20, 26); and the dynamic motions of the head and trunk during walking with no mass added to the head (5, 6, 7, 9, 10, 12, 15, 22).

However, relatively little is known about how mass added to the head affects the dynamic motions of the head and trunk when subjects are involved in natural activities such as running and walking where an objective of the activity is to maintain stable, clear vision.

Data from experiments where mass was added to the heads of subjects who were accelerated linearly on a sled indicated that the neck musculature worked actively to stabilize the head against the added mass. Although the mass added to the head was significant – in some cases the rotational inertia of the head in yaw was doubled and the rotational inertia in pitch was increased fivefold – the changes in the angular velocities



experienced by the head were small (position and acceleration were not recorded) (13). This is consistent with our hypothesis that the neck musculature will work actively to compensate for changes in mass added to the head in order to maintain the head as a stable platform for the sensory systems.

Numerous experiments have demonstrated that the neck system is able to stabilize the head against a wide range of trunk motions. Stable gaze was maintained against external perturbations that were applied to the trunk of sitting subjects (13), and only small changes in head motions occurred when subjects altered the motions of the trunk by moving their arms aggressively (5, 6). Tests where subjects walked at different speeds on a treadmill and over uneven ground have shown that the dynamic motions of the head in space did not change significantly despite significant changes to the motions of the trunk (7, 10, 15, 22). These experiments indicated that the vertical motion of the head was coupled directly to the up and down motion of the body, and could not be compensated for, while the rotational motion of the head in pitch (in space) was reduced by the neck musculature moving the head in an equal and opposite direction to the trunk. Since no mass was added to the subject's head, the results of these experiments do not support our hypotheses directly, but the results do indicate that stabilization mechanisms exist that limit the movements of the head.

It has also been shown that the addition of mass to the head results in the neck musculature working actively to maintain a stable platform for the head. Research into the effect of additional mass to the head under high accelerations has shown that neck

muscle strain increases due to the head being supported by the neck (1, 3, 24). Studies of movement of the head with, and without, additional mass have demonstrated that an increase in the mass decreases the isometric muscle strength and increases muscle activation (14, 20, 26). These results show that the changes to the mass attached to the head affect muscle activation and fatigue of the neck but do not give any measured data for the changes in the dynamic motions of the head and trunk. However, the subjects in these studies were able to maintain control of the head by either maintaining it in an upright position or in cases where active movements were made there were no changes to the ability of the subject to move and support their head. This supports the second hypothesis that the neck musculature will work to maintain a stable platform for the head but does not provide any information on the mechanisms at work during natural activity such as walking and running.

As discussed, researchers have demonstrated that the neck musculature system actively works to reduce dynamic motions of the head and maintain a stable platform for the head. The proposed testing protocol will provide additional information regarding the effect of mass on the head during walking and running.

## CHAPTER 2: METHODS

### 2.1 Testing Protocol

Subjects were asked to walk on a treadmill for three minutes followed by running on the treadmill for three minutes. Walking and running speeds were determined by asking the subject to walk and run on a treadmill at a comfortable pace for one minute prior to testing and the speeds were recorded. During the runs the subjects were instructed to watch a visual target placed in front of the treadmill at eye level. The visual target was used to ensure that that the subject maintained stability. Subjects were run for a total of six trials with a rest period of five minutes between each trial. Trial order was randomized between subjects.

Test conditions were designed to alter mass, moment of inertia, and torque applied to the head (Table 1). The conditions were as follows::

1. Wearing a lightweight climbing helmet (0.475 kg)
2. Wearing a football helmet (1.625 kg)
3. Wearing a football helmet with additional mass (0.750 kg) attached to the facemask (0.200 m)
4. Wearing a football helmet with additional mass (0.500 kg) attached to the facemask (0.300 m)
5. Wearing a football helmet with additional mass (0.750 kg) attached to the facemask (0.300 m)

6. Wearing a football helmet with additional mass (0.750 kg) attached to the facemask (0.200 m) and an additional mass (0.750 kg) attached to the back of the helmet (0.200 m)

**Table 1: Testing Conditions**

Condition	Mass (kg)	Total Mass (kg)	Distance (m)	Moment of Inertia (sagittal plane) (kg*m <sup>2</sup> )	Torque Applied about Center of Mass (N*m)
1	0.00	0.475	0.0	0.028	0
2	0.00	1.625	0.0	0.045	0
3	0.75	2.375	0.2	0.075	1.471
4	0.50	2.125	0.3	0.090	1.471
5	0.75	2.375	0.3	0.113	2.206
6	0.75 0.75	3.125	0.2 -0.2	0.105	0

The developed testing protocol allows for the testing of the hypotheses by testing the effect of changing both moment of inertia of the head and the torque applied to the head. Measuring positions, velocities, and acceleration show what changes are happening to the dynamic motions of the head and trunk and give an indication of what the neck musculature is doing to compensate for changes and if the position of the head and/or trunk is being adjusted to compensate for changes.

## 2.2 Development of the Testing Protocol

### 2.2.1 Preliminary Studies



**Figure 1: Sensors Coordinate System**

Trials were conducted ( $n = 2$ ) to investigate how mass (0.9 kg) added to the front of a helmet worn by a test subject affected the dynamic motions of the head and the trunk as the subject walked and ran. The addition of this mass resulted in a moment of inertia of  $0.08 \text{ kg}\cdot\text{m}^2$  about the sagittal plane and a static torque applied of  $1.8 \text{ N}\cdot\text{m}$  (Accelerations never exceeded +5 G resulting in a dynamic of torque of  $9 \text{ N}\cdot\text{m}$ ). Trials were conducted where subjects ran for five minutes on a treadmill while wearing a lightweight helmet (0.475 kg), a football helmet (1.625 kg), and a football helmet (1.625 kg) with the added mass (0.9 kg) and while watching a visual target placed directly in

front of the subject. Two three-axis rotational velocity and linear acceleration sensors were attached to the head and trunk, a strain gauge was attached between the head and shoulders to determine the head's position relative to the trunk, an Optotrak 3020 optical marker system was used to determine the position of the head and trunk in space, and a video camera was used so that movements could be analyzed and the data from all sensors verified and fused.

Results showed that the motions of the head in space did not change significantly for the three conditions. Position, velocity, and acceleration data for the head showed very similar values for each one of the three conditions indicating that the dynamic motions of the head did not change significantly despite the significant changes which had been made to the mass attached to the head. For the acceleration data the standard deviation for the lightweight helmet, football, helmet, and football helmet with additional mass respectively was as follows: x-acceleration; 0.019 m/s<sup>2</sup>, 0.035 m/s<sup>2</sup>, and 0.032 m/s<sup>2</sup>; y-acceleration; 0.017 m/s<sup>2</sup>, 0.023 m/s<sup>2</sup>, and 0.022 m/s<sup>2</sup>; z-acceleration; 0.03 m/s<sup>2</sup>, 0.028 m/s<sup>2</sup>, and 0.028 m/s<sup>2</sup>. Changes between trials were very small indicating that the musculature control system is working to compensate for the addition of mass resulting in few changes to the dynamic motions of the head, supporting the second hypothesis.

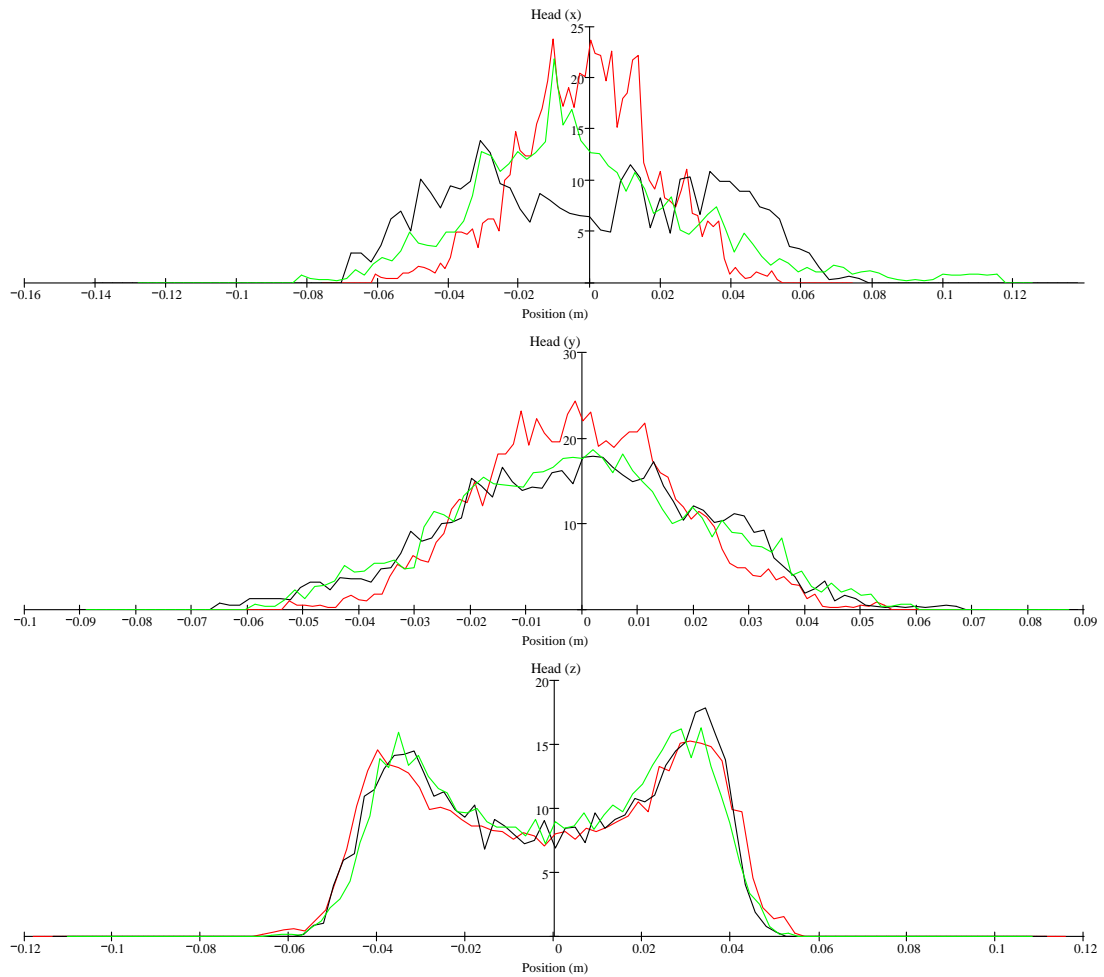


**Figure 2: Probability Distribution Function of Head Acceleration in x, y, and z. The lightweight helmet condition is in red, the football helmet condition is in green, and the football helmet with additional mass condition is in black.**

The velocity and acceleration of the trunk was similar for each of the trials but pitch angle of the trunk in space changed between the lightweight helmet condition and the two other conditions. This was clearly shown on the video data where the trunk was angled forward while running with the lightweight helmet and was brought closer to upright for the other two conditions. The upright position of the trunk provides better support for the

head reducing the fatigue experienced by the subjects. This supports the second hypothesis that musculature control system is working through changes in trunk position to compensate for the addition of mass to the head.

In order for the head to remain stable in space with changes in the position of the trunk, as discussed in paragraph one, the position of the head in space must change.

Measurements of head position relative to the trunk showed that the position of the head relative to the trunk changed significantly between the lightweight helmet condition and the two other conditions. Preliminary results showed a mean head relative to trunk position of  $-18^\circ$  for the lightweight helmet,  $-11^\circ$  for the football helmet, and  $-10.6^\circ$  for the football helmet with additional mass (Figure 3). Video of the trials indicated that head position in space was relatively unchanged between the different conditions and the trunk was held in a more upright position for the football helmet and football helmet with additional mass conditions. The standard deviation for the position of the head relative to the trunk for the lightweight helmet was  $2.3^\circ$ ; the football helmet was  $1.7^\circ$ , and  $2.2^\circ$  for the football helmet with additional mass. These data indicate that the neck musculature is working to reduce head motions and maintain a stable platform for the head. It also indicates that changes in the position of the trunk are used to help maintain this stability. These data support the second hypothesis.



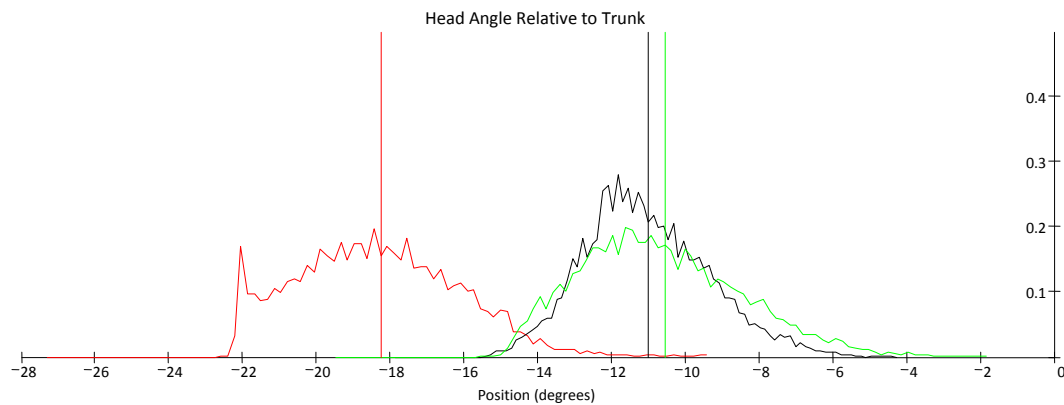


**Figure 3: Probability Distribution Function of Head Position Relative to Trunk. The lightweight helmet condition is in red, the football helmet condition is in green, and the football helmet with additional mass condition is in black.**

Results indicate that the neck musculature system works to reduce head motions in order to maintain a stable platform for the head despite large changes in the mass added to the head. Changes in position, velocity, and acceleration of the head in space were small despite the large changes in mass added to the head. Additionally changes in velocity and acceleration of the trunk were small but changes in the mean position of the trunk were observed. Further research was needed for two reasons; the subject pool was limited to those involved directly in the research resulting in  $n = 2$ , increasing the size of this subject pool allows for statistically significant data and the ability to make generalizations across the group tested. Additionally, the testing protocol was refined to allow for the researcher to test the effect of torque and moment of inertia as separate concepts.

This preliminary data formed the basis for developing the testing procedure described in this thesis and the refinement of the hypothesis developed for the research.

### **2.2.2 Acceptable Mass**

An important step in setting up the testing conditions was to ensure that enough mass is added to the head of the subjects to test the hypotheses but that it does not significantly increase the chance of injury occurring. In order to ensure that the mass will not cause harm to the subjects, the properties of commercially available NVDs and of masses used in research studies were considered to determine acceptable values for the mass, its moment of inertia, and the torque it applies to the subject's head. Among commercially available NVDs, the devices manufactured by Baigish and Vista Controls have some of the greatest mass. The Baigish-20A night-vision goggles have a mass of 0.9 kg, and when worn result in a moment of inertia of approximately  $0.2 \text{ kg}\cdot\text{m}^2$  in the sagittal plane and an applied torque of  $3.4 \text{ N}\cdot\text{m}$  about the center of mass of the head. A second device, the Vista Controls See-Thru Armor HMD, has a mass of 2.3 kg, and when worn at a distance of 0.2 m away from the CG of the head, results in a moment of inertia of approximately  $0.14 \text{ kg}\cdot\text{m}^2$  in the sagittal plane and a static torque of  $4.5 \text{ N}\cdot\text{m}$ . This torque would be expected to increase to in excess of  $40 \text{ N}\cdot\text{m}$  under high accelerations such as those experienced during an ejection from a plane.

Testing on pilots under high accelerations has shown the acceptable limits of helmet and NVD mass. Tests showed that the compressive forces imposed by a 2.2 kg helmet under +10 G of loading came to just under 1000 N, which is well below cadaver injury limits

(3). The maximum helmet mass under high accelerations, accelerations greater than +10 G, was determined to be 3.3 kg in order to prevent injury (3).

Research has shown that the neck strength of pilots does not differ greatly from that of the general population leading to the conclusion that loads applied to pilots in the experiments described above would be appropriate to apply to non-pilot subjects (23).

In order to ensure that the testing conditions are within safe limits the maximum dynamic torque applied to the head should never exceed 20 N\*m and the total mass attached to the head should not exceed 6 kg. This is well below the maximum dynamic torque applied by the Vista Controls HMD during flight; 44 N\*m at +10 G acceleration. Previous research has shown that the acceleration of the head never exceeds +5 G while running so to ensure that our testing conditions remain within an acceptable range the static torque applied must be under 4 N\*m. The total mass attached to the head, including the mass of the helmet, should not exceed 6 kg to ensure that the compressive forces imposed are below injury limits in running studies.

In order to determine the masses to be added to the head rotational inertia was calculated for the lightweight helmet and football helmet. Values for the rotational inertia and torque applied by additional mass were added to these values to calculate total rotational inertia and torque applied. The average head mass was taken to be 4.0 kg and average moment of inertia for the human head was taken as 0.021 kg\*m<sup>2</sup> about the sagittal plane (12, 28). The climbing helmet was modelled as half of a hollow sphere resulting in a moment of inertia of 0.0065 kg\*m<sup>2</sup> about the sagittal plane. The football helmet was

modelled as a hollow sphere resulting in a moment of inertia of  $0.024 \text{ kg}\cdot\text{m}^2$  about the sagittal plane. The additional mass added was taken as a point mass and the calculated moment of inertia was added to the values determined for the head and helmet. The total values for mass, torque applied, and moment of inertia about the sagittal plane were chosen to ensure that these values remained well within safety limits for test subjects. These safety limits are a maximum dynamic torque of  $20 \text{ N}\cdot\text{m}$  and maximum total mass of  $6 \text{ kg}$ .

## **2.3 Testing Equipment**

### **2.3.1 Treadmill**

Subjects ran on a treadmill (Merit Fitness 720T) which can operate at speeds of 0 to 10 miles per hour. The treadmill has safety handles on the sides of the subject and an emergency stop system if the subject is unable to keep pace with the treadmill.

### **2.3.2 Helmets and Added Mass**

#### **Petzel Ecrin Roc Climbing Helmet**

For trials using a lightweight helmet the Petzel Ecrin Roc Climbing Helmet was selected which has a mass of  $0.475 \text{ kg}$  and a moment of inertia of  $0.0065 \text{ kg}\cdot\text{m}^2$  about the sagittal plane. The helmet was selected because of its light weight and close fit on the head to reduce head motions within the helmet and obtain more accurate measures of position, velocity, and acceleration of the head.



**Figure 4: Petzel Ecrin Roc Climbing Helmet**

#### **Riddell Revolution IQ Football Helmet**

Trials using a football helmet used the Riddell Revolution IQ which has a mass of 1.625 kg and a moment of inertia of  $0.024 \text{ kg}\cdot\text{m}^2$  about the sagittal plane. The Revolution IQ is designed so that the center of gravity of the helmet is at the same point as the center of gravity of the head and is lined with inflatable pouches to fit to different sized heads. Subjects will also wear the Riddell Evolution V shoulder pads which will be used to mount equipment (strain gauge, IRLEDs).



**Figure 5: Riddell Revolution IQ Football Helmet**

### **Additional Masses**

Masses added to the head was added in increments of 0.25 kg and was mounted at the following positions; attached to the face mask (0.2 m from center of gravity of head), mounted further out from the face mask (0.3 m from center of gravity of head), and on the back of the helmet (-0.2 m from center of gravity of the head). Rotational inertia and torque for each of the conditions is given in Table 1.

Masses were attached to the helmet using a custom mounting system which allowed for the position of the mass to be modified.

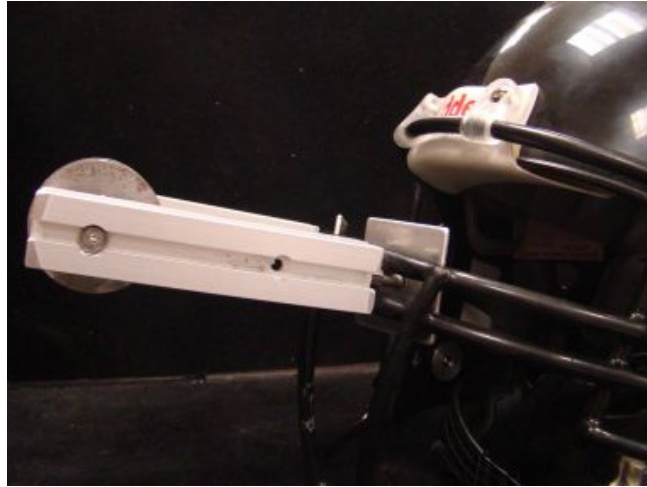


**Figure 6: Additional Mass Mounting System (Side View)**

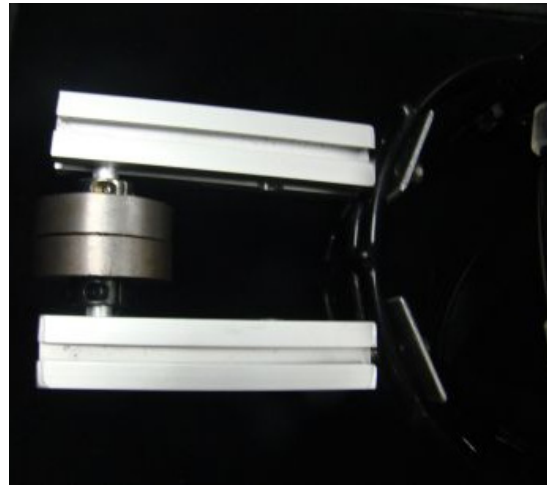


**Figure 7: Additional Mass Mounting System (Top View)**

### 2.3.3 Sensor System

Data from subjects was collected using a set of four instruments; ADIS16350 tri-axis accelerometer and rotational velocity sensor, strain gauge for displacement of the head, Optotrak 3020 for position in space, and DSC-H7 for video. Data from the sensors was collected at 100 Hz and the camera recorded video at 30 frames per second.

#### Analog Devices ADIS15350

Two ADIS16350s from Analog Devices were used, one mounted on the top of the helmet and the other mounted on the chest, to capture 3-axis acceleration and rotational velocity data. The sensor is attached by wires to a National Instruments USB-8451 I<sup>2</sup>C/SPI Interface which connects to the USB port of a desktop computer running LabView for data acquisition.

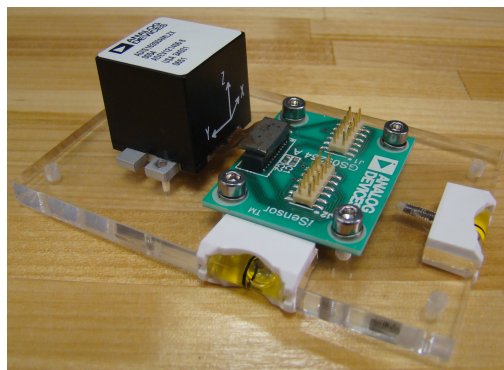


**Figure 8: ADIS16350 with Mounting Plate**



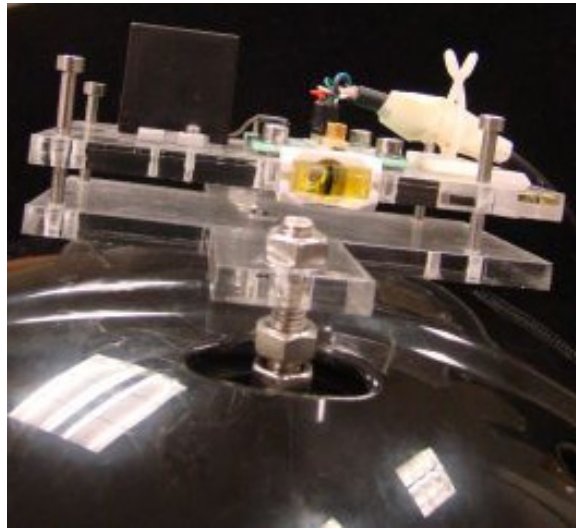


**Figure 9: ADIS16350 Mounted on Helmet (Side View)**

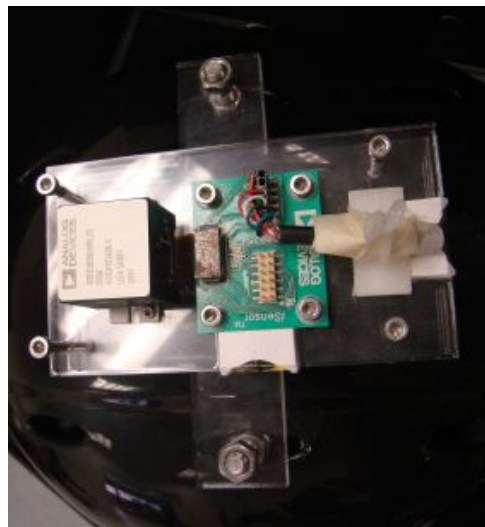


**Figure 10: ADIS16350 Mounted on Helmet (Top View)**



**Figure 11: ADIS16250 Torso Mounting Box**

### **Hokansen Strain Gauge**

A strain gauge (Hokansen) attached between the back of the helmet and the shoulder pads measures displacement of the head relative to the shoulders and allows angle of rotation to be calculated. This was attached to a National Instruments USB-6229 Data Acquisition Board connected to a desktop computer running LabView for data acquisition.

### **Northern Digital Optotrak 3020**

The Optotrak 3020 is an Infra-Red Light Emitting Diode (IRLED) system which captures position of the head and trunk using a camera system mounted to a desk on the opposite side of the room. The IRLEDs are placed on the helmet and the trunk using tape. NDI software running on a desktop computer records the position of each of the IRLEDs. NDI Toolbench software was used to record the position data.

### **Sony DSC-H7**

Video (DSC-H7) was to be taken of each run using a Sony DSC-H7 camera recording at 30 frames per second. Data from the video was to be used to verify that data from the other sensors gave an accurate representation of movements of the head and trunk, to aid in sensor fusion, and allow for calculation of footfall frequency.

### **Attachment of Sensors**

In order to accurately measure the dynamic motions of the subjects the accurate placement of the sensors is extremely important. One ADIS16350 sensor was attached to the top of the helmet using a mounting plate with built in bubble levels. The levels were used to ensure that the sensor was aligned with the axes of the head. The second ADIS16350 was mounted inside of a box and attached to the torso of the subject using an elastic band around the trunk. The Optotrak IRLLEDs were attached in groups of four to the helmet and the shoulder. Again, a bubble level was used to ensure proper alignment with the axes of the head and trunk. The strain gauge was attached between the back of the helmet and the shoulder pads using Velcro strips and was calibrated at the beginning of each trial.

## **2.4 Data Acquisition**

The strain gauge was attached to a power supply generating a constant current of 0.3 A. As the length of the strain gauge changed the resistance changed resulting in a change in the voltage running across the strain gauge. The strain gauge was wired in parallel to a

National Instruments BNC-2110 breakout board connected to a PC running LabView 8.2. Figure 12 shows the front panel of the LabView data acquisition program which was written to acquire the voltage data from the strain gauge. The program allows for the modification of the acquisition rate and duration. The collected data is displayed on the graph and saved in to a text file with the raw voltage readings.

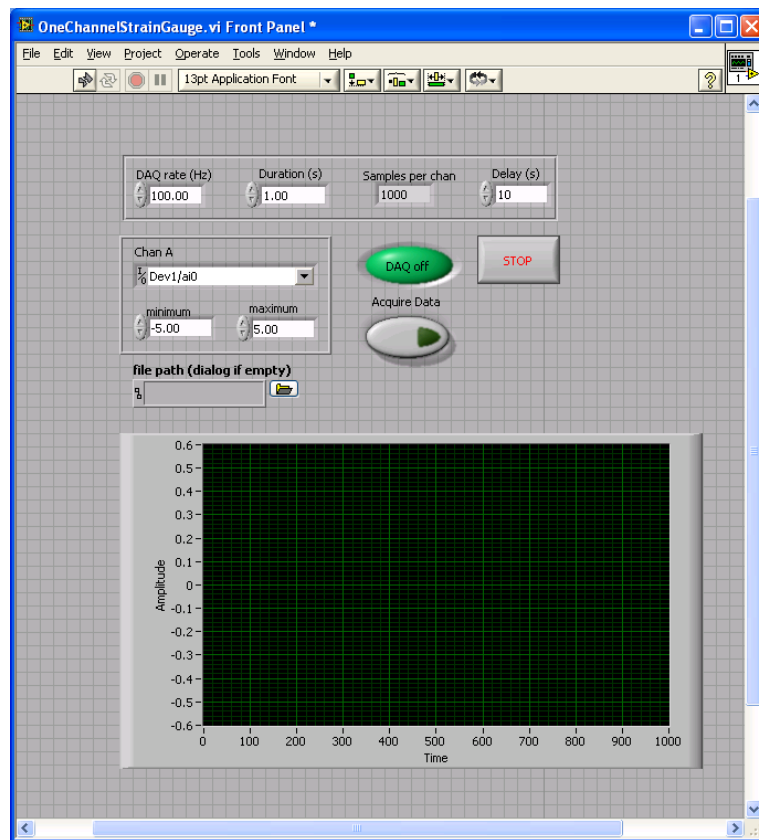


**Figure 12: Strain Gauge LabView DAQ Program Front**

The ADIS16350 sensors are connected to a National Instruments USB-8451 I<sup>2</sup>C/SPI/SMBus Interface utilizing the SPI communication protocol. A custom LabView application is used to acquire data from the sensors. Figure 13 shows the front of the data acquisition program which allows the acquisition rate to be modified and gives a real time view of the output data as well as reporting any errors from the sensors. Figure 14 shows the calculations performed by LabView to convert the raw sensor data to acceleration ( $\text{m/s}^2$ ) and rotational velocity ( $\text{deg/s}$ ). The data is output to a text file with six readings from each sensor.

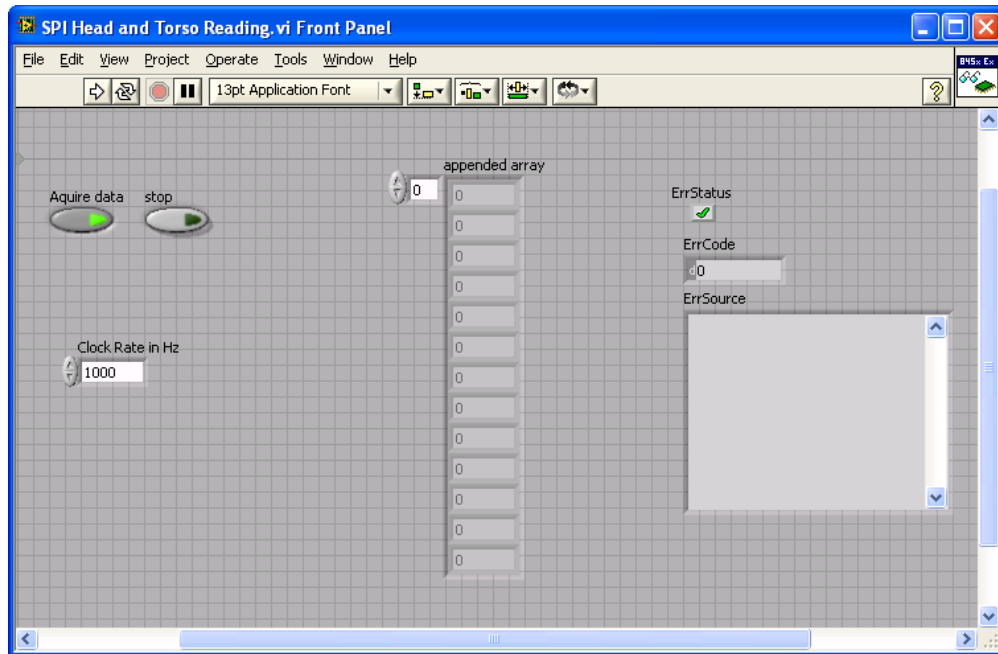


**Figure 13: ADIS16350 LabView DAQ Program Front**

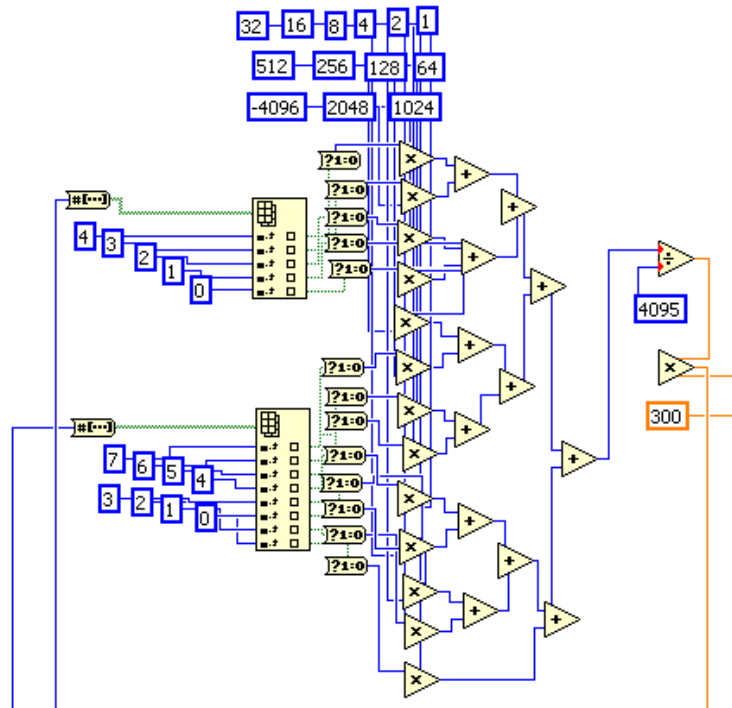


**Figure 14: ADIS16350 LabView DAQ Raw Data Conversion**

## 2.5 Subjects

Trials were run with adults due to restrictions on working with minors. Therefore, five subjects were recruited from the student population at Drexel University. They were recruited by word of mouth and bulletins posted around the Drexel University main campus. The inclusion criterion for subjects is that they are in good health without history of neck trauma or any other neck pathology. Subjects in poor general health were not included in this study.

The subjects recruited were four males between the ages of 22 and 28 and one female aged 25. All of the subjects were in good health and exercised regularly. The female subject was unable to complete Conditions 4 and 5 because she felt uncomfortable with the mass added but the other subjects were able to complete all of the trials.

The decision was made to recruit only college-age students to avoid the additionally complications inherent in testing on minors. Future studies may involve younger subjects in order to test the effects of additional mass on the undeveloped neck which may provide further insight in to the effect of helmets on non-adults.

## **2.6 Data Processing**

Collected data was analyzed using MathCAD 11. Raw data was collected from the sensors as X, Y, and Z position for the Optotrak IRLEDs, X, Y, and Z acceleration for the accelerometers, and Pitch, Yaw, and Roll rotational velocity for the rotational velocity sensors. Initially the raw data was rotated to ensure that it was aligned with the global reference frame. All of the data was filtered using a low-pass filter (**B.1 Low Pass Filter**) with a passband of 20 Hz and stopband of 21 Hz to remove noise and a median filter looking at 6 points on either side of the data point to remove outliers.

Each one of the trials was broken up in to a sixty second walk and sixty second run period with the position, velocity, and acceleration data aligned to ensure that the start and end times were the same. This allowed for easy comparison between conditions and across subjects.

X, Y, and Z positions of the head and trunk were calculated by finding the mean position of the four IRLEDs attached to the head and the trunk. Pitch, Roll, and Yaw rotations were calculated by finding the rotation of the four IRLEDs in space.

The power spectrums for each of the positions, velocities, and accelerations was found using the built in pspectrum function in the MathCAD signal processing extension pack in order to determine the frequency content of the data and this was normalized to allow for easy comparison of relative power at each frequency.

Probability distribution functions were plotted for the positions to determine how much time was spent at each position and the same was done for velocities and accelerations.

For the pitch rotation the moving average was calculated using a two second window to determine the general position of the head and trunk during the trials and this moving average was removed from the original data so that the high frequency movement of the head and trunk could be compared.

Means and standard deviations for the data were calculated to allow for comparison between the conditions. These statistics are given in full in Appendix D: Raw Statistical Data.

Once the data was processed comparisons were made from both raw statistics and graphs of the data to determine the effect of changes in mass, moment of inertia, and torque applied.



## CHAPTER 3: RESULTS



**Figure 15: Subject running with mass and counterbalance**

The data collected from testing shows the motions of the head and trunk in space. The positioning of the mass at the front and back of the helmet was expected to have the most effect on the motions in the sagittal plane, specifically the pitch rotation and the Z-direction movement so these motions are analyzed. The yaw rotations should have also been effected with fewer changes in roll rotations because the mass is placed on axis.

### **3.1 Control Condition**

Condition 1 with the lightweight helmet gives a picture of how the head and trunk move naturally during walking and running. This condition provides a baseline for natural head movement upon which increases in mass, moment of inertia, and torque applied can be compared.

Overall the data shows that the motions of the head and trunk occur at either half of the footfall rate or at the footfall rate and that the magnitudes of the head and trunk motions are very similar while walking but the yaw, roll, and Z-direction motions of the trunk are much greater than the head during running.

The head pitch rotation is an oscillatory motion with the head rotating forward with every footfall and backwards in between footfalls. This was confirmed by looking at the frequency spectrum which showed major peaks at the footfall frequency which was determined from the video taken during each trial (Figure 17). The mean position of the head varied across the subjects and the position of the head varied within trials with subjects holding their head at different positions throughout each trial with a oscillatory motion around this moving average (Figure 16). Standard deviations of pitch rotation were generally low for the head, never exceeding  $2.2^\circ$  for walking and  $2.9^\circ$  for running. The magnitude of pitch rotations generally increased when changing from walking to running. Rotational velocities also followed a oscillatory motion with zero-velocities occurring at the peaks and troughs of the rotation when the motion of the head changes direction (Figure 18). Velocities were not consistent across the subjects but all subjects experienced higher velocities of the head while running.

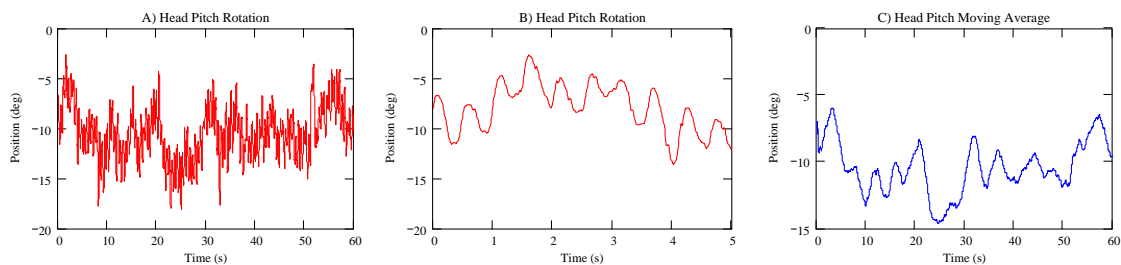


**Figure 16: Representative Head Pitch Rotation plots over A) Complete Trial, B) Five Second Window, and C) Moving average showing mean head position over a two second window**

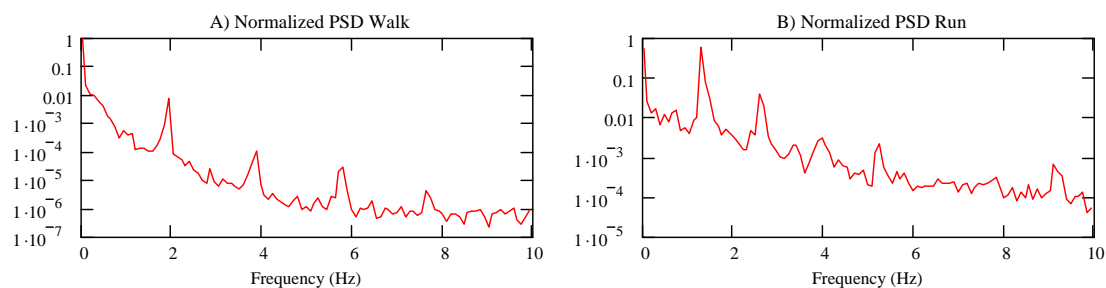


**Figure 17: Representative Frequency Content of Pitch Rotations while A) Walking and B) Running**

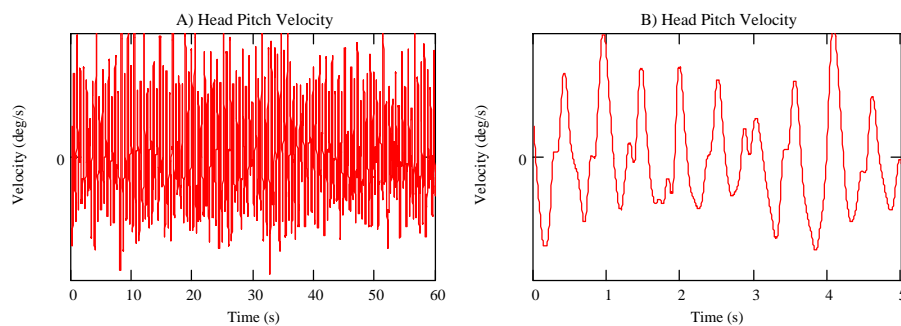


**Figure 18: Representative Head Pitch Velocity plots over A) Complete Trial and B) Five-second window**

Trunk motions followed the same oscillatory motion of the head and were similar in magnitude to those of the head while walking but generally higher than the head while running. Like the head the mean pitch position of the trunk was not consistent across the subjects and the subjects changed the position of their trunk within trials but the standard deviation of the moving average was almost always lower than that of the head indicating that the positioning of the trunk in space did vary greatly within trials. The power spectrum density showed that the head and trunk have very similar frequency content (Figure 19, Figure 20).

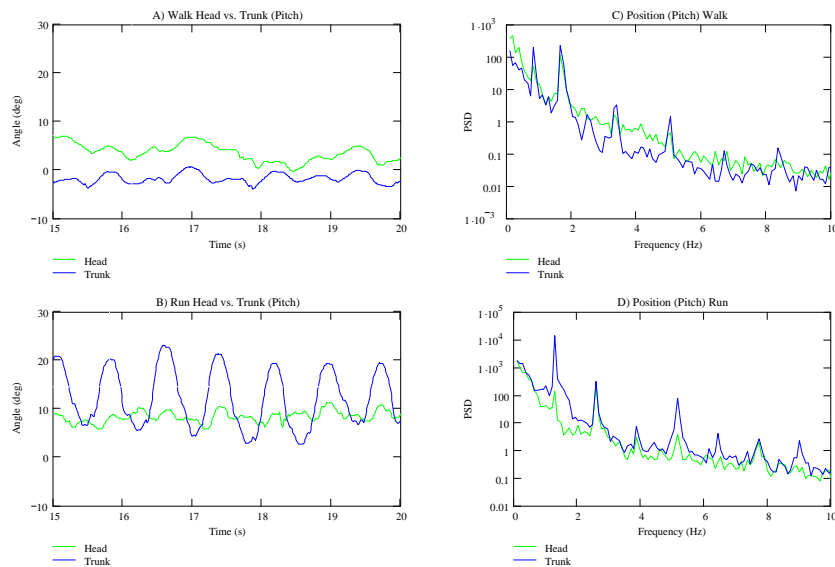


**Figure 19: Representative Head and Trunk Pitch Rotation while A) Walking and B) Running. Frequency Analysis of Head and Trunk Pitch Rotation while C) Walking and D) Running.**

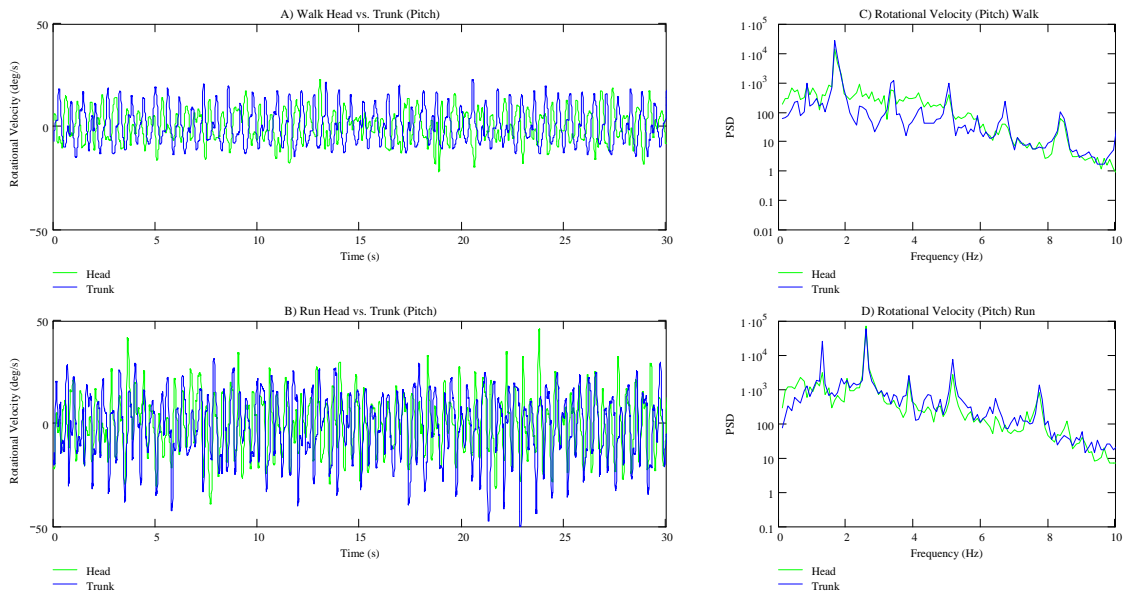


**Figure 20: Representative Pitch Rotational Velocity A) Walking B) Running. Frequency Spectrum A) Walking B) Running**

The yaw motion of the head goes through a complete cycle every two footfalls with the head turning left and right as the left and right feet come down. This was confirmed by the power spectrum analysis of the yaw rotation which showed most of the power concentrated at half of the footfall frequency (Figure 22). The motion is oscillatory with a zero mean as subjects move their heads around the center position (Figure 21).

Standard deviations of yaw rotation for all of the subjects were under  $2.7^\circ$  for walking and  $3.6^\circ$  for running showing that rotations of the head were small.

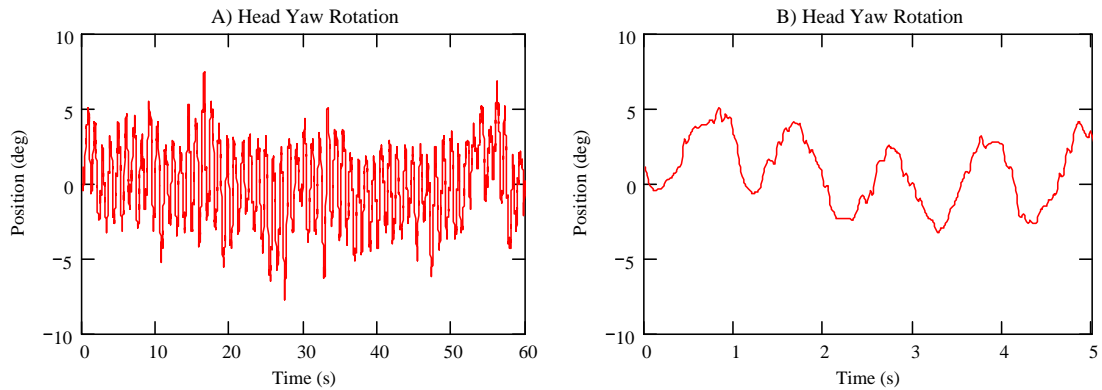


**Figure 21: Representative Head Yaw Rotation plots over A) Complete Trial and B) Five-second window**

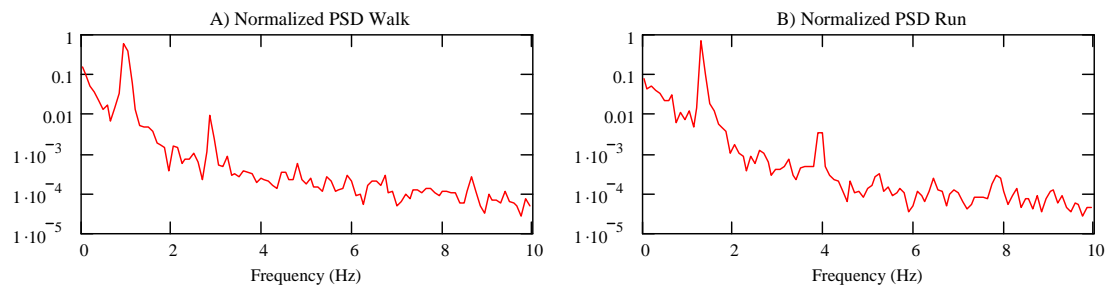


**Figure 22: Representative Frequency Content of Yaw Rotations while A) Walking and B) Running**

Trunk motions were similar to the head motions with similar frequency content with the power highest at the footfall rate. However, head motions were slightly higher while walking and significantly higher while running (Figure 23).

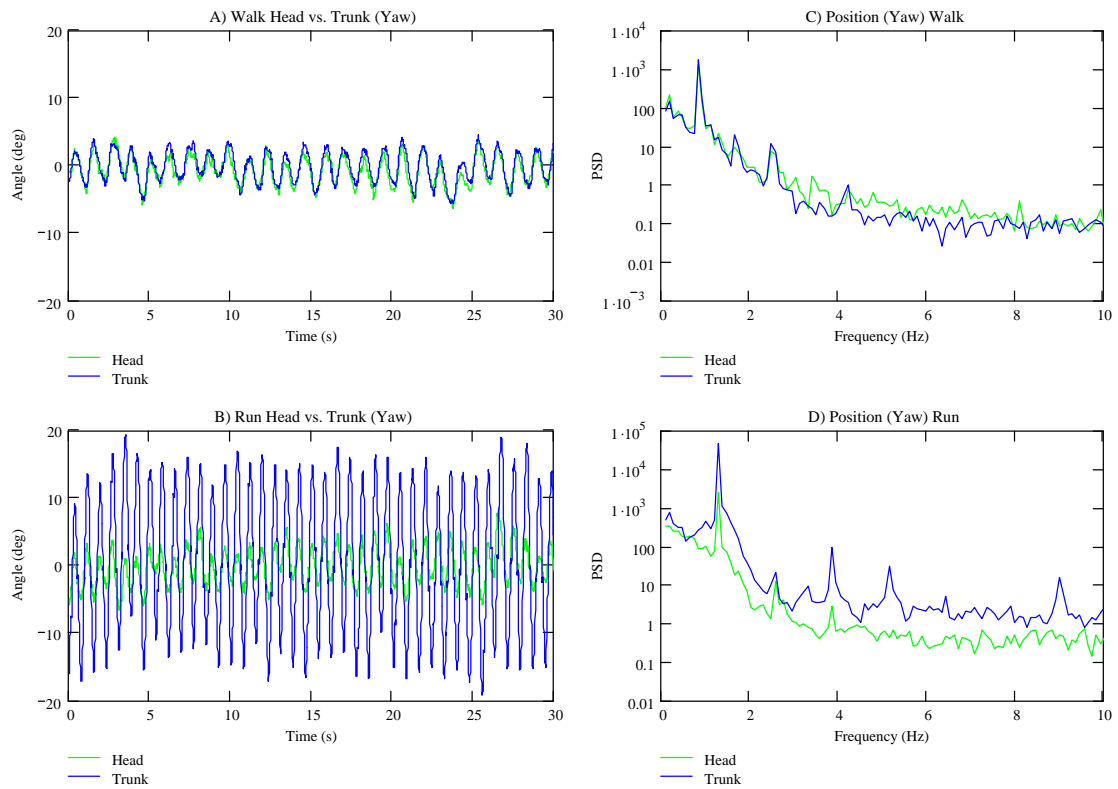


**Figure 23: Head and Trunk Yaw Rotation while A) Walking and B) Running. Frequency Analysis of Head and Trunk Yaw Rotation while C) Walking and D) Running.**

The head roll rotation occurs with each footfall with a complete cycle occurring every two footfalls with the head leaning left when the left foot comes down and right when the right foot comes down. This was confirmed by the power spectrum density which showed a major peak at half of the footfall frequency (Figure 25). The motion of the head was oscillatory with some higher frequency content as the head reached the limits of its rotation. The mean position was at zero degrees as the head was rotating about the center point. Standard deviations of pitch rotation for the head were low with a maximum of  $1.9^\circ$  while walking and running.

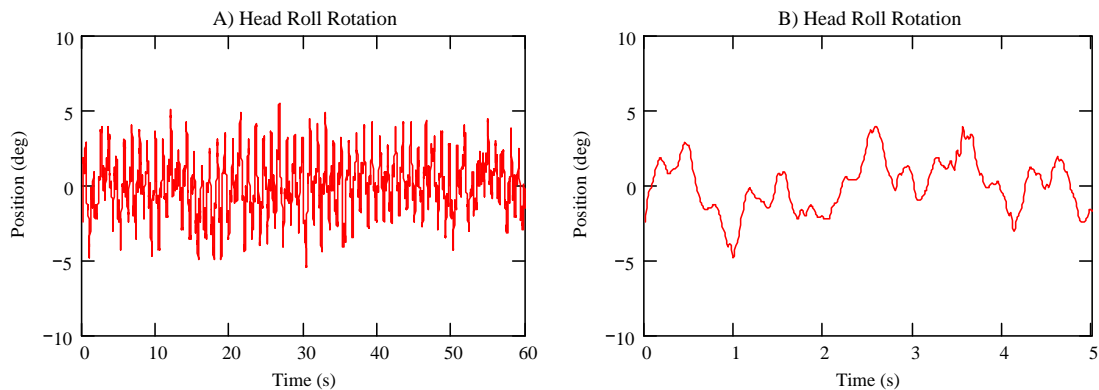


**Figure 24: Representative Head Roll Rotation plots while walking over A) Complete Trial and B) Five-second window**



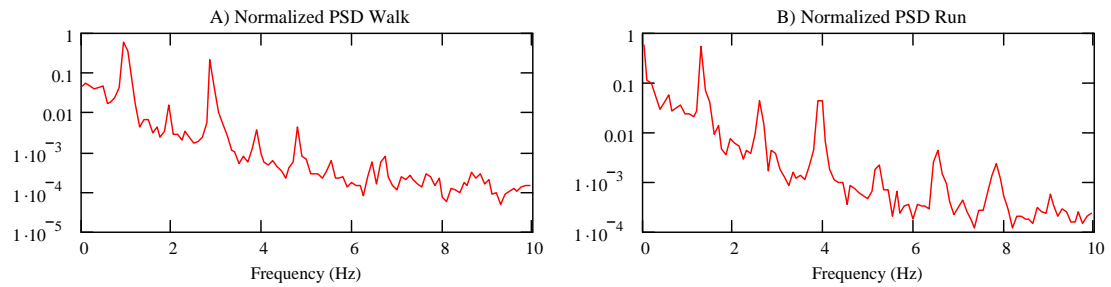


**Figure 25: Representative Frequency Content of Roll Rotations while A) Walking and B) Running**

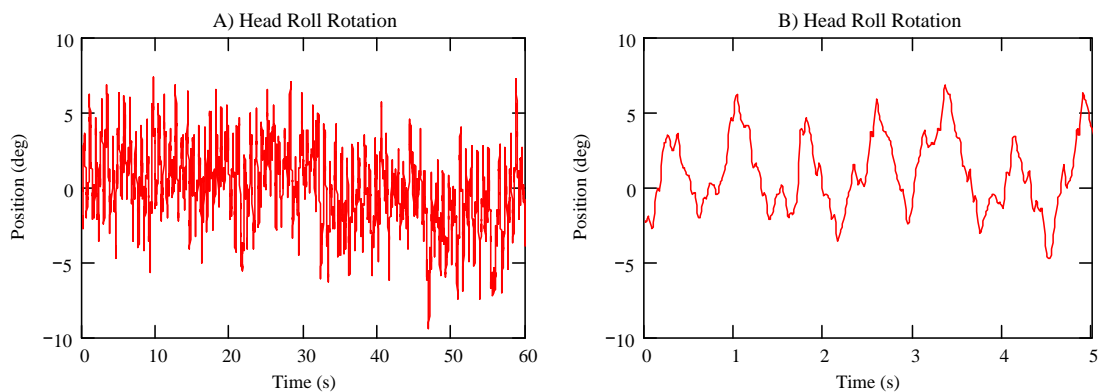


**Figure 26: Representative Head Roll Rotation plots while running over A) Complete Trial and B) Five-second window**

The roll rotational motion of the trunk was similar to that of the head with similar frequency content and the same oscillatory motion. The standard deviation of trunk rotation was almost always higher than that of the head and was significantly higher while running (Figure 27). Maximum standard deviations of pitch rotation for the trunk

were  $2.7^\circ$  while walking and  $5.1^\circ$  while running. Velocities were also much higher for the trunk during running and walking.

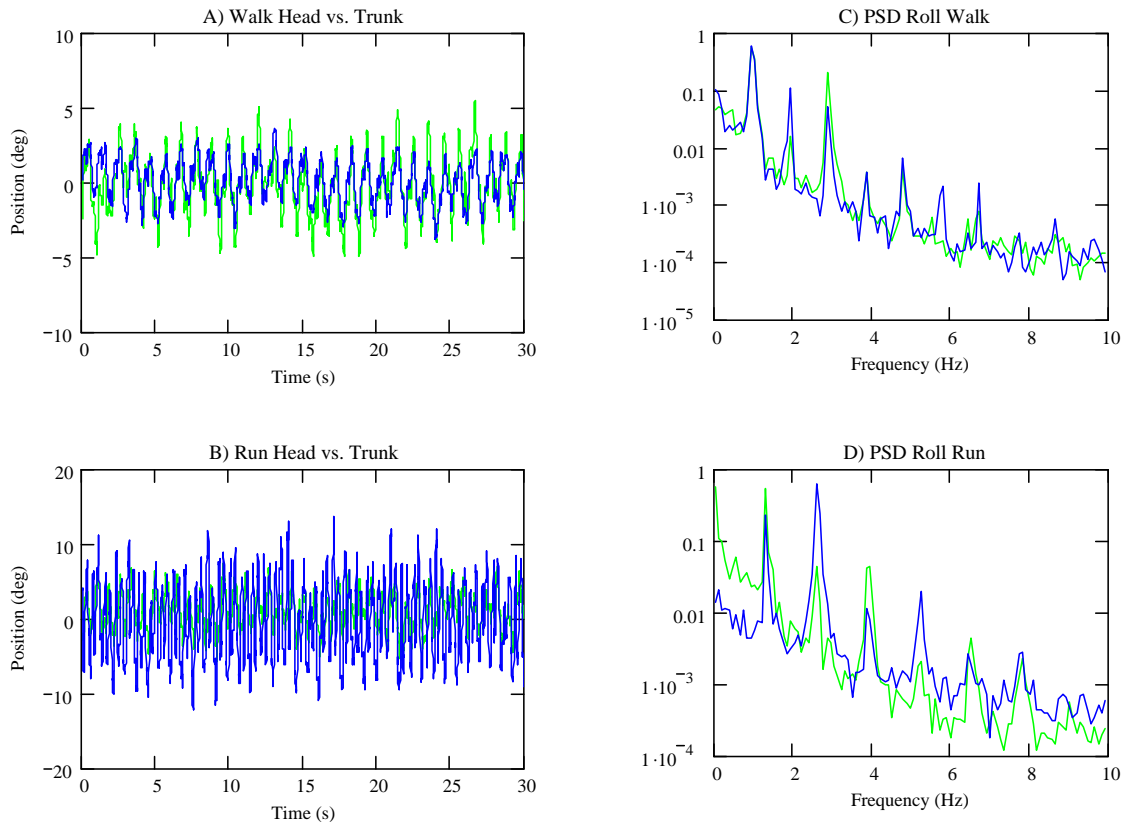


**Figure 27: Head and Trunk Roll Rotation while A) Walking and B) Running. Frequency Analysis of Head and Trunk Roll Rotation while C) Walking and D) Running.**

As subjects walk or run they are pushing off of the ground with their feet resulting in an up and down motion. The head moves up and down with the footfalls resulting in a

oscillatory motion with major frequency content at the footfall rate (Figure 28, Figure 29).

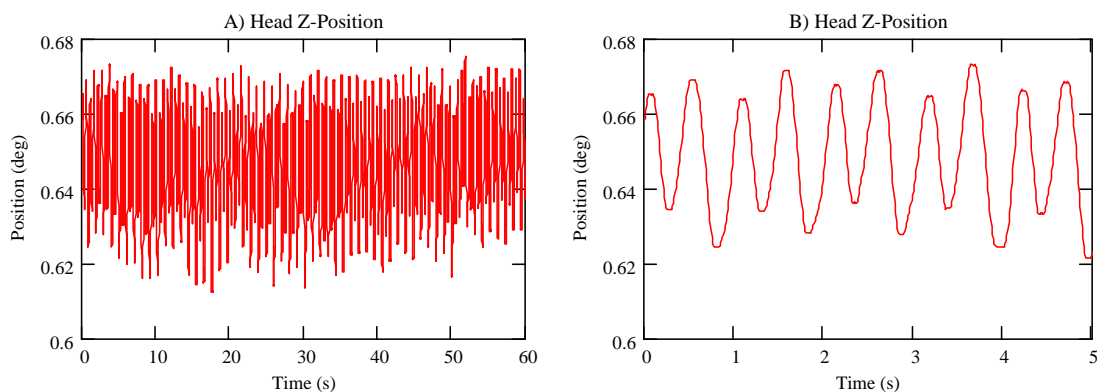


**Figure 28: Representative Head Z-direction position plots while walking over A) Complete Trial and B) Five-second window**

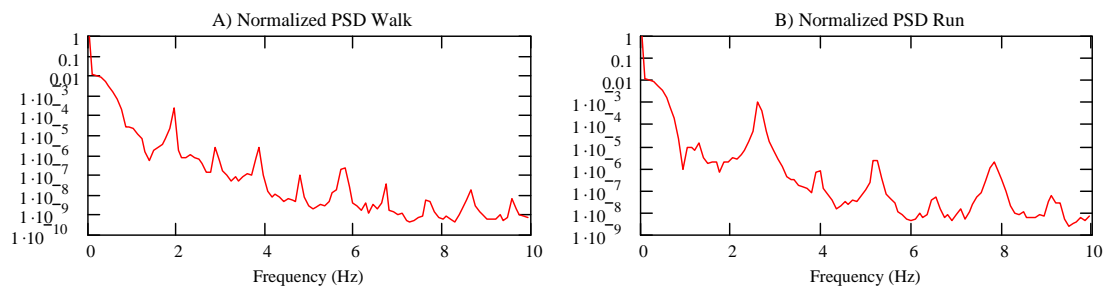


**Figure 29: Representative Frequency Content of Z-direction motions while A) Walking and B) Running**

The trunk also moves up and down with footfalls in the same motion as the head. The standard deviation of trunk position is always higher than that of the head and the root mean square values of acceleration were also always higher indicating that the up and

down motion of the trunk is translated directly to the head with a damping factor (Figure 30).

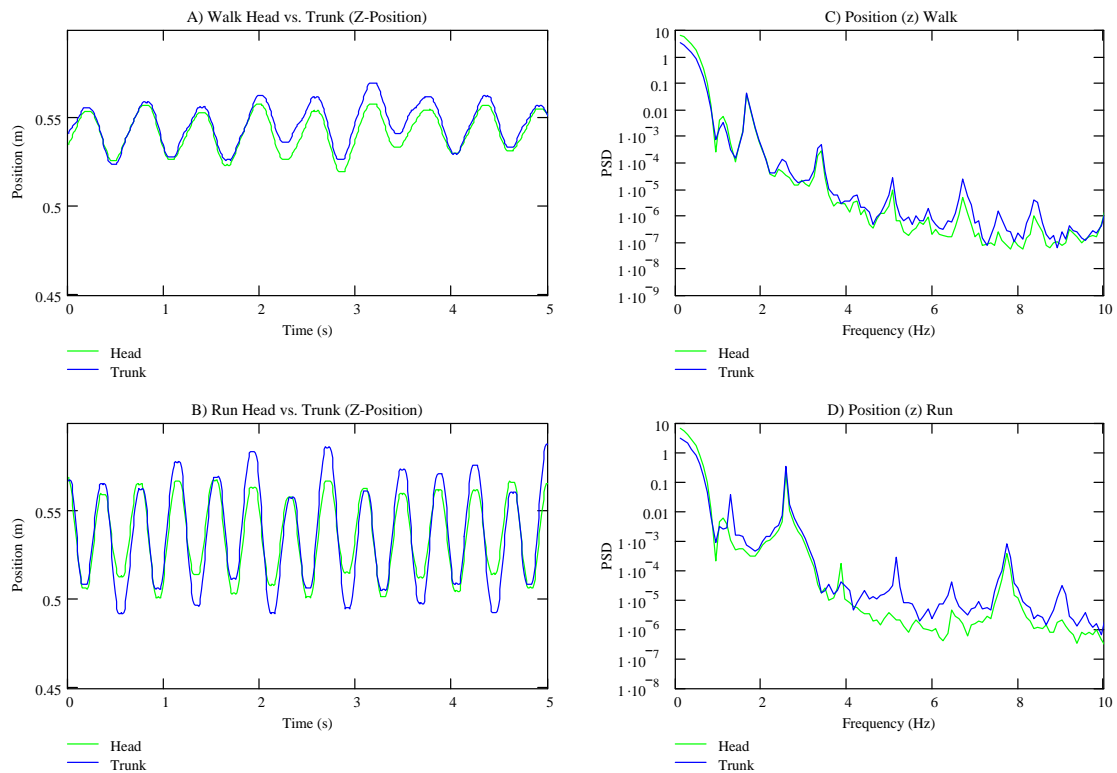


**Figure 30: Head and Trunk Z-Position while A) Walking and B) Running. Frequency Analysis of Head and Trunk Motion while C) Walking and D) Running.**

### 3.2 Pitch Motion

The pitch motion of the trunk is one of the main inputs in to the motion of the head so looking at the relative motions of the head and trunk gives an indication of how much the neck musculature is working to stabilize the head in pitch.

Results showed that the pitch rotational motion of the head followed the same oscillatory motion across the conditions. The pitch movement of the head around the moving average did not change significantly across the conditions despite large changes in the moment of inertia of the head and the torque applied to the head. The mean pitch position of the head changed between the runs and the moving average of the position changed within the runs but there was no correlation between the pitch position of the head and the changes in mass, moment of inertia, or torque applied.

The standard deviation of the pitch rotation of the head varied less than  $1^\circ$  across the conditions for all of the subjects while walking and for four of the five subjects while running showing that the rotation motion of the head was similar for all of the conditions. There was no correlation between changes in standard deviation for increases in mass, moment of inertia, or torque applied with the standard deviations staying in a small range (Figure 32). Distributions of pitch rotation around the moving average were similar across the conditions for all subjects while walking and running indicating similar motions of the head about the moving average (Figure 33). Power spectral analysis showed that the power for each condition was concentrated at the footfall frequency and the footfall frequency did not vary across the conditions. Power content was similar for all of the conditions with no evidence of higher peaks for different conditions or any faster falloff of power for any of the conditions (Figure 34).

Root-Mean-Square velocity of pitch rotation varied between conditions and subjects but there was no relationship between the addition of mass, increasing moment of inertia, or increased applied torque across the subjects (Figure 36).

Head mean pitch position in space stayed between  $-15^{\circ}$  and  $15^{\circ}$  for all subjects while running and walking with no changes in mean pitch position related to mass, moment of inertia, or torque applied. Within trials the moving average of the pitch position varied with standard deviations of the moving average reaching as high as  $3.8^{\circ}$  showing that subjects varied their head position within trials but there was no correlation between increasing standard deviation of moving average and increases in mass, moment of inertia, or torque applied (Figure 38, Figure 39).

The pitch rotation standard deviation of the trunk about the moving average did not vary with mass applied, increased moment of inertia, or increased torque applied (Figure 40). While running the standard deviation was generally higher than that of the head but it was similar while walking. Root mean square of rotational velocity showed that the trunk rotational velocity did not change significantly across the conditions (Figure 41).

The mean pitch position of the trunk varied between trials but the standard deviation of the moving average was generally lower than that of the head indicating that the subjects did not vary the pitch position of their trunks as much as the head within trials (Figure 42).

The pitch movements of the head and trunk were fairly similar while walking but the movement of the trunk increased greatly compared to the head while running (Figure 43, Figure 44, Figure 45). While running the standard deviation of the trunk position was generally higher than that of the head and when the opposite was true the values were not significantly different. Standard deviation of trunk position reached as high as  $7.2^{\circ}$  while

standard deviation of head position never exceeded  $3.0^\circ$ . Standard deviations of the moving averages were generally higher for the head than the trunk.

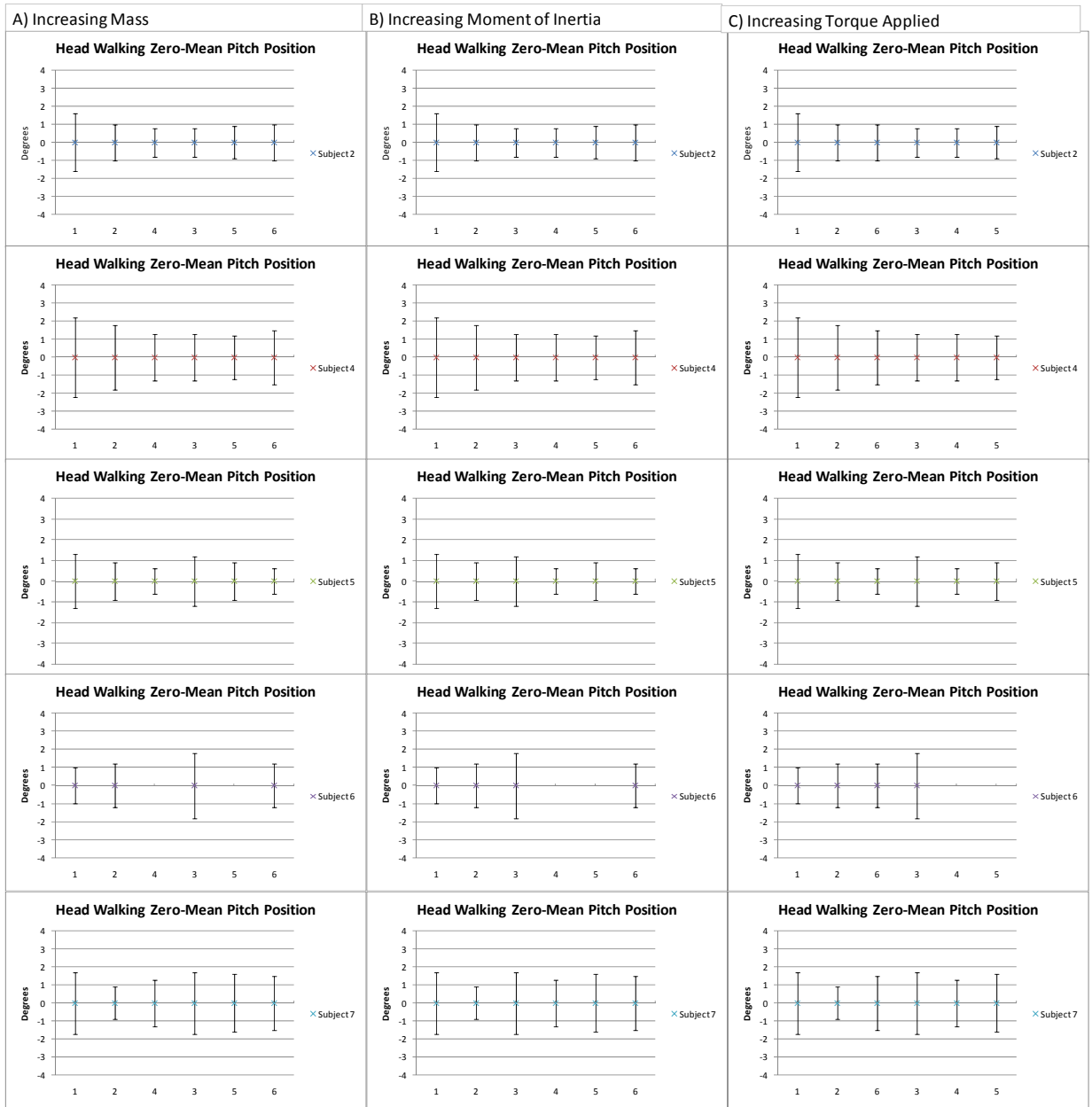


**Figure 31: Mean Walking Head Pitch Rotation around Moving Average with Standard Deviation for A) Increasing Mass, B) Increasing Moment of Inertia, and C) Increasing Torque Applied**



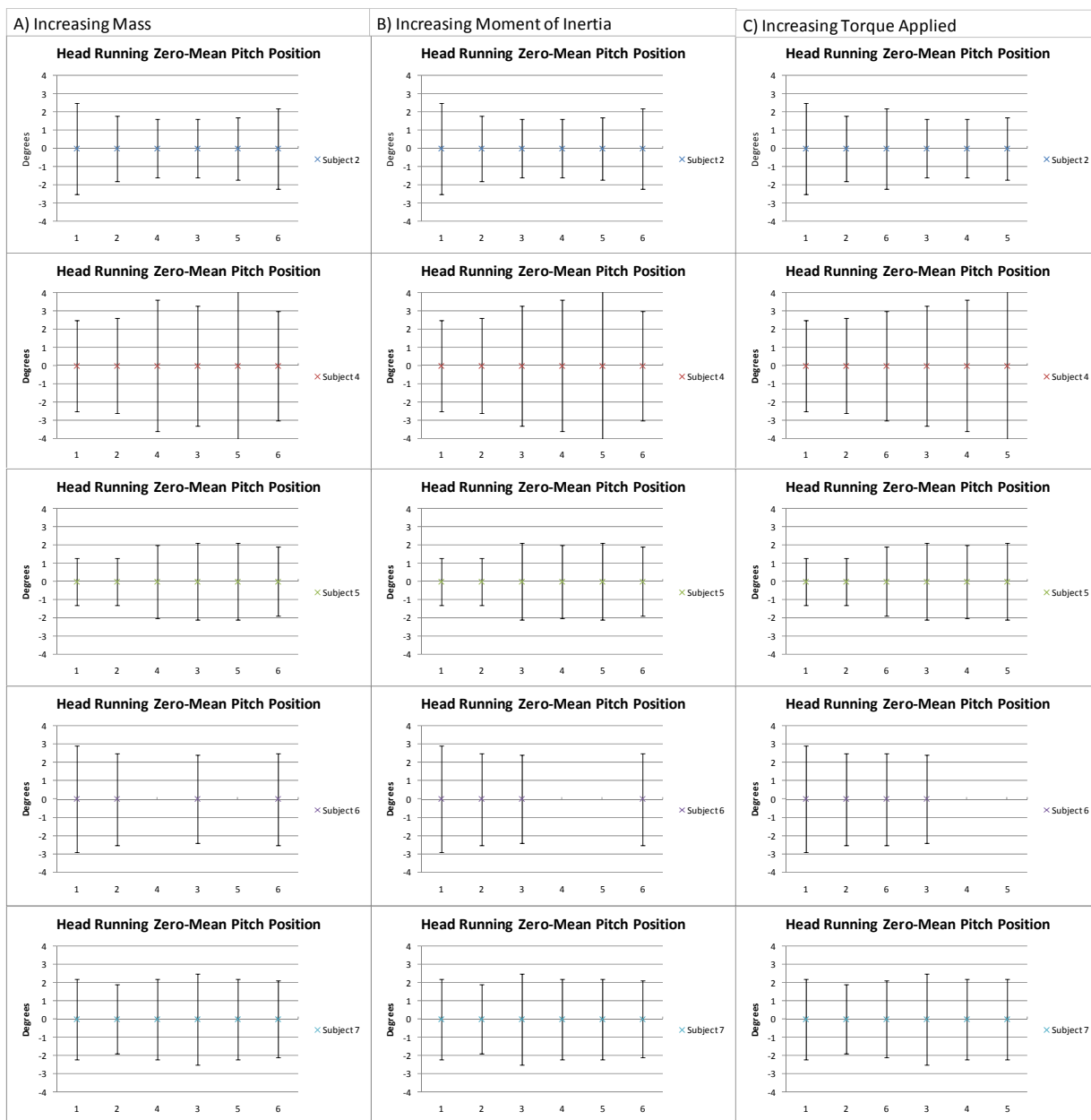


**Figure 32: Mean Running Head Pitch Rotation around Moving Average with Standard Deviation for A) Increasing Mass, B) Increasing Moment of Inertia, and C) Increasing Torque Applied**

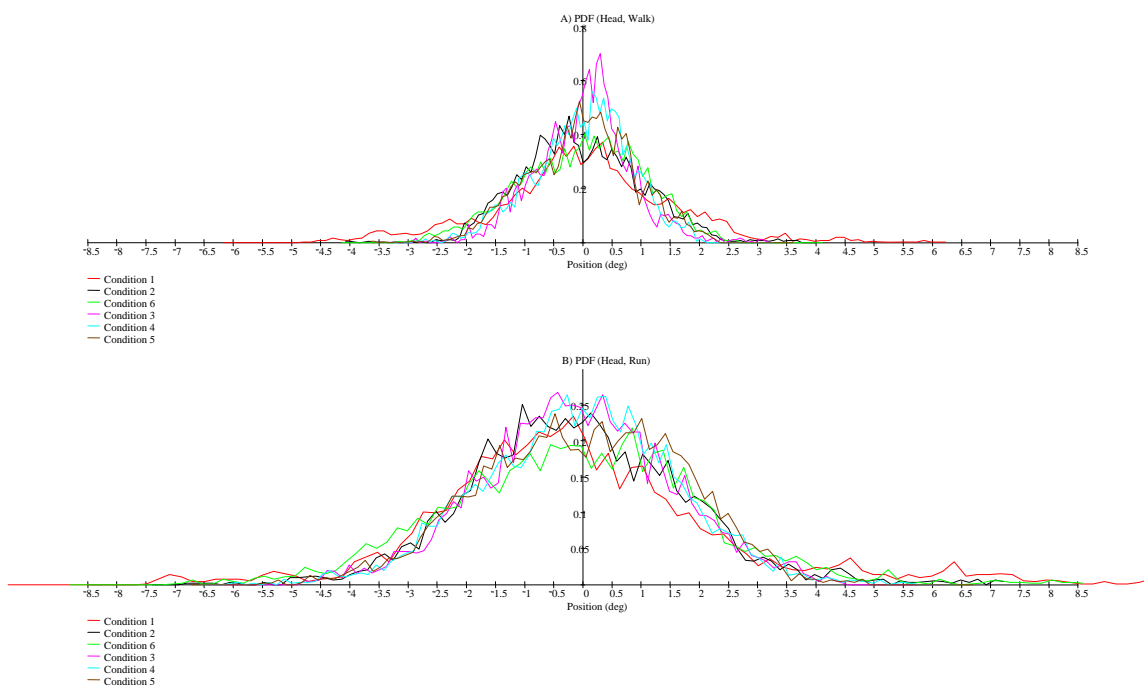


**Figure 33: Representative Probability Distribution Function of Head Pitch Rotation around moving average A) Walking B) Running**

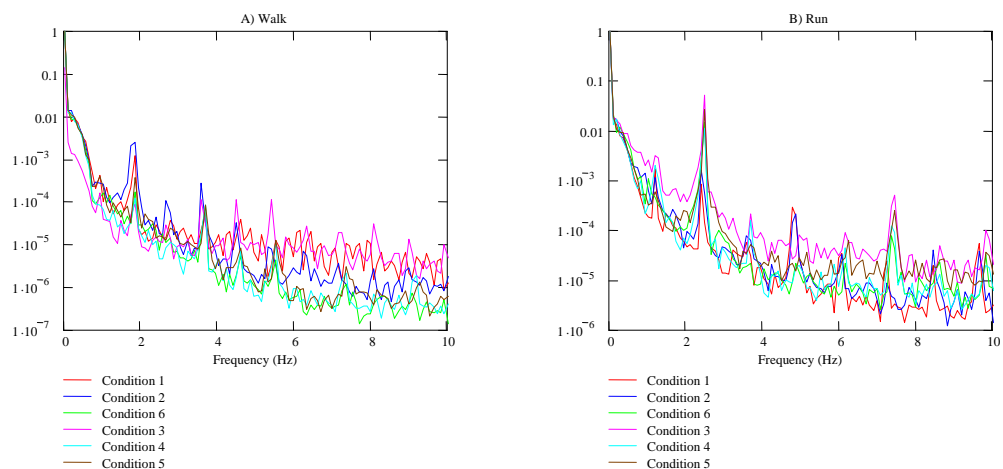


**Figure 34: Representative Normalized Power Spectrum Density of Head Pitch Rotation A) Walking B) Running**

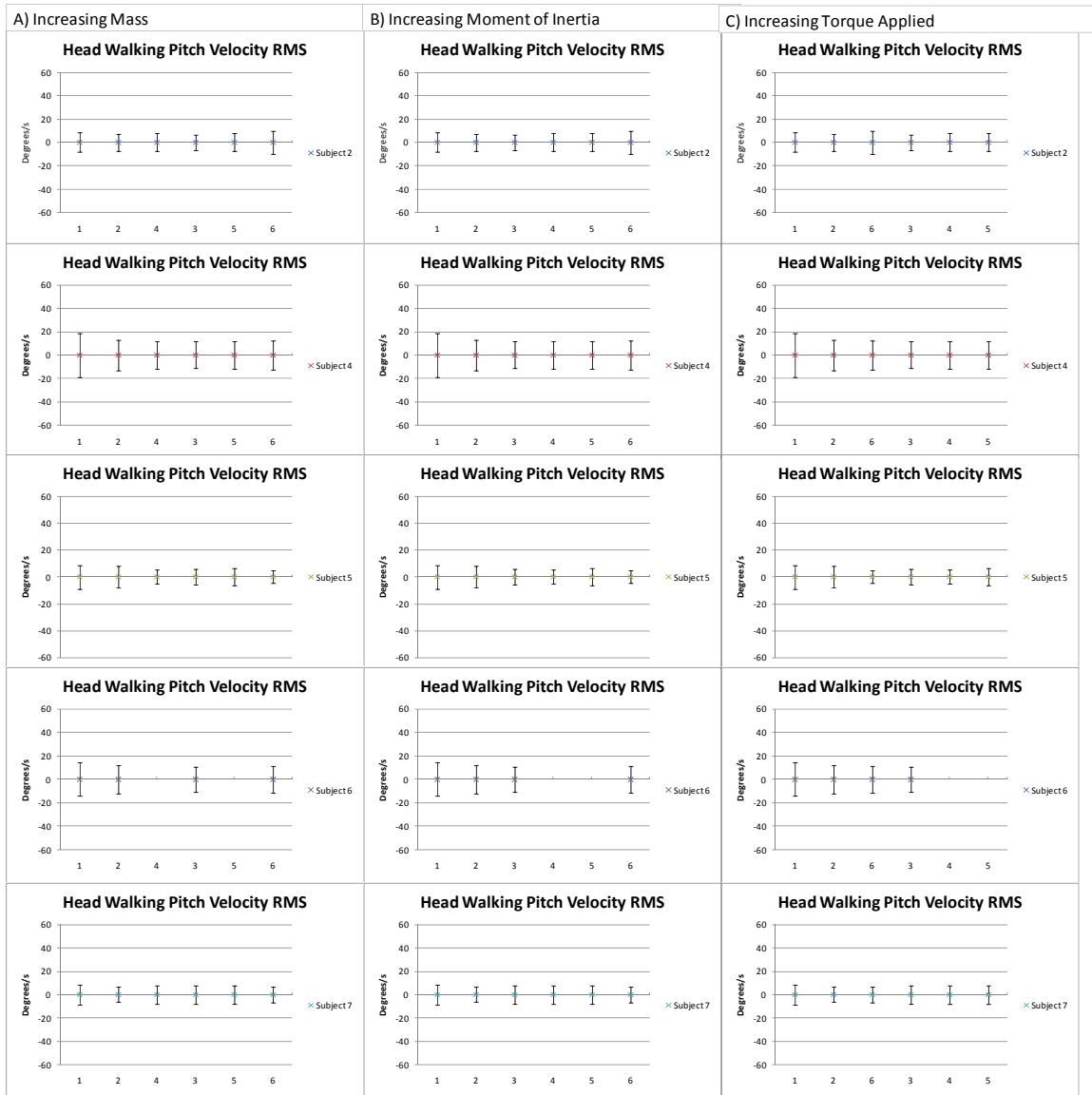


**Figure 35: Mean Walking Head Pitch Rotational Velocity with Root Mean Square for A) Increasing Mass, B) Increasing Moment of Inertia, and C) Increasing Torque Applied**

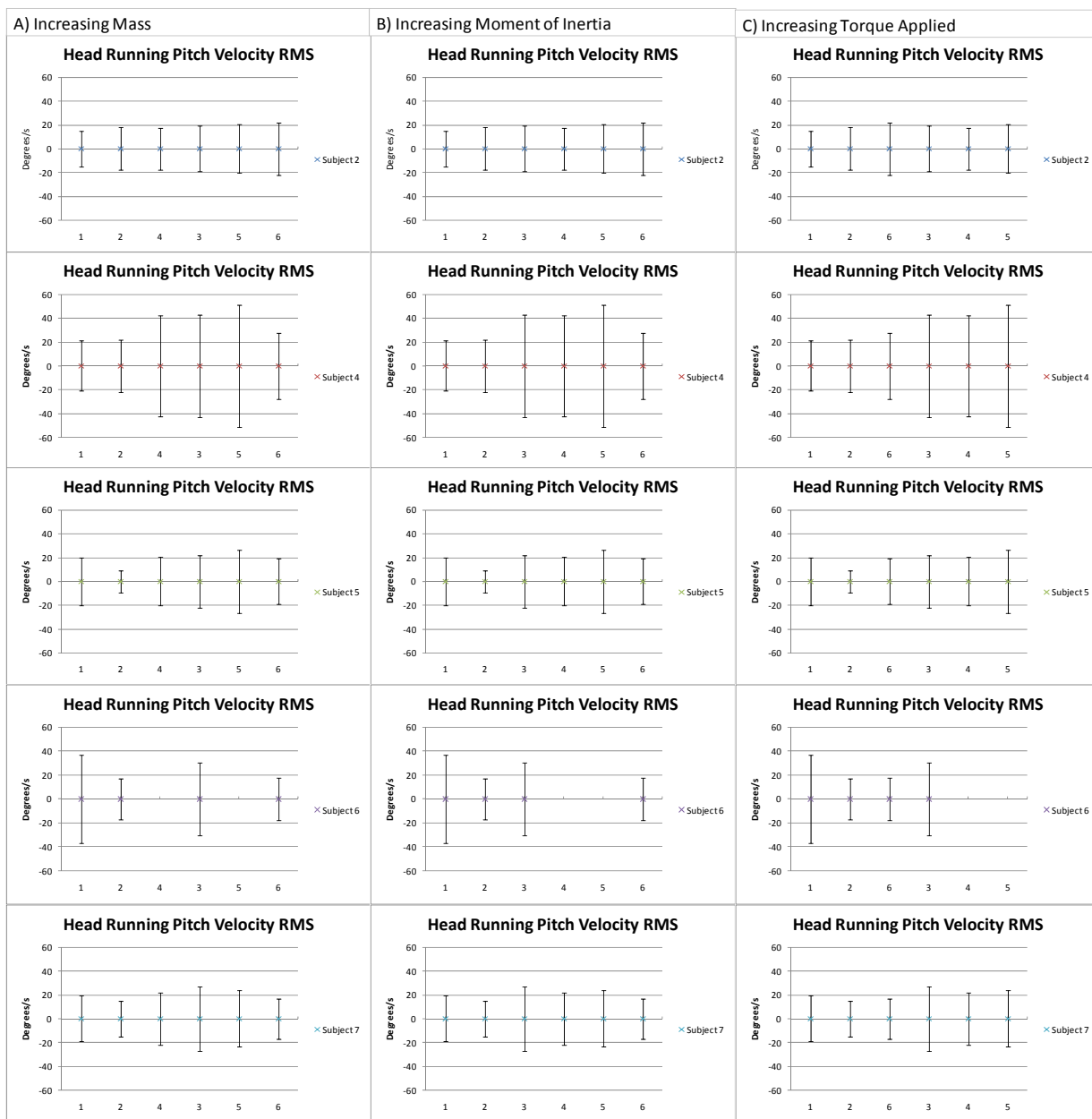


**Figure 36: Mean Running Head Pitch Rotational Velocity with Root Mean Square for A) Increasing Mass, B) Increasing Moment of Inertia, and C) Increasing Torque Applied**

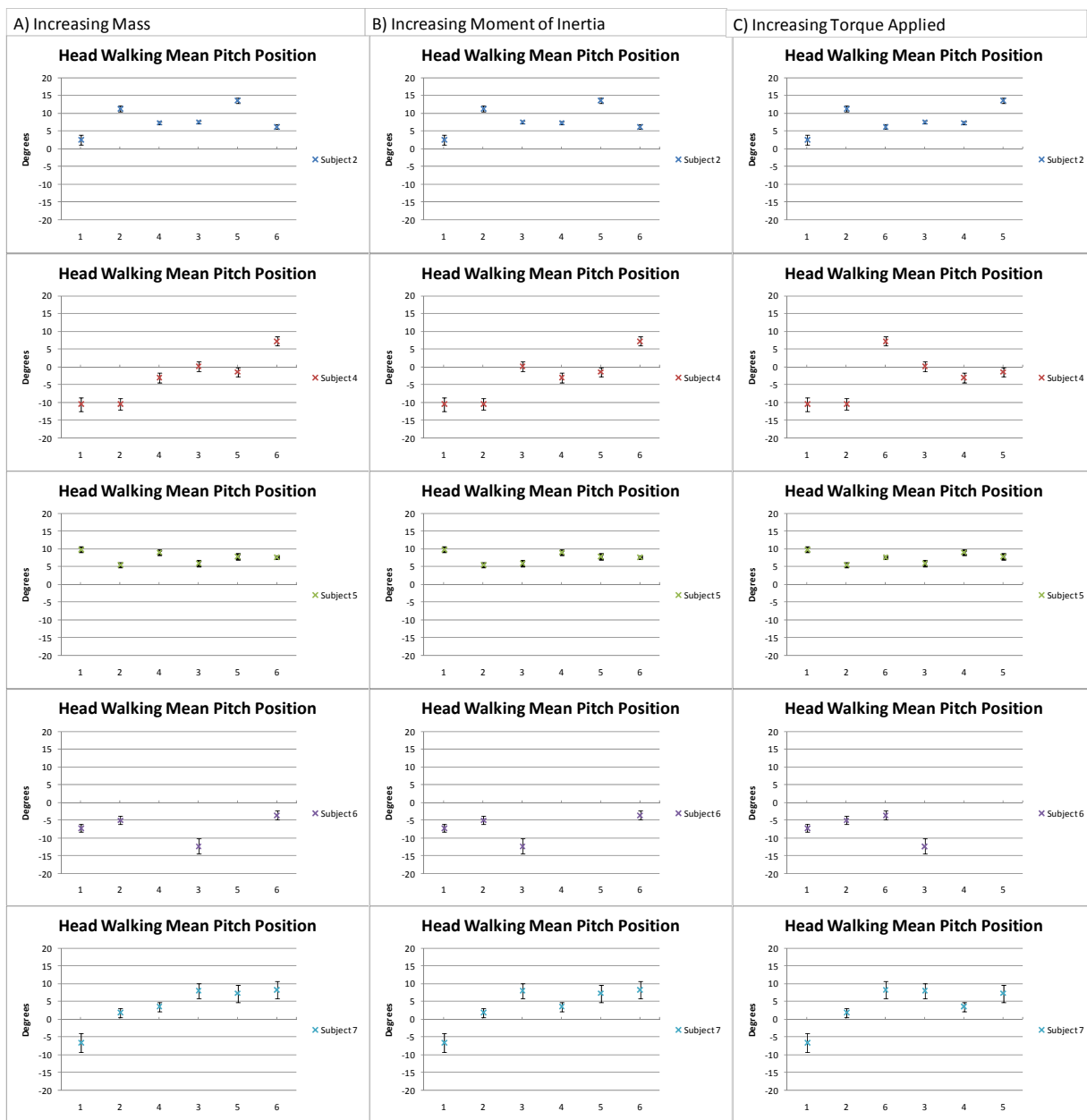


**Figure 37: Mean Walking Head Pitch Rotation with Standard Deviation for A) Increasing Mass, B) Increasing Moment of Inertia, and C) Increasing Torque Applied**



**Figure 38: Mean Running Head Pitch Rotation with Standard Deviation for A) Increasing Mass, B) Increasing Moment of Inertia, and C) Increasing Torque Applied**

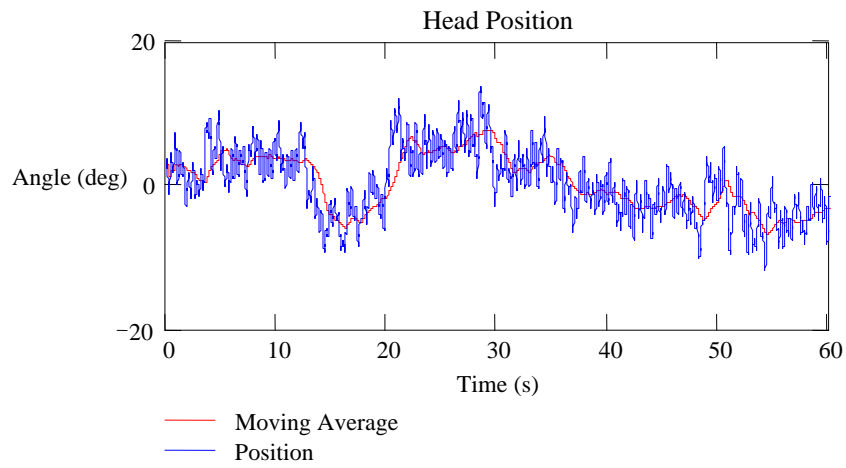


**Figure 39: An example of significant changes in moving average during a run**

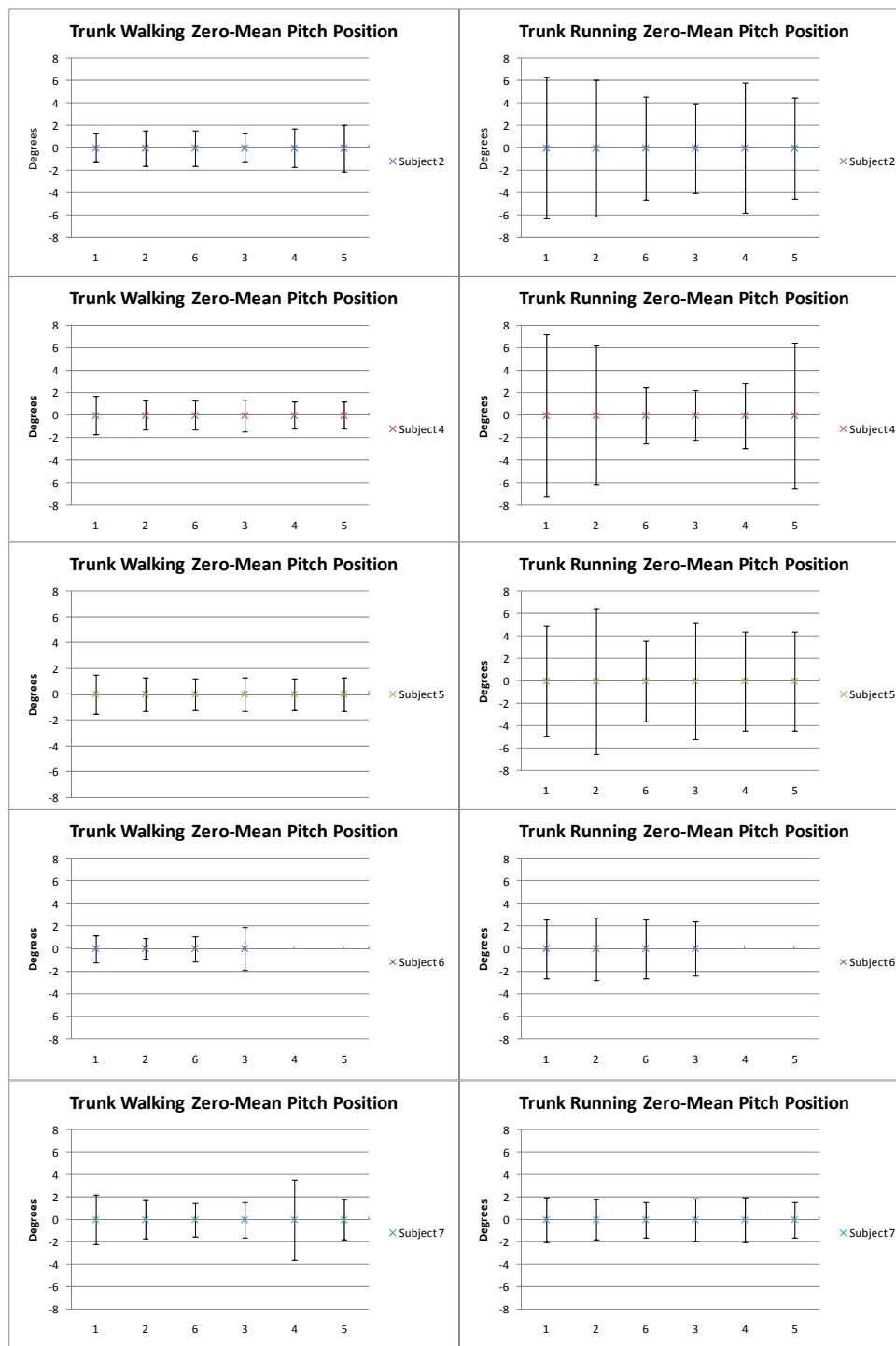


**Figure 40: Mean Running Trunk Pitch Rotation around Moving Average with Standard Deviation**



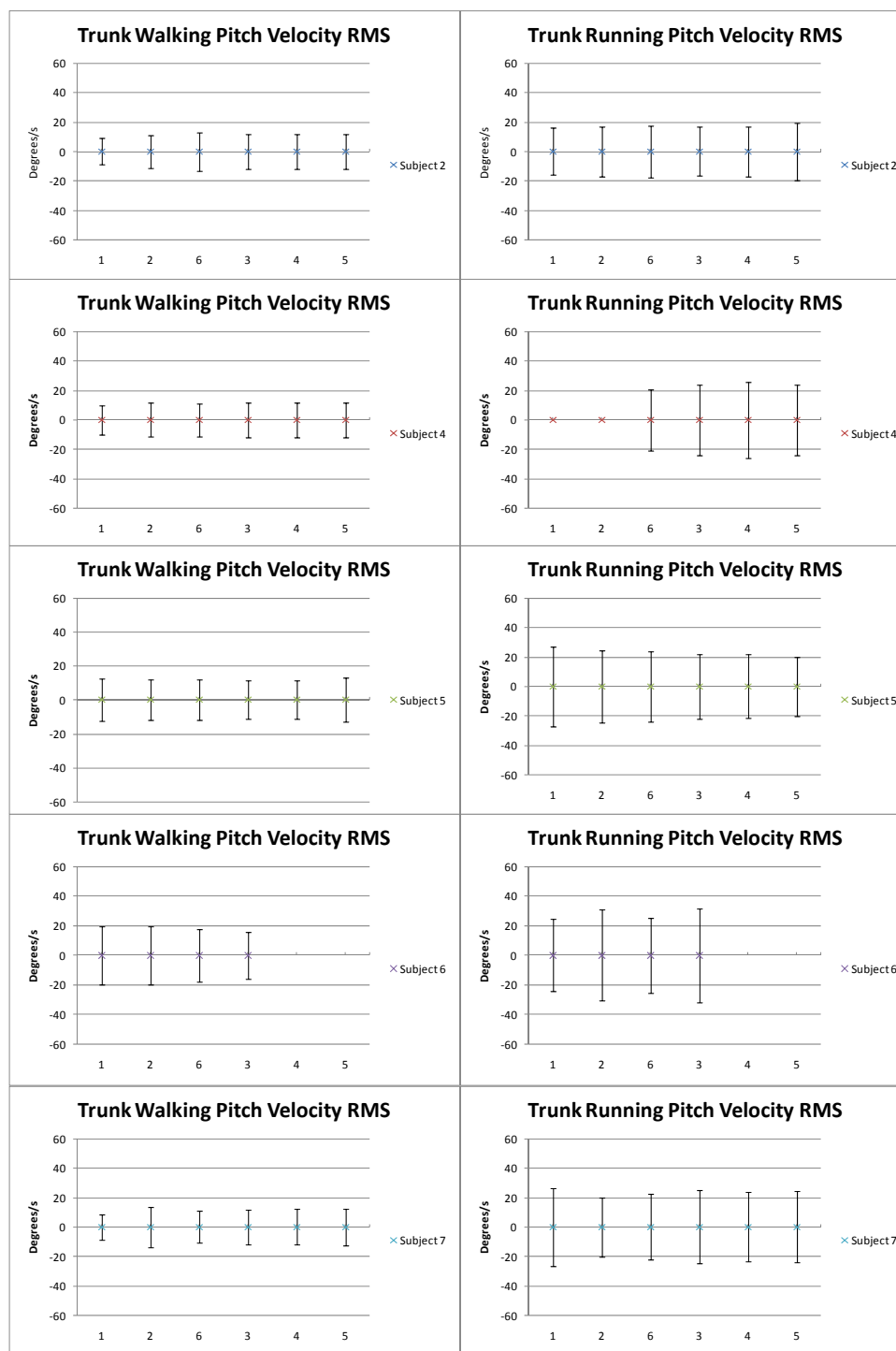


**Figure 41: Mean Running Trunk Pitch Rotational Velocity with Root Mean Square**

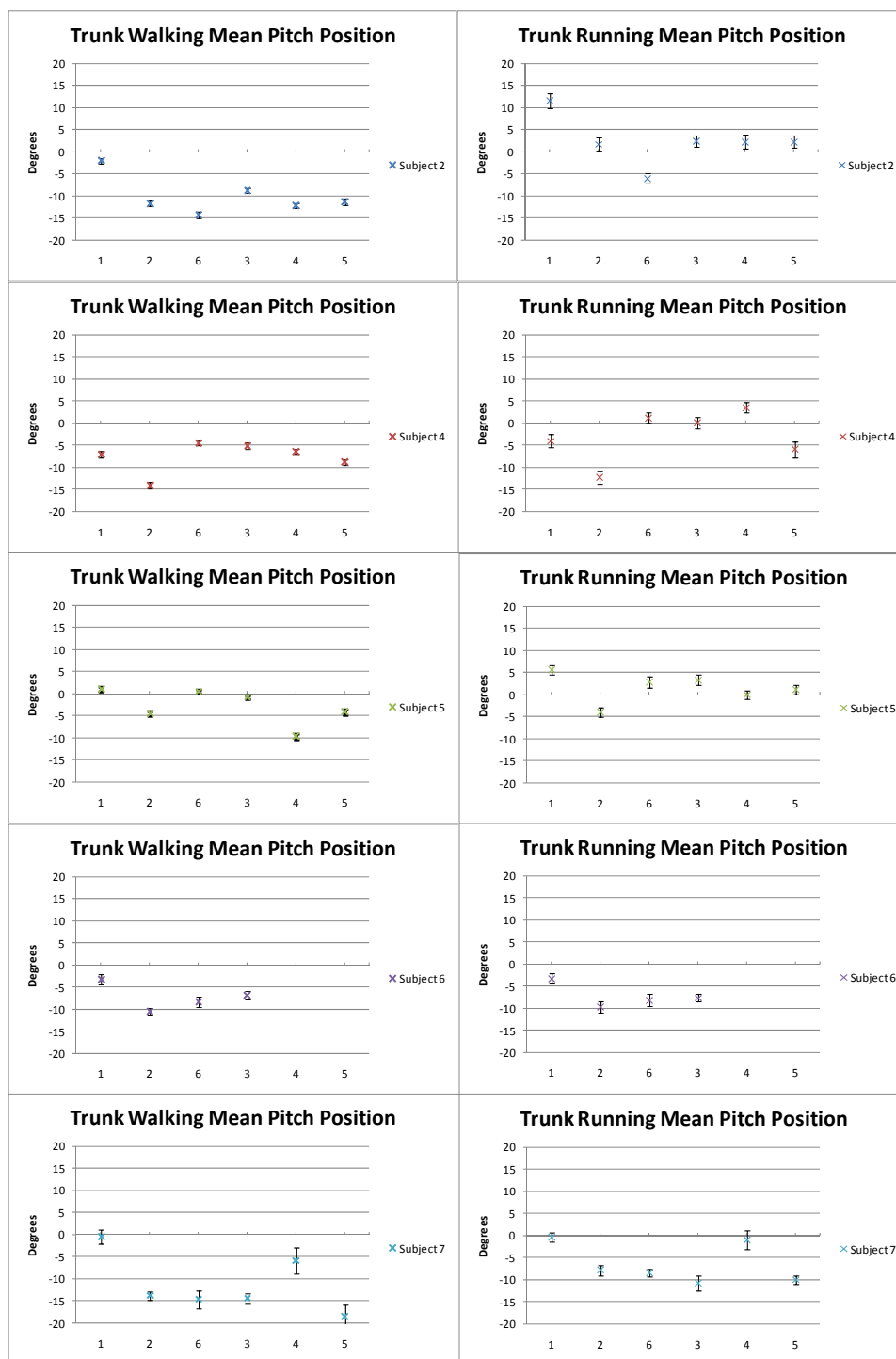


**Figure 42: Mean Running Trunk Pitch Rotation with Standard Deviation**

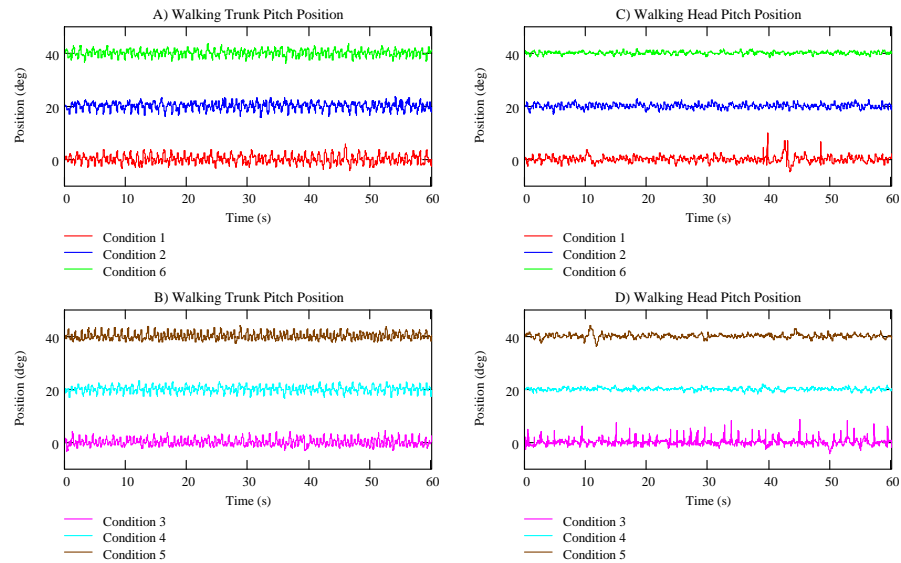


**Figure 43: Walking Pitch Rotation with Moving Average Removed A) Trunk Conditions 1, 2, 6; B) Trunk Conditions 3, 4, 5; C) Head Conditions 1, 2, 6 D) Head Conditions 3, 4, 5. The plots are all zero mean but offset for comparison purposes.**

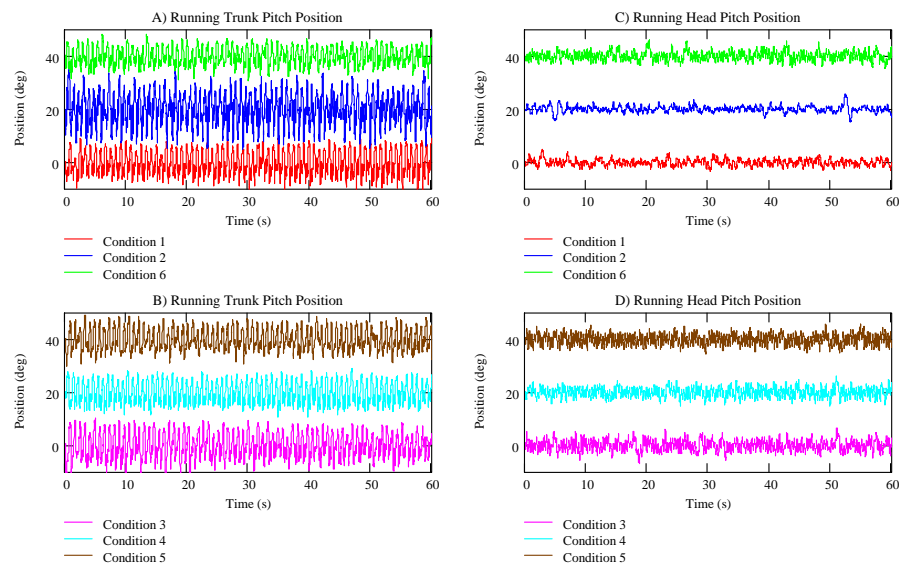


**Figure 44: Running Pitch Rotation with Moving Average Removed A) Trunk Conditions 1, 2, 6; B) Trunk Conditions 3, 4, 5; C) Head Conditions 1, 2, 6 D) Head Conditions 3, 4, 5. The plots are all zero mean but offset for comparison purposes.**

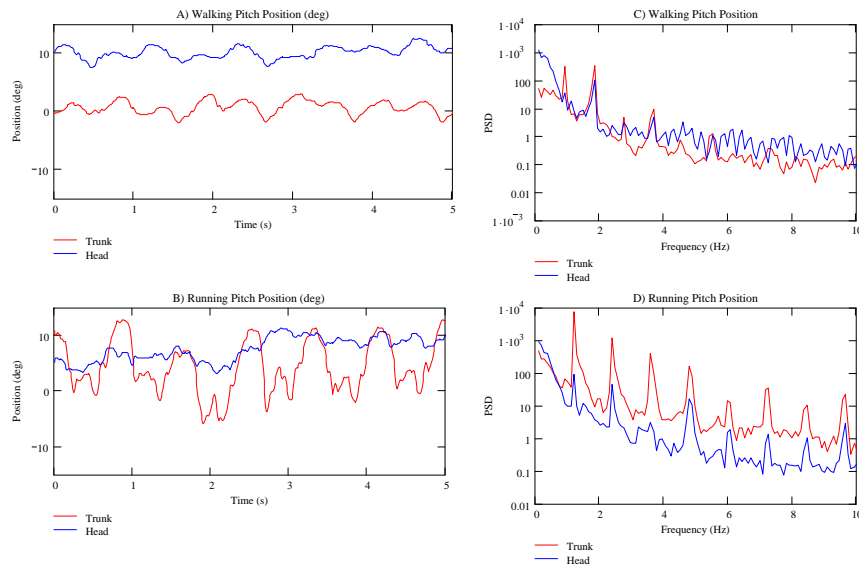


**Figure 45: Pitch Position A) Walking B) Running. Frequency Analysis C) Walking D) Running**

### 3.3 Yaw Motion

Yaw motions in the trunk occur as the body is turned with footfalls. These motions provide an input to the head and can be used to assess ability of the neck musculature to stabilize the head in space.

The results showed that the yaw motion of the trunk is always greater than or equal to the yaw motion of the head. There was no obvious relationship between the standard deviation of yaw rotation or velocity with changes in mass, moment of inertia, or torque applied.

Standard deviations of yaw rotations for the head generally did not vary more than  $1.5^\circ$  across the conditions and never exceeded  $2.7^\circ$  for walking and  $4.2^\circ$  for running (Figure

46). Root mean square of rotational velocity also remained similar across the conditions (Figure 47). Probability density functions for the head yaw rotation showed very similar curves across the conditions (Figure 49). Plotting the power spectral density of the yaw rotation showed similar power across the conditions with power concentrated at half the footfall frequency (Figure 48).

The standard deviation of pitch rotation was higher for the trunk than the head in fifty-four out of fifty-six trials with the two exceptions having equal standard deviations for the head and trunk. The root mean square velocity was also higher for the trunk in fifty-four out of fifty-six trials. The motions of the head and trunk are in phase with greater amplitude for the trunk, especially during running (Figure 52, Figure 53, Figure 54).

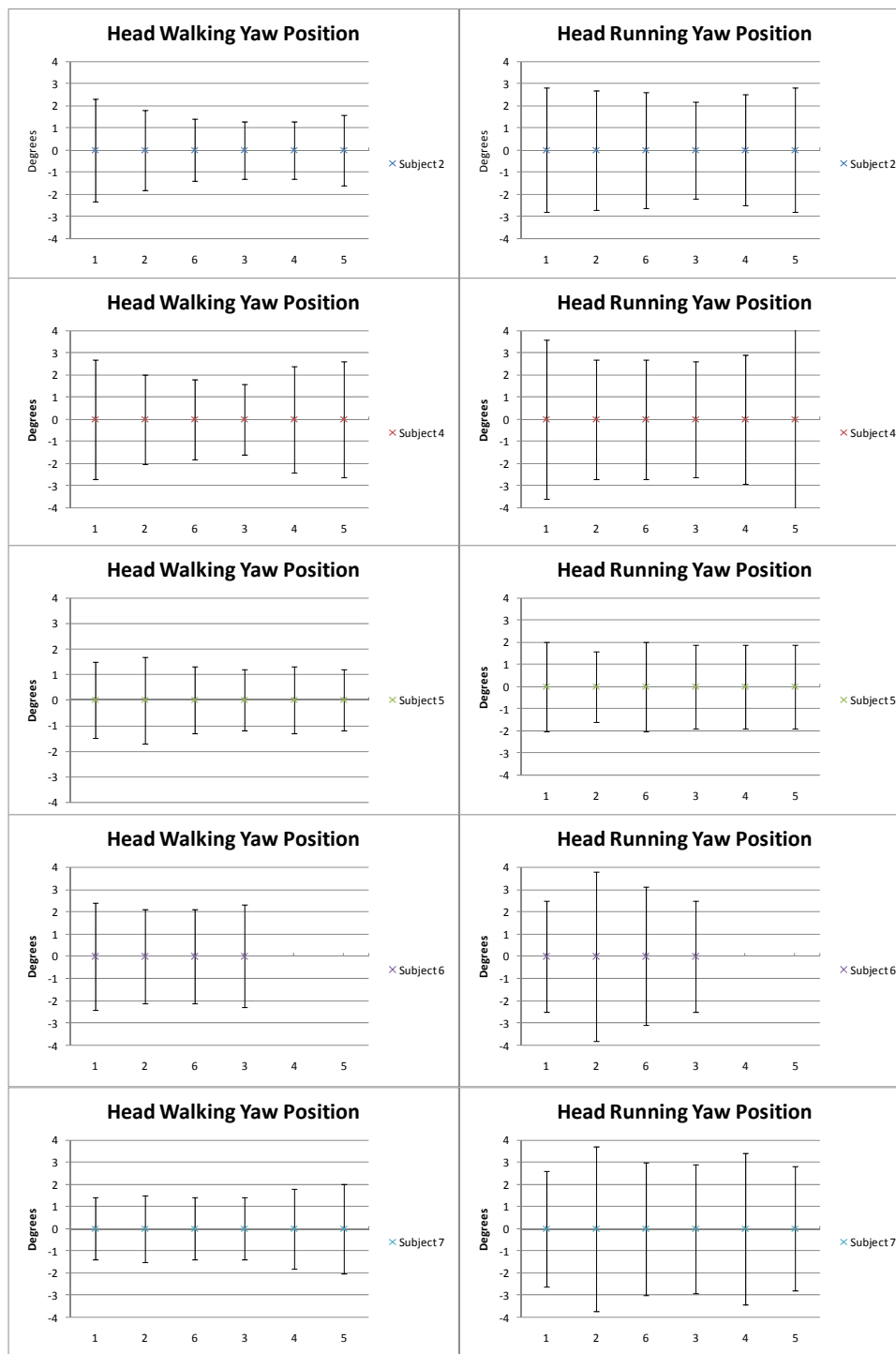


**Figure 46: Mean Walking and Running Head Yaw Rotation with Standard Deviation**

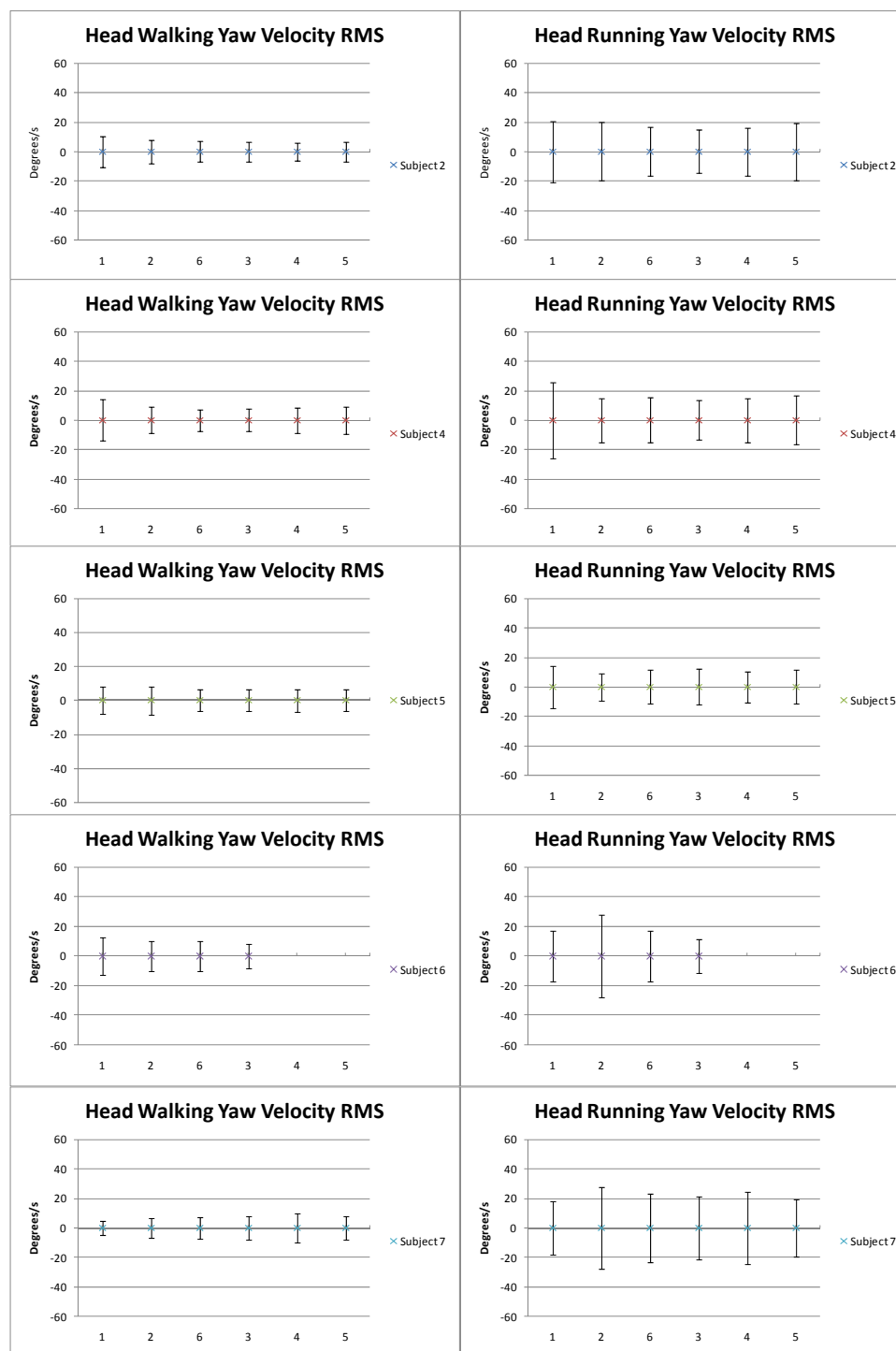


**Figure 47: Mean Walking and Running Head Yaw Rotational Velocity with Root Mean Square**

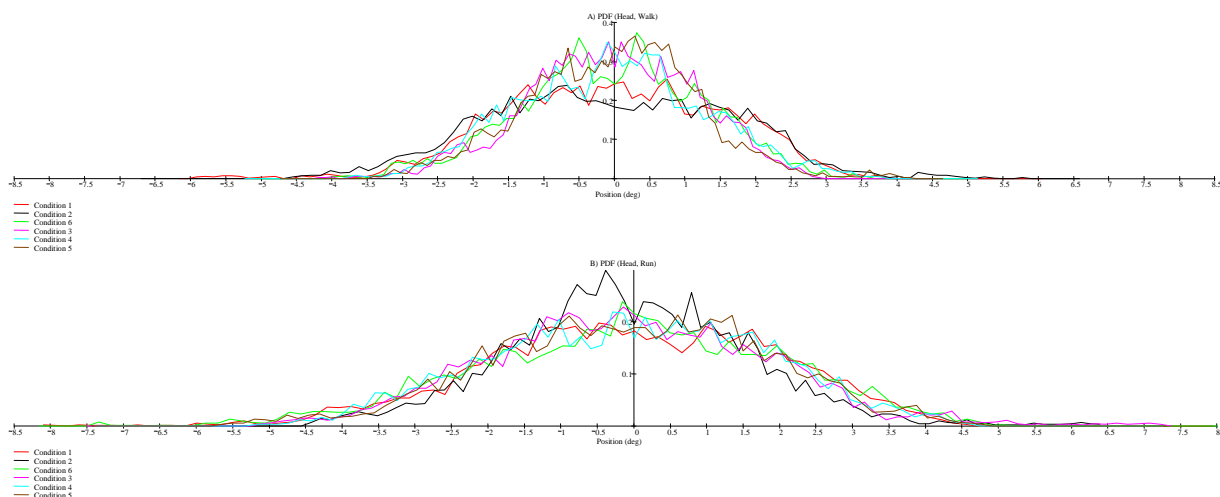


**Figure 48: Representative Probability Distribution Function of Head Yaw Rotation around moving average A) Walking B) Running**

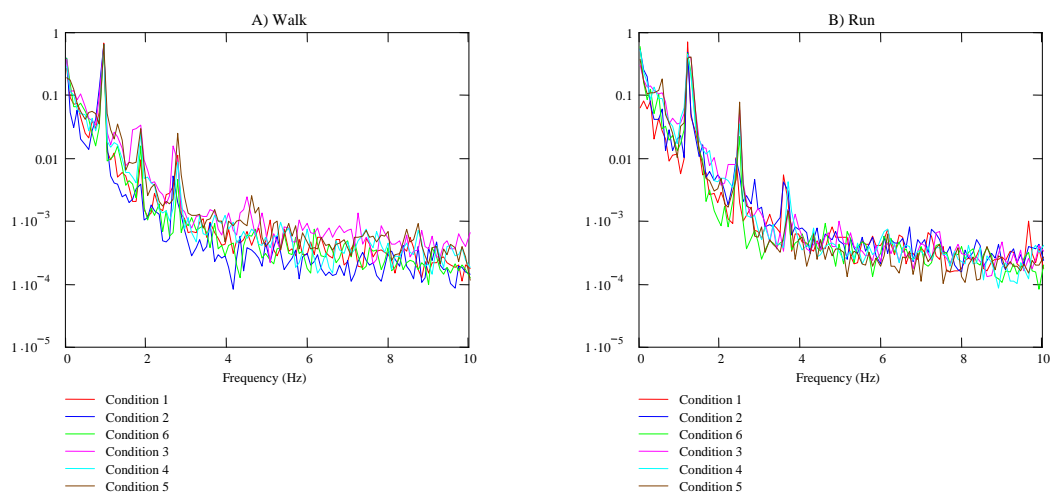


**Figure 49: Representative Normalized Power Spectrum Density of Head Yaw Rotation A) Walking B) Running**



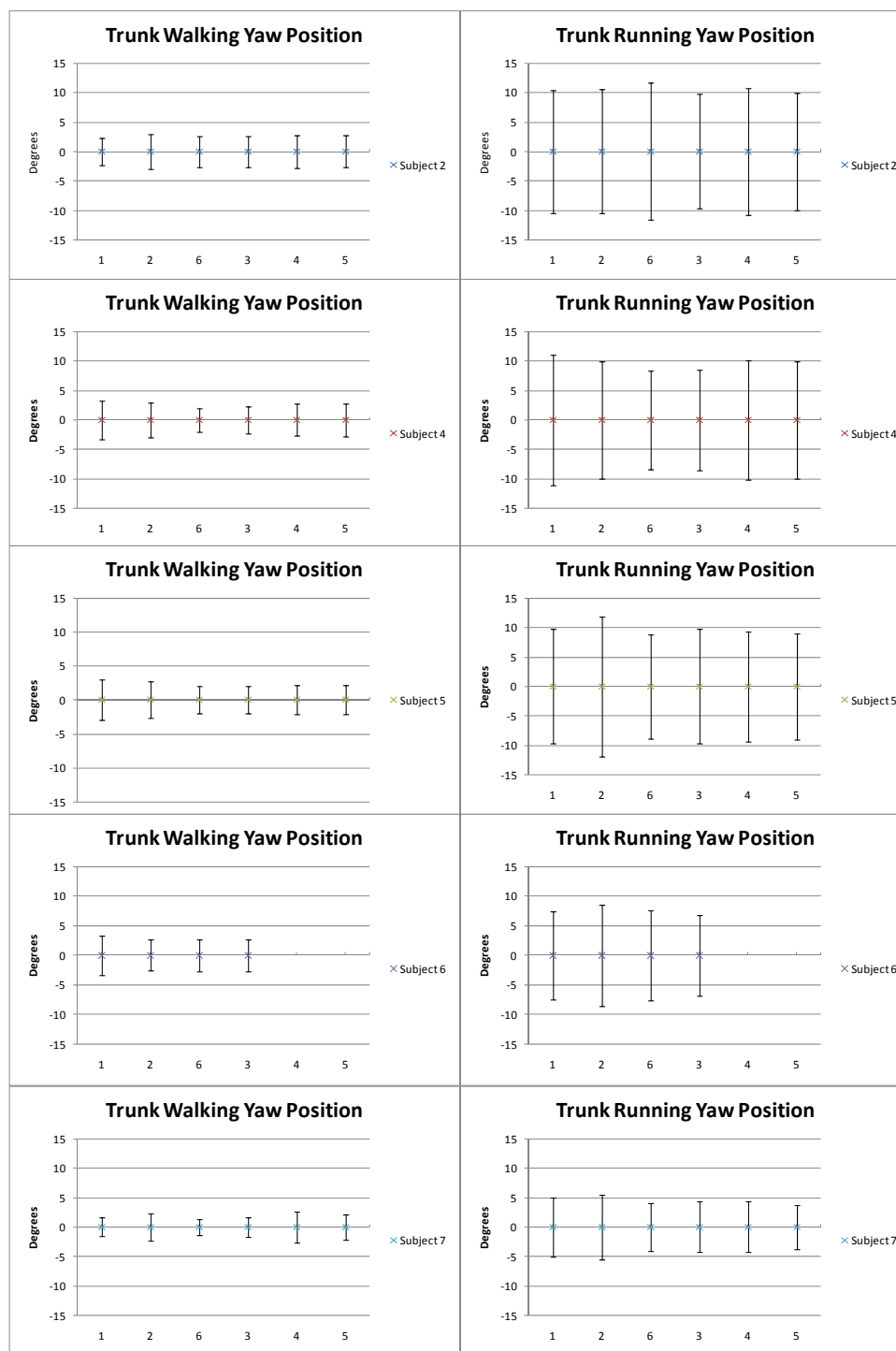


**Figure 50: Mean Walking and Running Trunk Yaw Rotation with Standard Deviation**

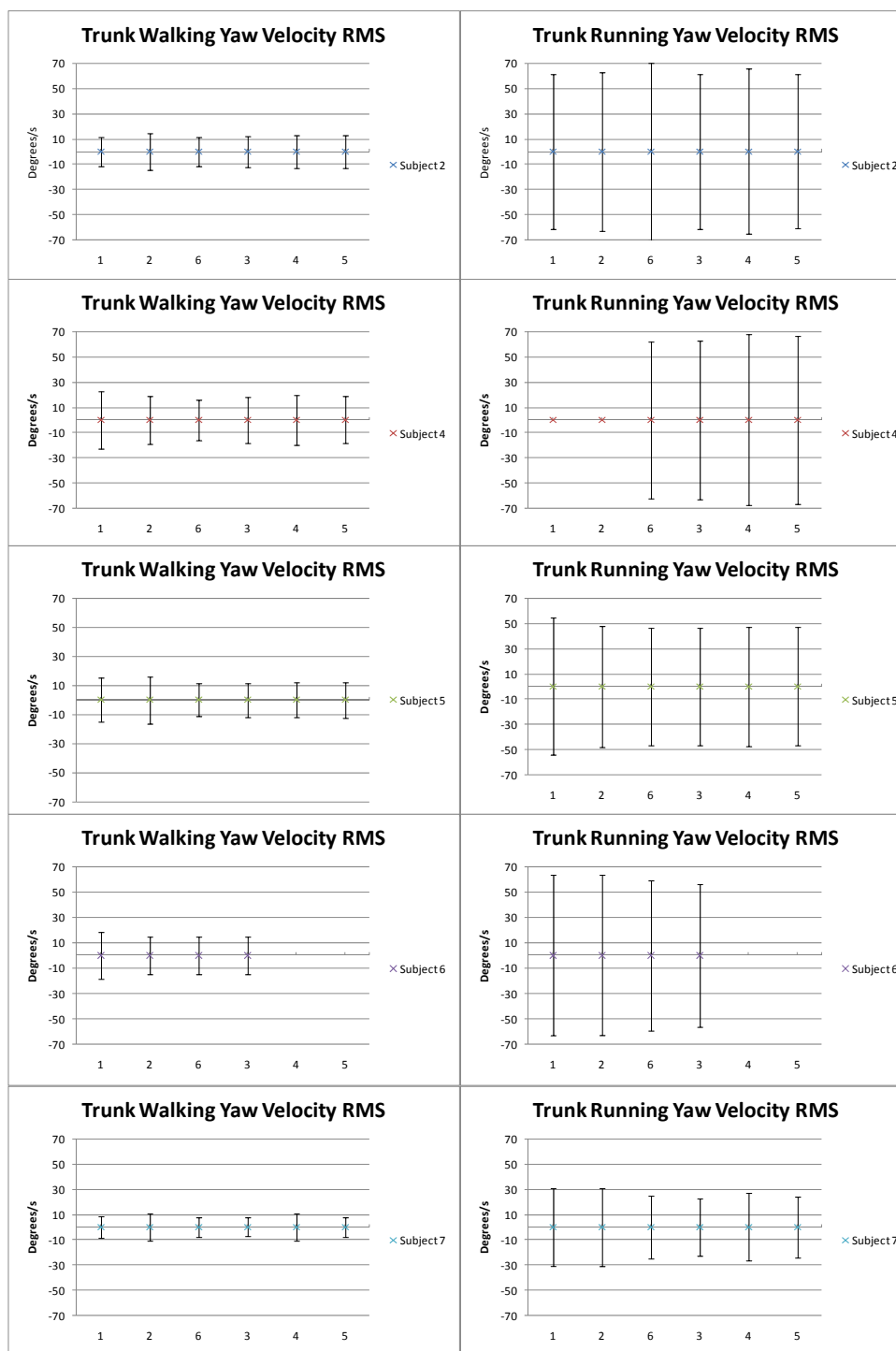


**Figure 51: Mean Walking and Running Yaw Trunk Rotational Velocity with Root Mean Square**

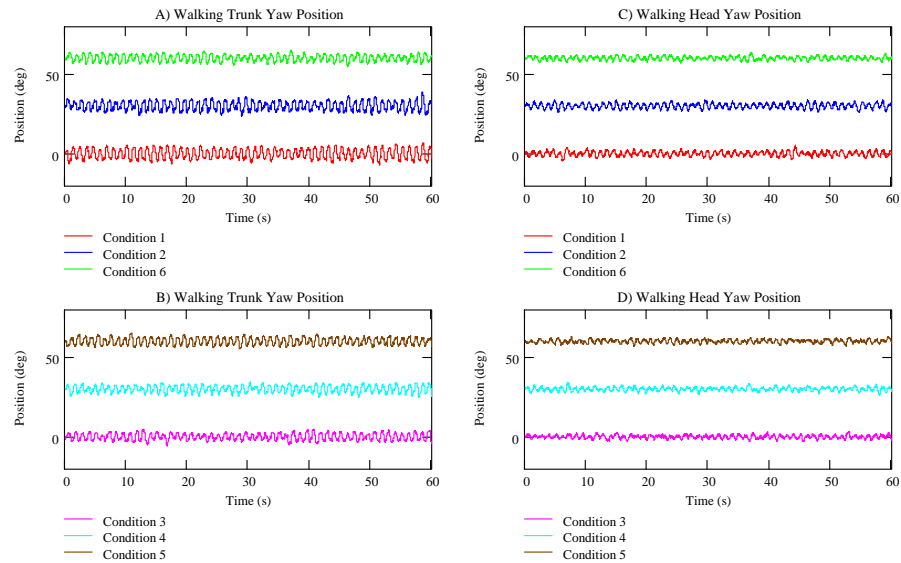


**Figure 52: Walking Yaw Rotation with Moving Average Removed A) Trunk Conditions 1, 2, 6; B) Trunk Conditions 3, 4, 5; C) Head Conditions 1, 2, 6 D) Head Conditions 3, 4, 5. The plots are all zero mean but offset for comparison purposes.**

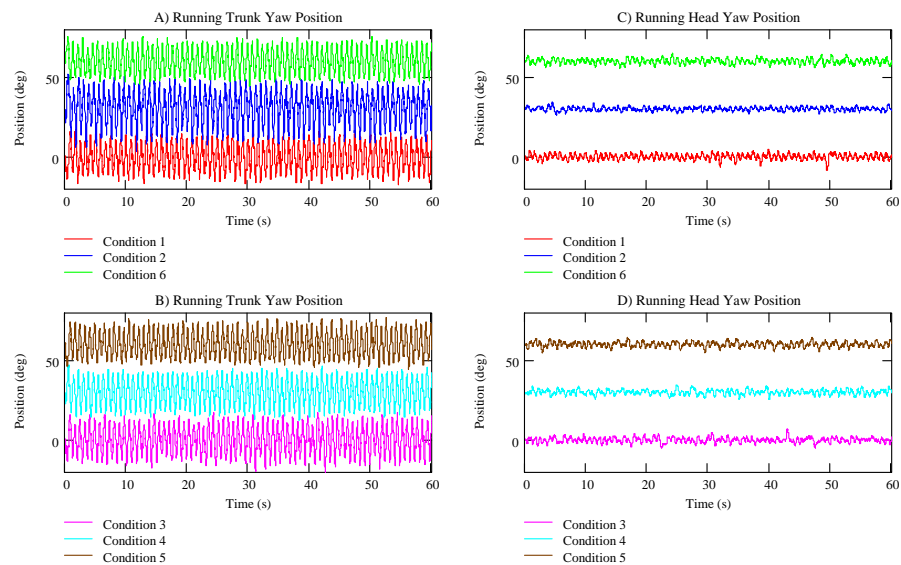


**Figure 53: Running Yaw Rotation with Moving Average Removed A) Trunk Conditions 1, 2, 6; B) Trunk Conditions 3, 4, 5; C) Head Conditions 1, 2, 6 D) Head Conditions 3, 4, 5. The plots are all zero mean but offset for comparison purposes.**

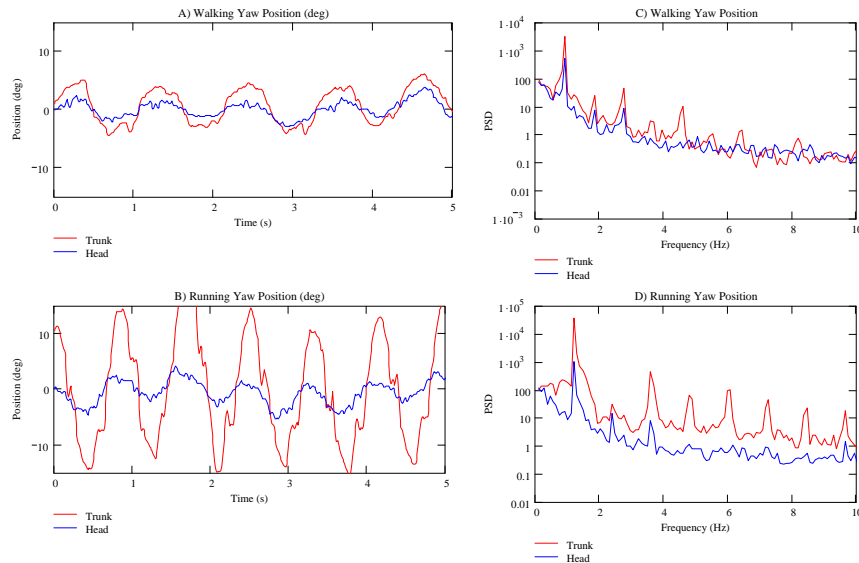


**Figure 54: Yaw Position A) Walking B) Running. Frequency Analysis C) Walking D) Running**

### 3.4 Roll Motion

Both the head and the trunk exhibited roll motion during walking and running. The roll motion of the trunk comes from the effect of the body leaning side to side as each foot comes down and this motion provides a direct input in to the motion of the head.

Looking at the roll motion of the head and the trunk allows us to see how much the neck musculature is compensating for the input from the trunk in order to maintain stable vision. The standard deviation of the roll position in degrees gives a good assessment of the relative magnitudes of roll across the different conditions while walking and running.

The results showed that the roll motion of the head was similar across the conditions and the roll motion of the trunk was almost always higher than that of the head.

The standard deviation of roll rotation did not vary greatly across the conditions with standard deviations for each subject staying within a  $1.1^\circ$  range across all of the conditions for both walking and running. Standard deviation of the roll rotation ranged from  $0.9^\circ$  to  $1.6^\circ$  for walking and from  $1.1^\circ$  to  $2.7^\circ$  for running. There was no correlation between roll motion and mass, moment of inertia, or torque applied. Root mean square velocity also stayed fairly consistent across the conditions and did not exhibit a dependency on mass, moment of inertia, or torque applied (Figure 55, Figure 56). Power spectral analysis of the roll motion showed similar spectra across the conditions with no consistent change in the maximum power or drop-off rate across the subjects. Power was concentrated at half the footfall rate (Figure 57). Probability density functions were similar across the conditions (Figure 58).

Trunk positions and velocities showed variations across the conditions but did not show any correlation to mass, moment of inertia, or torque applied (Figure 59, Figure 60).

While walking the pitch standard deviation of the head position was equal to or lower than that of the trunk for nineteen of the twenty-eight trials and it was lower for running it was lower in twenty-seven of the twenty-eight trials. While running the standard deviation of roll position of the trunk was generally much greater than that of the head (Figure 61, Figure 62, Figure 63).

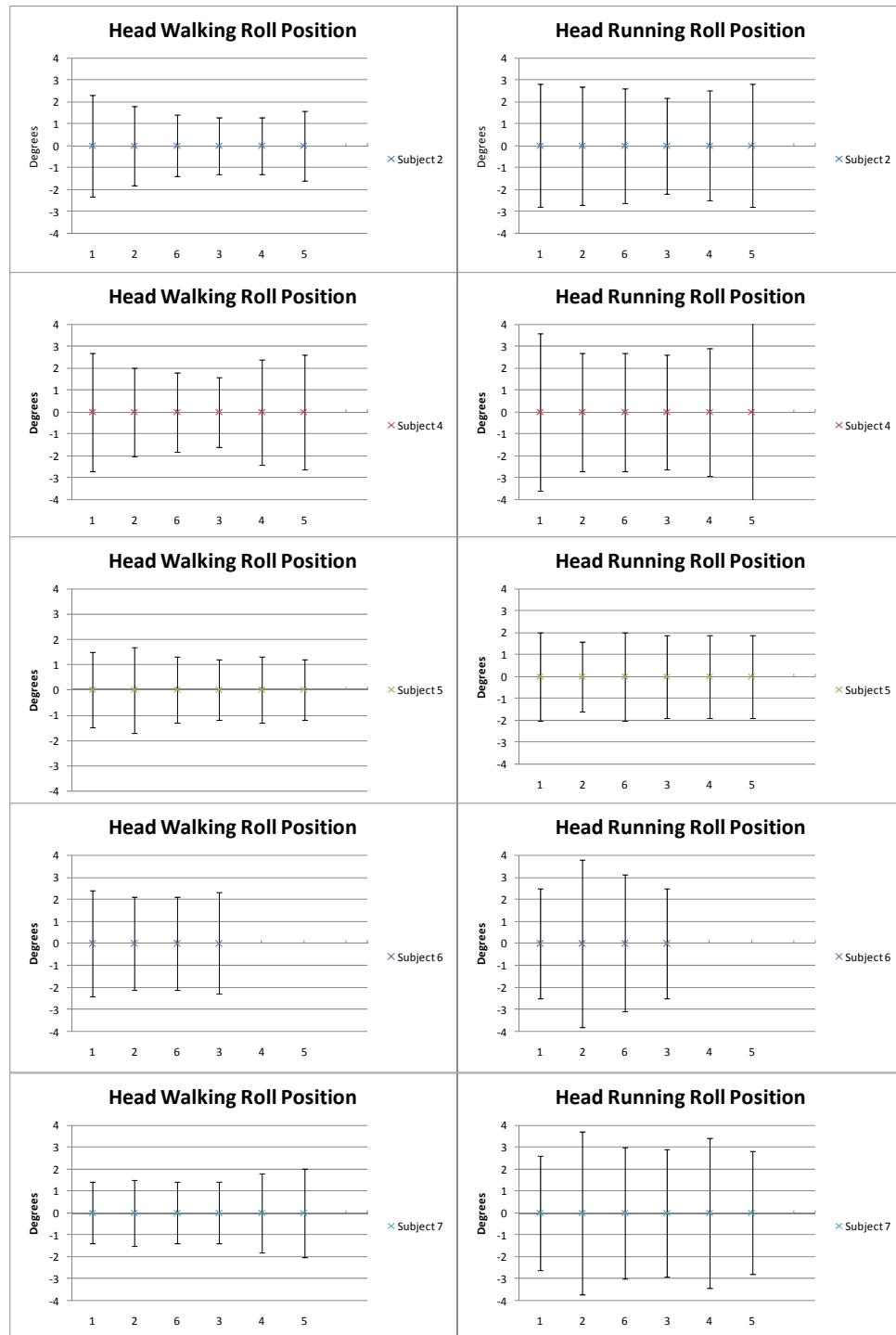


**Figure 55: Mean Walking and Running Head Roll Rotation with Standard Deviation**

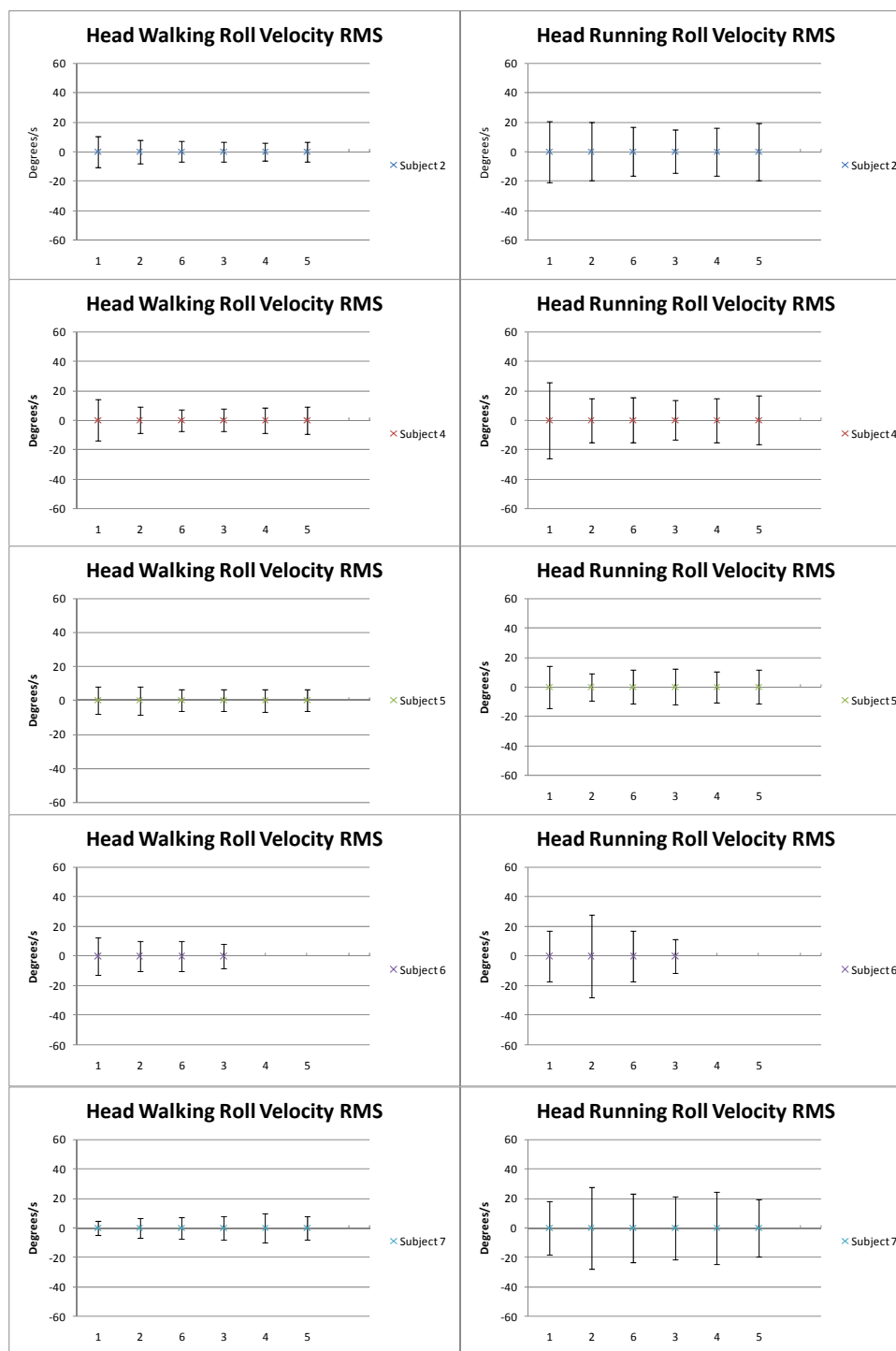


**Figure 56: Mean Walking and Running Roll Head Rotational Velocity with Root Mean Square**

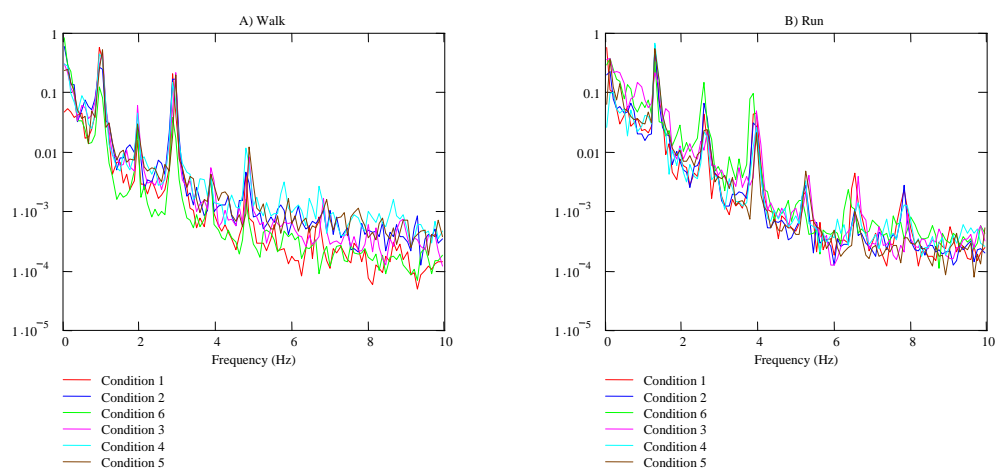


**Figure 57: Representative Normalized Power Spectrum Density of Head Roll Rotation A) Walking B) Running**



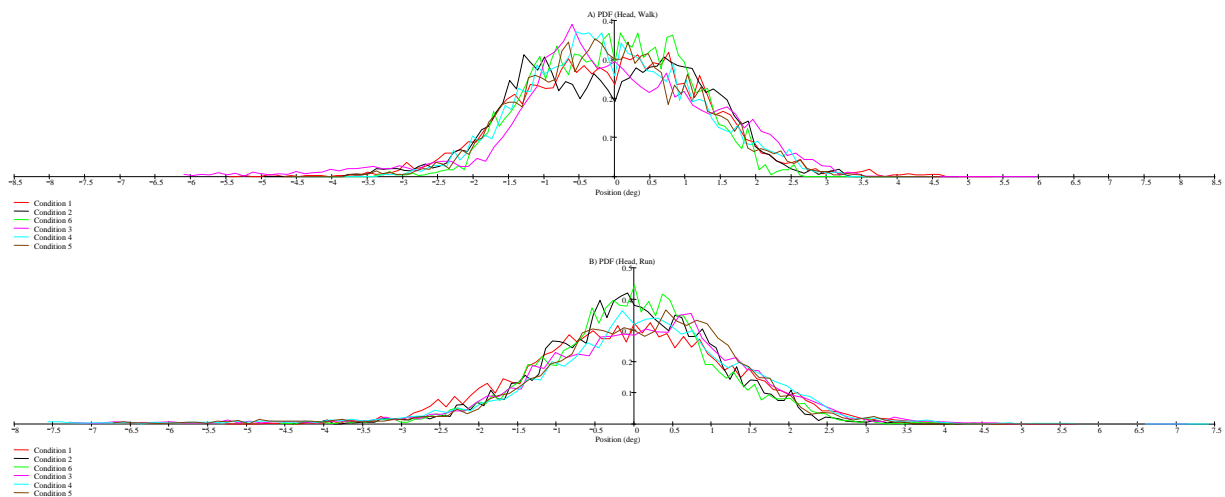


**Figure 58: Representative Probability Distribution Function of Head Roll Rotation around moving average A) Walking B) Running**

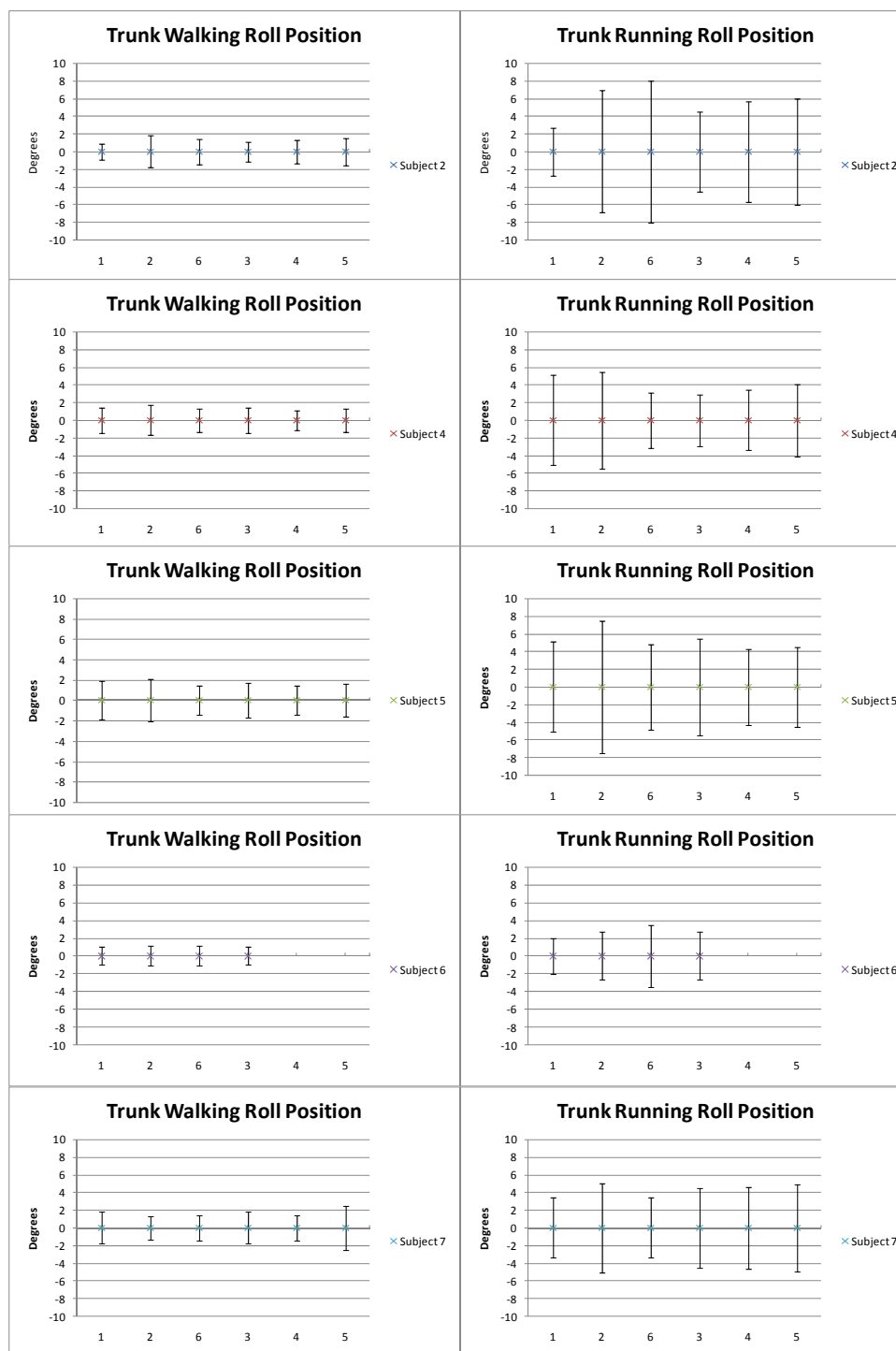


**Figure 59: Mean Walking and Running Trunk Roll Rotation with Standard Deviation**

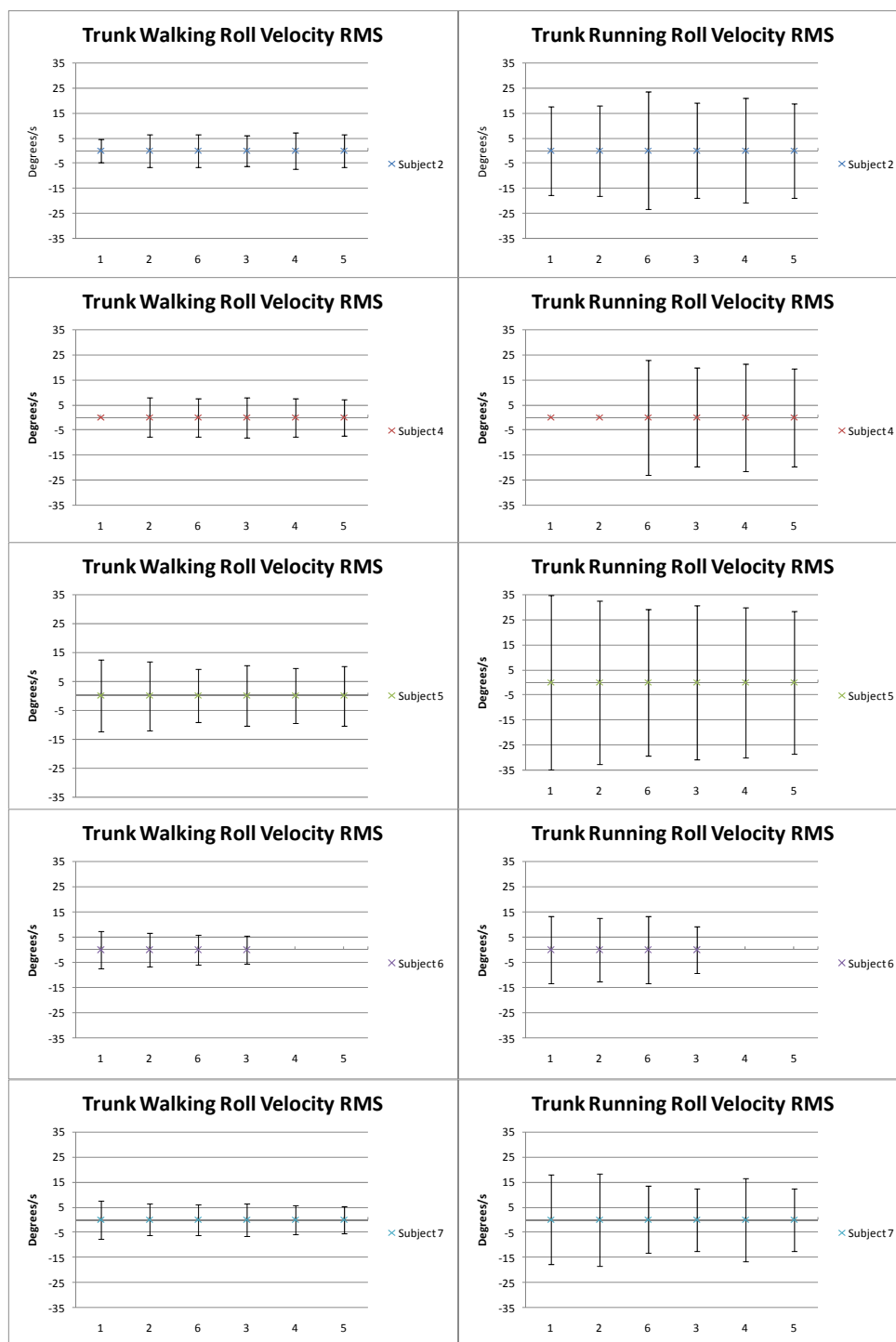


**Figure 60: Mean Walking and Running Roll Trunk Rotational Velocity with Root Mean Square**

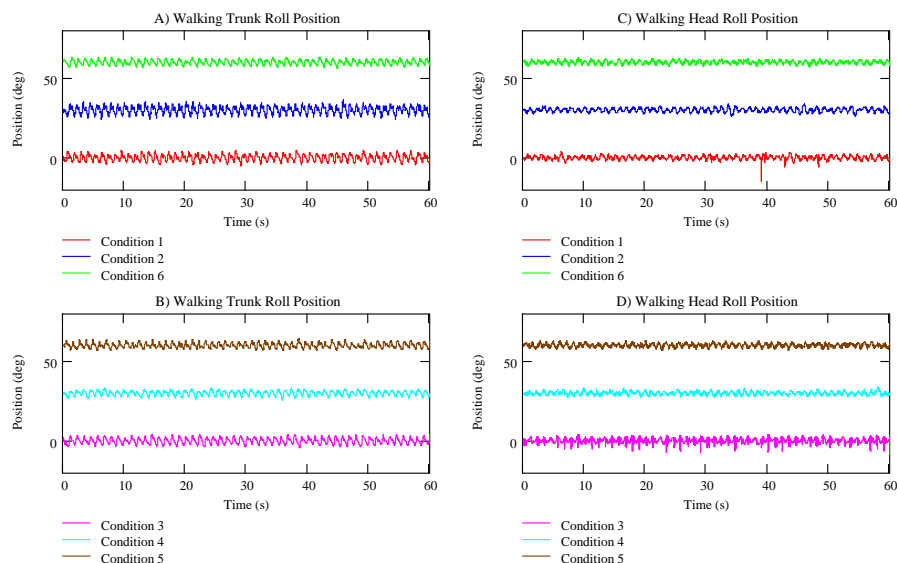


**Figure 61: Walking Roll Rotation with Moving Average Removed A) Trunk Conditions 1, 2, 6; B) Trunk Conditions 3, 4, 5; C) Head Conditions 1, 2, 6 D) Head Conditions 3, 4, 5. The plots are all zero mean but offset for comparison purposes.**

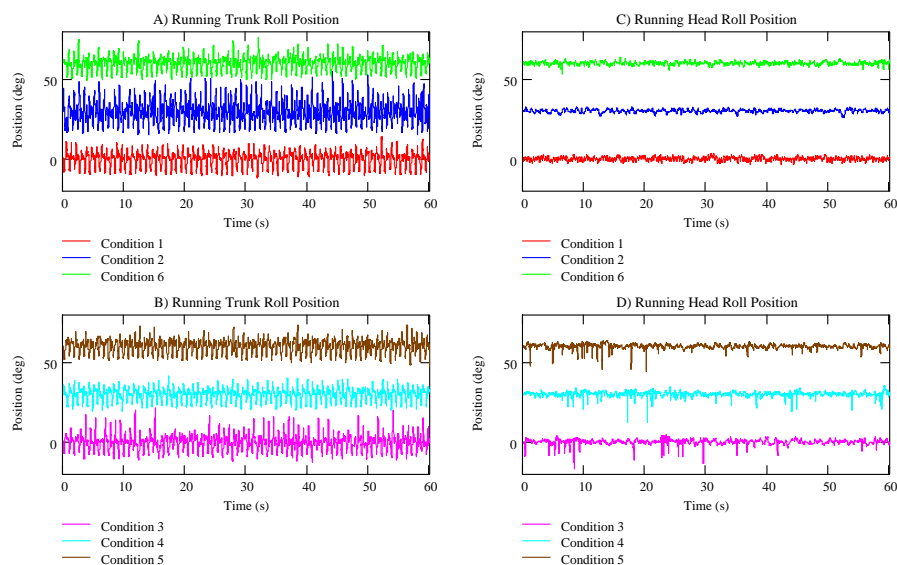


**Figure 62: Running Roll Rotation with Moving Average Removed A) Trunk Conditions 1, 2, 6; B) Trunk Conditions 3, 4, 5; C) Head Conditions 1, 2, 6 D) Head Conditions 3, 4, 5. The plots are all zero mean but offset for comparison purposes.**

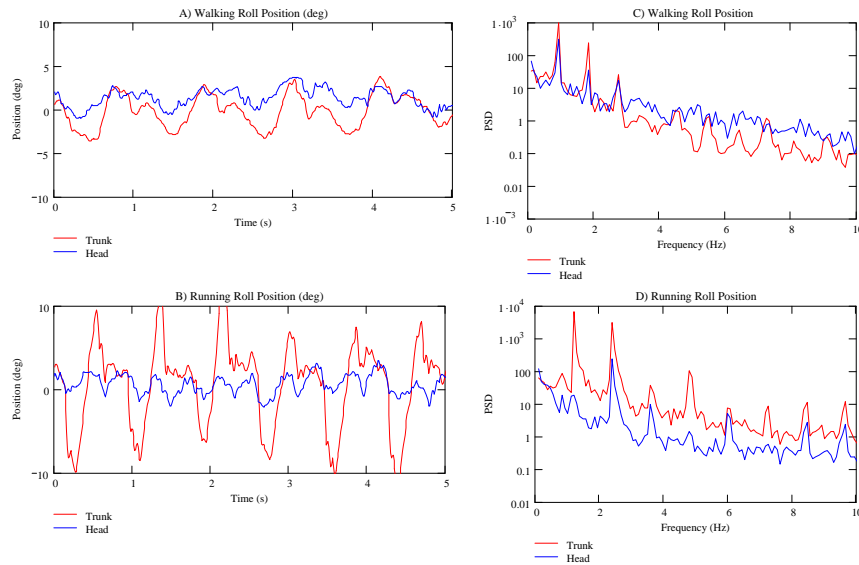


**Figure 63: Roll Position A) Walking B) Running. Frequency Analysis C) Walking D) Running**

### 3.5 Z-Direction Motion

During running and walking the trunk moves up and down with the footfalls and the head moves along with the trunk. Comparing the relative magnitudes of the Z-direction motions of the head and trunk gives an indication of how much of the trunk motion is translated in to head motion.

Standard deviations of Z-direction position and root mean square of accelerations of the head and trunk remained similar across the conditions with no correlation between Z-direction motions and increasing mass, moment of inertia, or torque applied (Figure 64, Figure 65, Figure 69, Figure 70). The standard deviation of the Z-direction position for the head stayed within a 7mm range for the head and an 8mm range for the trunk indicating little change in the motion of the head and trunk. The power spectral density

of the head Z-position showed that the power is concentrated at the footfall frequency with very little change between the conditions (Figure 68).

Across the walking and running conditions it was found that the displacement of the head was always less than that of the trunk in the Z-Direction. The same was true for the acceleration of the head and trunk in the Z-Direction.

The motion of the head and trunk were in phase and both had similar power spectrums with higher power at the peaks for the trunk (Figure 71).

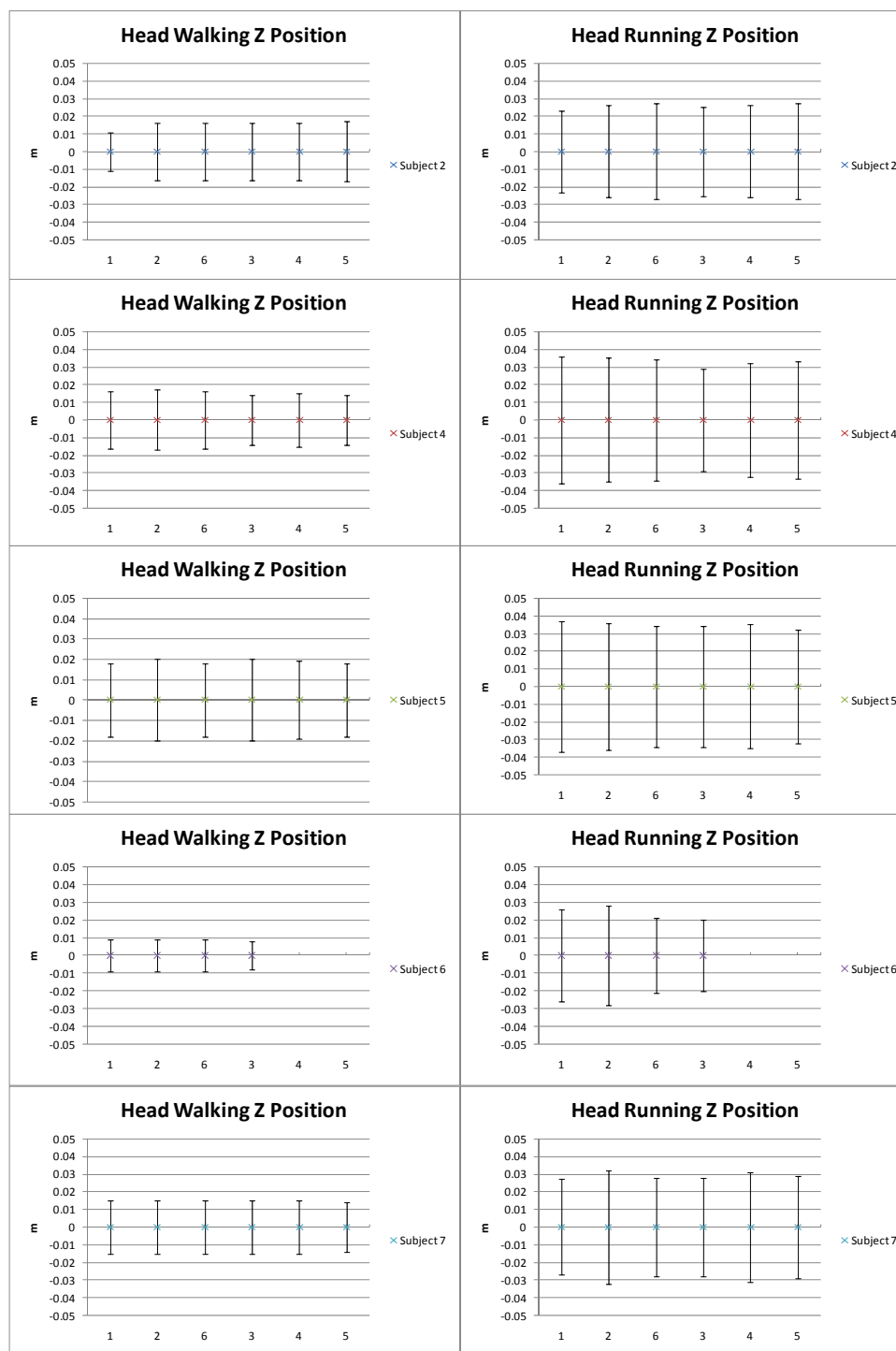
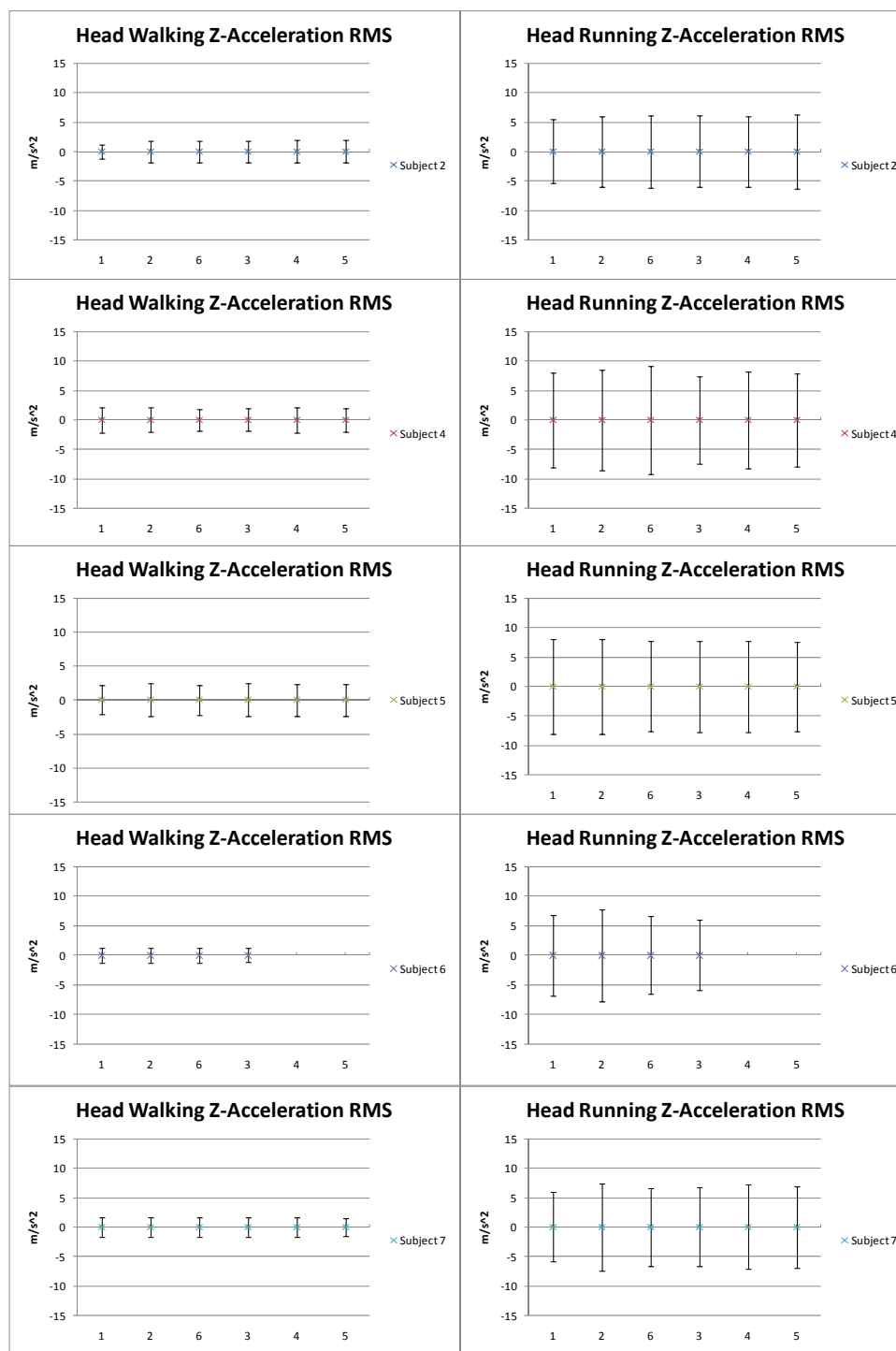
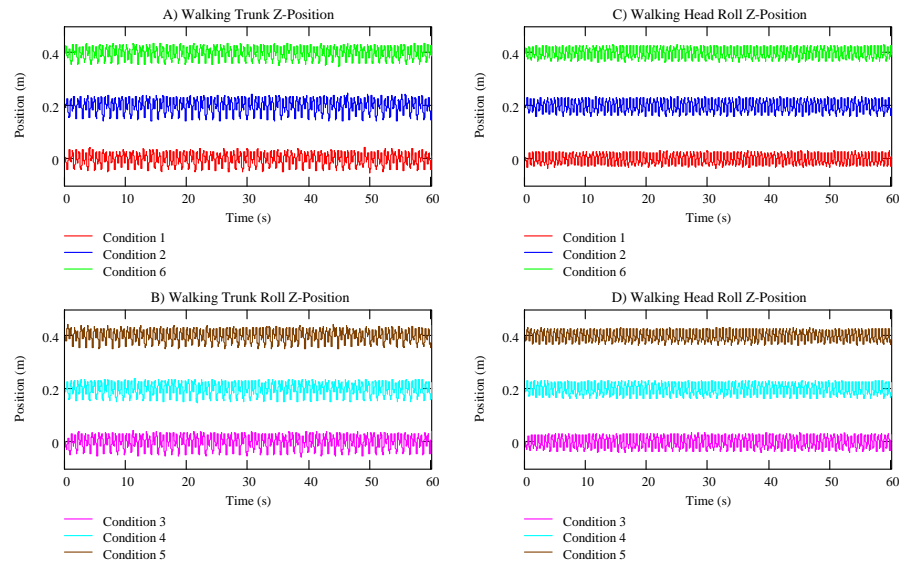


Figure 64: Walking and Running Head Z-Position Standard Deviation



**Figure 65: Mean Walking and Running Head Z-Acceleration with Root Mean Square**





**Figure 66: Zero-Mean walking Z-direction position A) Trunk Conditions 1, 2, 6; B) Trunk Conditions 3, 4, 5; C) Head Conditions 1, 2, 6 D) Head Conditions 3, 4, 5. The plots are all zero mean but offset for comparison purposes.**

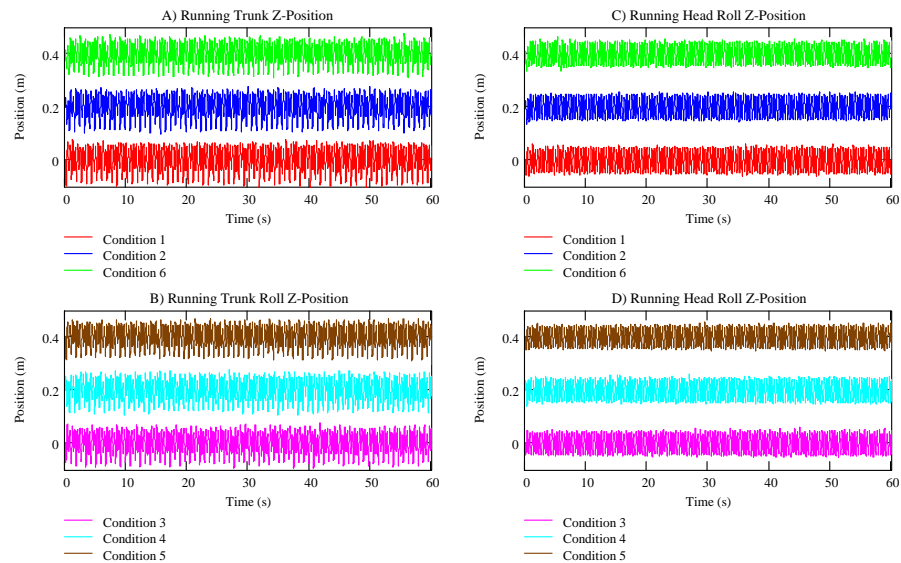


**Figure 67: Zero-Mean running Z-direction position A) Trunk Conditions 1, 2, 6; B) Trunk Conditions 3, 4, 5; C) Head Conditions 1, 2, 6 D) Head Conditions 3, 4, 5. The plots are all zero mean but offset for comparison purposes.**

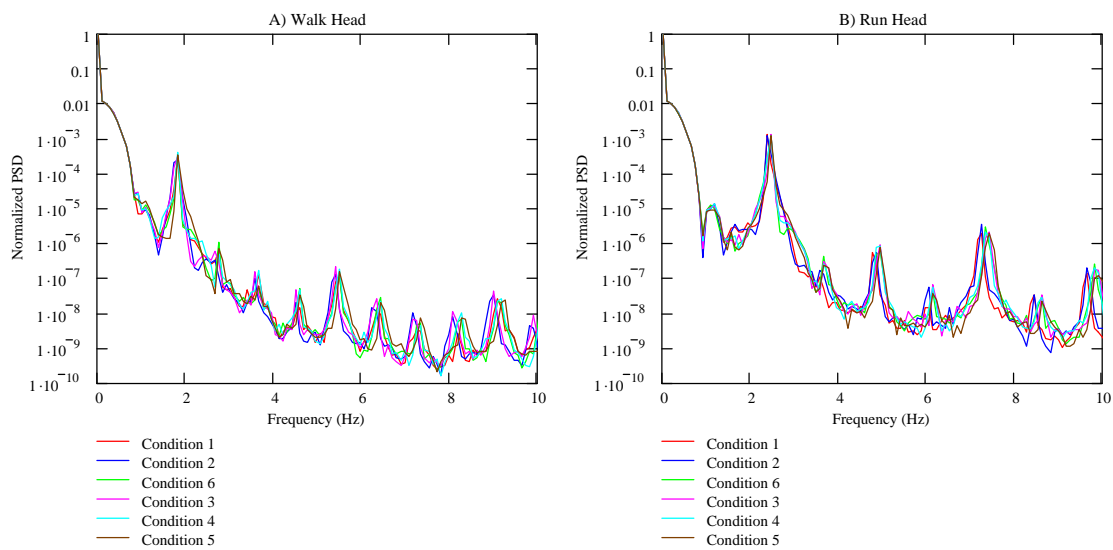


**Figure 68: Power Spectral Density of Head Z-Position while A) Walking and B) Running**

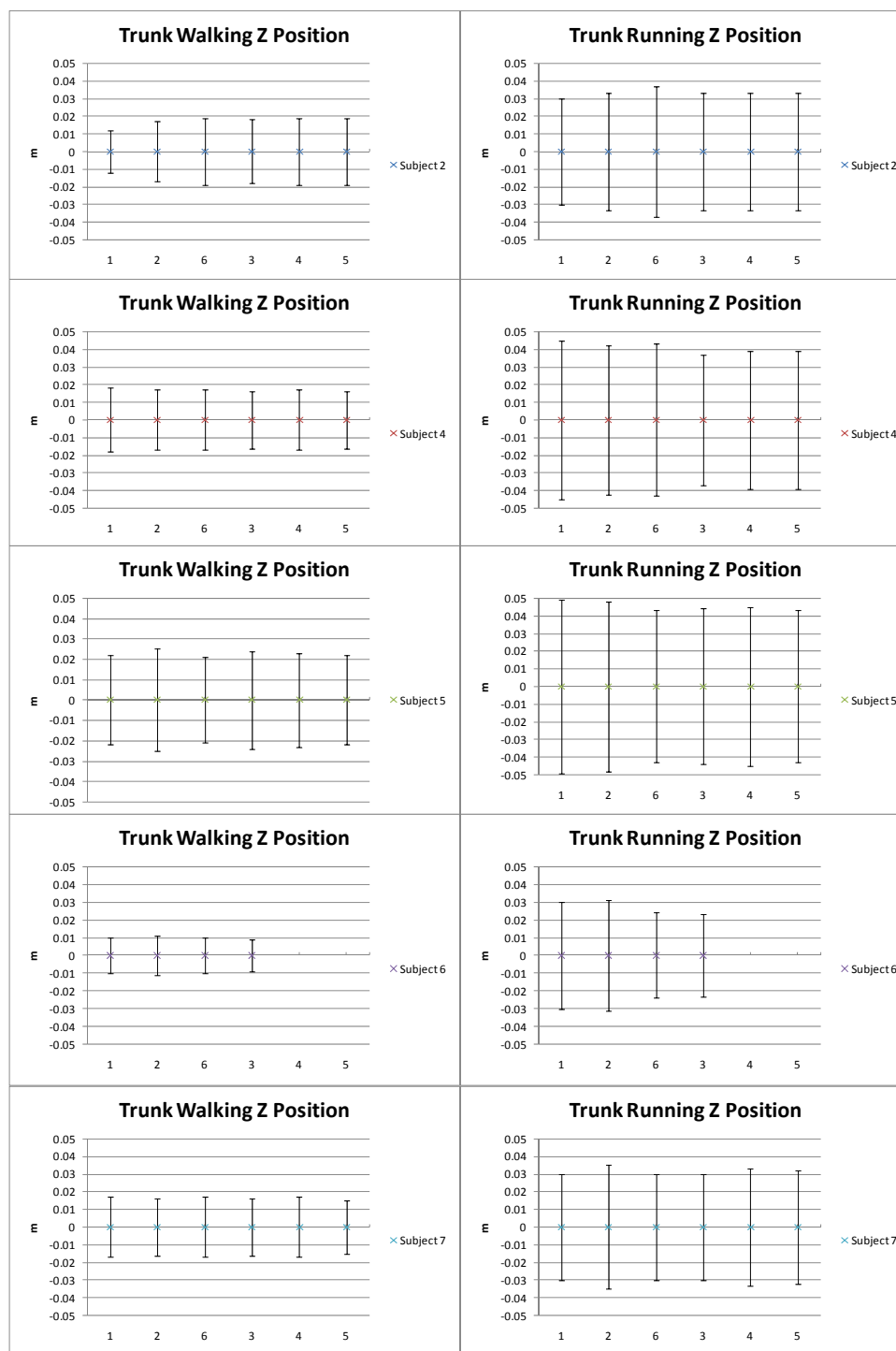


**Figure 69: Walking and Running Trunk Z-Position Standard Deviation**

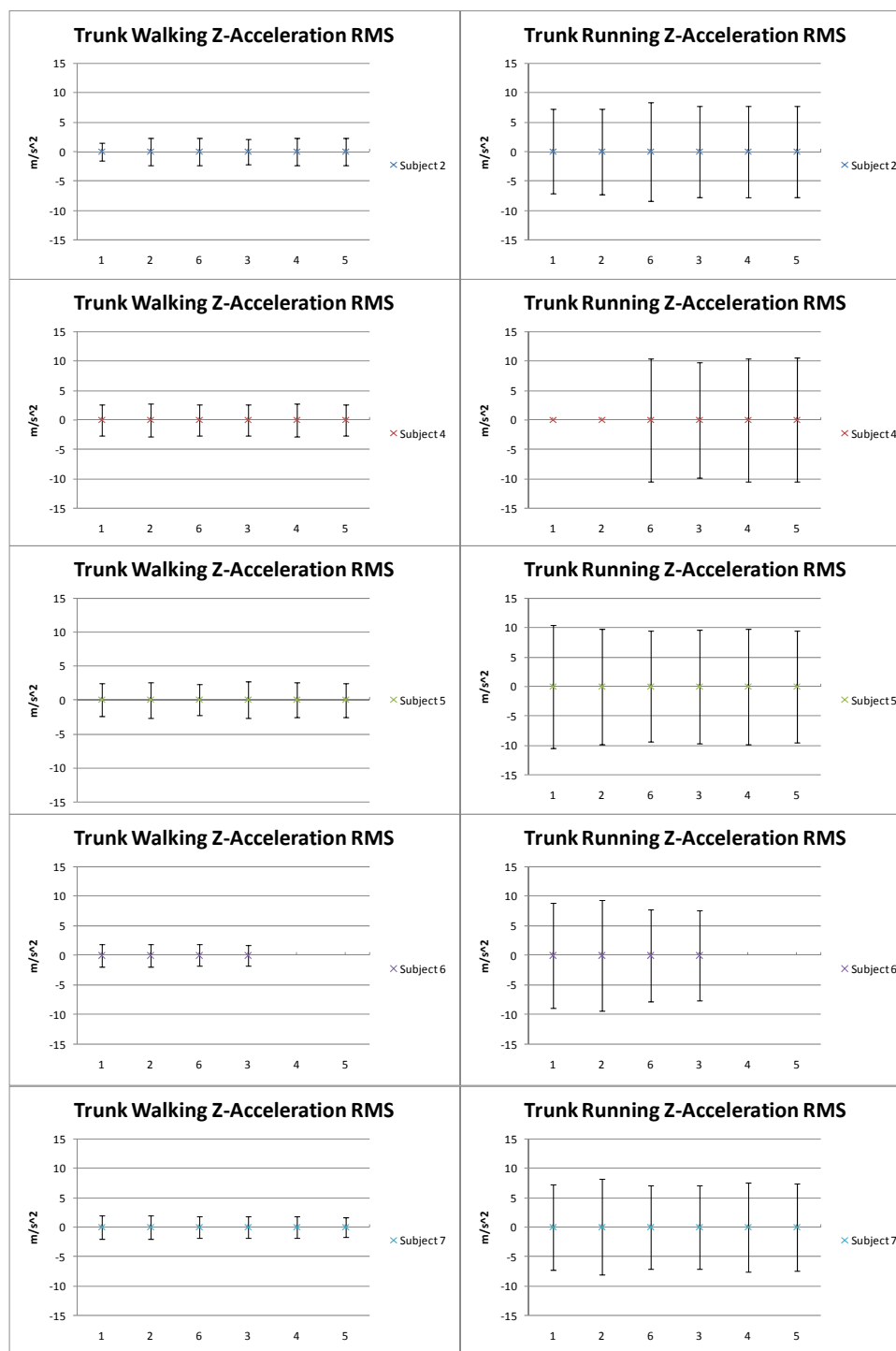


**Figure 70: Mean Walking and Running Trunk Z-Acceleration with Root Mean Square**

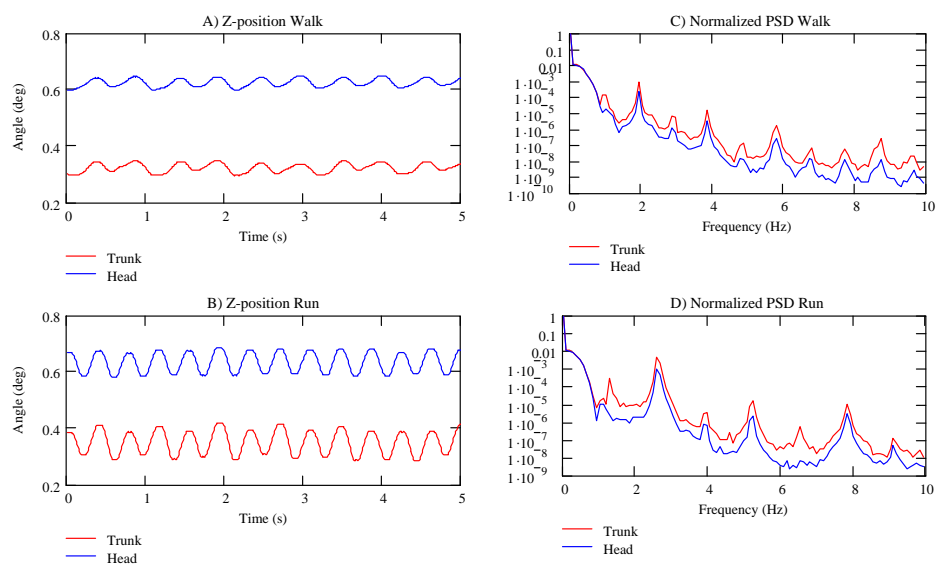


**Figure 71: Z-position A) Walking B) Running. Frequency Analysis C) Walking D) Running**

## CHAPTER 4: DISCUSSION

Across the conditions and subjects there were changes in the motions of the head and trunk but they were generally not very significant and there was no correlation between the changes and increases in mass, moment of inertia, or torque applied. It was expected that the application of a mass would have an effect on the magnitude and frequency content of position, velocity, and acceleration of the head but these changes were not evident.

When adding a significant amount of mass to the head it would be expected that there would be changes in the positioning and motions of the head in space with a consistent input from the trunk. An increase in the moment of inertia results in an object having a greater resistance to change in rotational velocity. If the system were passive, such as a second-order system, and not resonant it would be expected that as the moment of inertia increased subjects would exhibit lower rotational velocities of the head and decreased overall movement so lower standard deviations of position. Since the masses added were in the sagittal plane these changes should have been most evident in the pitch rotation of the head. Results showed that the pitch motion of the head did not change significantly across the conditions despite increasing the moment of inertia from  $0.028 \text{ kg}\cdot\text{m}^2$  to  $0.113 \text{ kg}\cdot\text{m}^2$ . Subjects in general held their heads between  $-20^\circ$  and  $20^\circ$  when looking at the target and moved their heads through a variety of positions throughout the trials. During one trial the moving average of the subject's trunk pitch rotation moved between  $-2^\circ$  and

4° while the head moved between -8° and 8° (Figure 72). It was seen that the position of the head could vary considerably throughout the sixty second of the run and the changes were not just for short periods but were actually positions which the subject held their head at for a significant period of time.

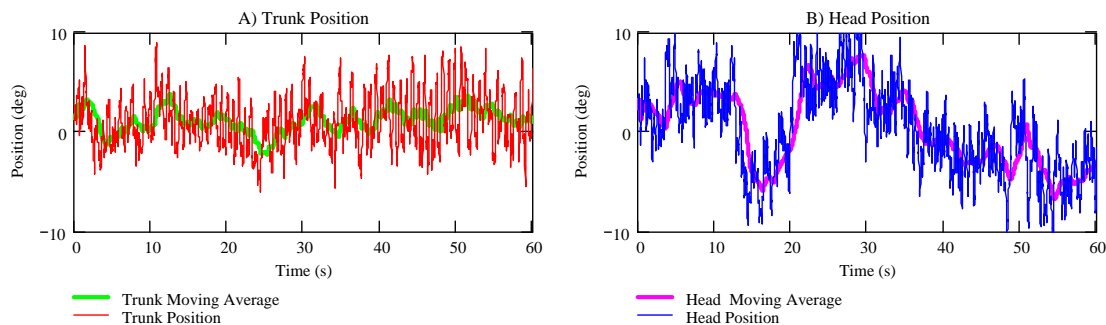


**Figure 72: Pitch Position and Moving Average for A) Trunk and B) Head**

Increasing the torque applied was expected to result in changes in the mean position of the head in space because the additional mass would pull the head forward and/or perhaps the subjects would pull their head back to compensate for the torque applied. The three balanced conditions applied no torque to the head but the three unbalanced conditions all applied a torque. For the unbalanced conditions we would expect the mean pitch angle of the head to be brought forward from the three balanced conditions. However, there was no evidence that additional torque pulled the head forward.

The preliminary data collected indicated that subjects compensated for the addition of mass by changing head position, trunk position, and footfall rate. In particular it was seen that the subjects moved their heads further back with an increase in the amount of torque applied. This change was not seen in the data collected with very little changes evident across the conditions.

The mean pitch position of the head was shown to change throughout each of the runs indicating that subjects were comfortable holding their head in various positions and the standard deviation around the moving mean for the head remained fairly consistent across the conditions for both walking and running indicating that the neck musculature is able to compensate for changes in the motion of the trunk to keep a consistent motion for the head. The small standard deviations of the head motion indicate that a stable platform for vision is being maintained despite the changes to the external load.

Yaw rotation of the trunk occurs when walking and running and the yaw motions of the trunk were almost always higher than those of the head indicating that the subjects were controlling the yaw motion of the head. Yaw motion of the head increased when running compared to walking but not nearly as much as the increase shown by the trunk. Since a high yaw motion would make it harder for subjects to watch the visual target controlling these motions is important and the neck musculature appears to be able to compensate for the much greater input from the trunk.

Roll motions of the head and trunk were similar across all the conditions with the trunk roll motion always higher than the head during running. During the running trials the



large difference between trunk and head movement showed that the compensatory mechanisms are controlling the head motion to maintain a stable platform for vision.

Analysis of the Z-position and acceleration of the head and trunks showed that the head exhibits less motion than the trunk and since there is no greater movement in pitch it can be assumed that this reduced motion is because of a damping factor in neck as opposed to the up and down motion being translated in to a pitch rotation.

Subjects were asked to report back after the trials were complete as to how difficult each of the conditions made running. Each one of the subjects reported that the unbalanced conditions were more tiring and that the use of the counterbalance in Condition 6 made the run easier. One subject did not feel comfortable running with the heavier masses of Conditions 4 and 5 so did not complete those trials indicating that despite the lack of changes to the motions the subjects were aware of the changes which were made and found that applying a torque made running a more difficult task.

Overall the lack of significant changes in head motion across the conditions indicates that neck musculature is controlling head motions despite changes to the mass, moment of inertia, and torque applied to the head. This shows that the head-neck system is not purely passive, but instead actively compensates for changes which are made in order to control head motions and maintain a stable platform for vision. Changes in motions when moving from walking to running were significant for the trunk but much smaller changes in head motions were observed indicating that the muscular control system is actively working to compensate for the much greater input from the trunk.

#### **4.1 Limitations and Assumptions**

The data presented helps give an understanding of how the neck musculature is able to control for a variety of inputs in order to maintain a stable platform for vision. However, assumptions needed to be made about the setup in order to make conclusions about the positioning and motions of the head and trunk. A major assumption is that the alignment of the sensors is correct to allow for comparison between conditions. A bubble level was used to ensure that the mounting of the IRLEDs and ADIS16350 was consistent and they were aligned in the same plane. Slight changes in the attachment of the sensors could result in small changes to the reported angles of the head and trunk and lead to inconclusive results. Hence, reported mean pitch positions could be offset by a few degrees because of differences in how the sensors were mounted.

## CHAPTER 5: CONCLUSIONS AND FUTURE WORK

The data presented shows clearly that the neck musculature is able to control for changes in input from the trunk and changes to the mass, moment of inertia, and torque applied to the head. The trend across the data was that there were very few changes in how the head moves despite the large changes made across the conditions. While this does not support the first hypothesis because there were no consistent changes evident from the data, it does support the second hypothesis that the neck musculature is able to compensate for the changes in the system. The changes which were applied were significant with the moment of inertia and torque applied starting at  $0.028 \text{ kg}\cdot\text{m}^2$  and  $0 \text{ N}\cdot\text{m}$  for Condition 1 and increasing all the way up to  $0.113 \text{ kg}\cdot\text{m}^2$  and  $2.206 \text{ N}\cdot\text{m}$  for Condition 5.

Since the motions of the head and trunk did not change significantly despite these significant changes to the system it can be concluded that the neck musculature is able to compensate for significant changes in order to ensure that the motions of the head stay within a comfortable zone where subjects are able to maintain stable vision.

While there were not significant changes noticed across the conditions the subjects reported that the use of a counterbalance was very effective in reducing the amount of discomfort felt during the trials. This finding implies that the application of a torque to the head would result in greater fatigue and should be used by designers of head mounted equipment.

## **5.1 Future Work**

While the results from this research have provided some valuable insights in to the effect of added mass on the dynamic motions of the head and trunk during running and walking there are areas where the research can be improved and expanded to obtain more valuable data.

### **5.1.1 Changes to the Sensor System**

Immediate changes which could be made to the sensor system would include integrating the Optotrak IRLEDs in to the helmet to ensure that they are always positioned in the same orientation. The sensors were mounted on the shoulder pads to ensure that they are moving with the torso as opposed to the arms of the subject but there may have been some movement of the shoulder pads so setting up a new attachment system would ensure that all movement captured is that of the torso.

Advancements in sensor technology allow for more accurate sensors with a variety of on-board algorithms to provide on-board filtering and calculations of heading. An example of this is the MicroStrain 3DM-GX3™-25 which includes a triaxial accelerometer, triaxial gyro, triaxial magnetometer, temperature sensor, and an on-board processor. The addition of a magnetometer to the setup allows for more accurate heading readings and aids in sensor fusion. Initially attempts were made at adding a magnetometer to the current setup but the readings were affected by the motor attached to the treadmill.

The development on a low-power portable sensor system which can be used in the field would be very beneficial to this area of research. Using a low power microcontroller to collect the data from a sensor would eliminate the need for a computer setup and would allow for testing to take place in a variety of conditions such as during a football game.

### **5.1.2 Changes to the Testing Protocol**

While the testing conditions used during this research provide a good initial picture of the effect of mass on the dynamic motions of the head and the trunk there are more conditions which could be tested to give a complete picture of these effects. These testing conditions could include the addition of a mass offset from the sagittal plane which may induce greater changes in roll and yaw. Since the current masses were symmetrical about the sagittal plane the anticipated changes should have been in the pitch motions of the head and trunk with few changes in yaw and roll motions. Additional testing conditions might include the addition of mass to the back of the head on its own rather than as a counterbalance and the addition of mass which has no effect on the center of gravity such as heavier helmets with a center of gravity which lines up with that of the head.

Extending the length of each trial run would allow for the effect of fatigue to be assessed as the neck muscles would be working for a longer period and would be less likely to be able to compensate for the changes in mass, moment of inertia, and torque applied.

Additionally, adding even greater masses to the head could lead to subjects being unable to control for the changes and give an understanding of what the limits are for head

mounted loads. If evidence of fatigue is found then the use of external devices such as a cervical spine protective device to help limit motions of the head could be included as a testing condition to evaluate the potential benefits of artificially controlling head movements (18).

### List of References

1. Ashrafiuon, H., N. Alem, et al. (1997). "Effects of weight and center of gravity location of head-supported devices on neck loading." Aviat Space Environ Med **68**(10): 915-22.
2. Bhattacharya, A., E. P. McCutcheon, et al. (1980). "Body acceleration distribution and O<sub>2</sub> uptake in humans during running and jumping." J Appl Physiol **49**(5): 881-887.
3. Buhrman, J., Perry C., (1994). "Human and manikin head/neck response to +Gz acceleration when encumbered by helmets of various weights." Aviat Space Environ Med **65**(12): 1086-90.
4. Crane, B., Demer J., (1997). "Human gaze stabilization during natural activities: translation, rotation, magnification, and target distance effects." Journal of Neurophysiology **78**: 2129-2144.
5. Cromwell, R., Newton, R., Carlton, L., (2001). "Horizontal plane head stabilization during locomotor tasks." Journal of Motor Behavior **33**: 49
6. Cromwell, R., Schurter, J., et al. (2004). "Head stabilization strategies in the sagittal plane during locomotor tasks." Physiotherapy Research International **9**: 33-42
7. Grossman, G. E., Leigh R. J., et al. (1988). "Frequency and velocity of rotational head perturbations during locomotion." Exp. Brain Res. **70**: 470-476
8. Hämäläinen, O. (1993). "Flight helmet weight, +Gz forces, and neck muscle strain." Aviat Space Environ Med **64**(1): 55-7.
9. Hicheur, H., Vieilledent, S., et al. (2005). "Head motion in humans alternating between straight and curved walking path: Combination of stabilizing and anticipatory orienting movements." Neuroscience Letters **383**: 87-92
10. Hirasaki, E., Moore, S. T., et al. (1999). "Effects of walking velocity on vertical head and body movements during locomotion." Exp. Brain Res. **127**: 117-130
11. Keshner, E. A. (1990). "Controlling Stability of a Complex Movement System." Physical Therapy **70**(12): 98-108
12. Keshner, E. A. (2003). "Head-Trunk Coordination During Linear Anterior-Posterior Translations." J Neurophysiol **89**(4): 1891-1901.

13. Keshner, E. A., T. C. Hain, et al. (1999). "Predicting control mechanisms for human head stabilization by altering the passive mechanics." Journal of Vestibular Research **9**(6): 423-434.
14. Knight, J. F. and C. Baber (2004). "Neck Muscle Activity and Perceived Pain and Discomfort Due to Variations of Head Load and Posture." Aviation, Space, and Environmental Medicine **75**: 123-131.
15. Menz, H. B., Lord, S. R., et al. (2003). "Acceleration patterns of the head and pelvis when walking on level and irregular surfaces." Gait and Posture **18**: 35-46
16. Merkle, A., M. Kleinberger, et al. (2005). "The Effects of Head-Supported Mass on the Risk of Neck Injury in Army Personnel." Johns Hopkins APL Technical Digest **26**(1): 75-83.
17. McEntire, B. J., Shanahan, D. F. (1997). "Mass Requirements for Helicopter Aircrew Helmets." U.S. Army Aeromedical Research Laboratory
18. Milone, M. (2009). "The development of a Cervical Spine Protective Device for Youth Athletes in American Tackle Football" Master's Thesis, Drexel University
19. Nakaza, E. T. (2007). Assessment of Injury Risks Associated with Wearing the Enhanced Combat Helmet and Night Vision Goggle - Driver: Frontal Vehicle Collision Study. School of Safety Science. Sydney, University of New South Wales. **MS**: 166.
20. Oppenheim, A., Schafer, R. (1999). *Discrete-Time Signal Processing*. Upper Saddle River, NJ: Prentice-Hall, Inc.
21. Phillips, C. and J. Petrofsky (1983). "Neck muscle loading and fatigue: systematic variation of headgear weight and center-of-gravity." Aviat Space Environ Med **54**(10): 901-5.
22. Pozzo, T., Berthoz, A., et al. (1990). "Head stabilization during various locomotor tasks in humans." Experimental Brain Research **82**: 97-106
23. Seng, K.-Y., P.-M. Lam, et al. (2003). "Acceleration Effects on Neck Muscle Strength: Pilots vs. Non-Pilots." Aviation, Space, and Environmental Medicine **74**: 164-168.
24. Sovelius, R., J. Oksa, et al. (2008). "Neck Muscle Strain When Wearing Helmet and NVG During Acceleration on a Trampoline." Aviation, Space, and Environmental Medicine **79**: 112-116.



25. Tangorra, J. L., L. A. Jones, et al. (2003). "Dynamics of the Human Head-Neck System in the Horizontal Plane: Joint Properties with Respect to a Static Torque." Annals of Biomedical Engineering **31**(5): 606-620.
26. Thuresson, M., B. ng, et al. (2003). "Neck Muscle Activity in Helicopter Pilots: Effect of Position and Helmet-Mounted Equipment." Aviation, Space, and Environmental Medicine **74**: 527-532.
27. Viviani, P. and A. Berthoz (1975). "Dynamics of the head-neck system in response to small perturbations: Analysis and modeling in the frequency domain." Biological Cybernetics **19**(1): 19-37.
28. Walker, L. B., E. H. Harris, et al. (1973) "Mass, Volume, Center of Mass and Mass Moment of Inertia of Head and Head and Neck of the Human Body." Proc 17th STAPP Car Crash Conference, 525-537.

## Appendix A: Torque and Moment of Inertia Calculations

### Moment of Inertia of Head\*

head :=

	0	1	2
0	$2.835 \cdot 10^3$	$2.54 \cdot 10^5$	$4.47 \cdot 10^5$
1	$4.703 \cdot 10^3$	$2.36 \cdot 10^5$	$5.33 \cdot 10^5$

mass := head<sup><0></sup>

Ihead := head<sup><1></sup>

mass := mass·kg

Ihead := Ihead·gm·cm<sup>2</sup>

avg\_mass := mean(mass)

I<sub>h</sub> := mean(Ihead)

avg\_mass =  $4.376 \times 10^3$  kg

I<sub>h</sub> =  $0.021 \text{kg m}^2$

\*Walker, L. B., E. H. Harris, et al. (1973) "Mass, Volume, Center of Mass and Mass Moment of Inertia of Head and Neck of the Human Body." Proc 17th STAPP Car Crash Conference, 525-537.

### Moment of Inertia of Helmets

$$I = \frac{2 \cdot m \cdot r^2}{3}$$

I - Football Helmet

I - Climbing Helmet

mf := 1.625 kg

mc := 0.475 kg

r := 0.15 m

r := 0.15 m

$$I_f := \frac{2 \cdot m_f \cdot r^2}{3}$$

$$I_c := \frac{2 \cdot m_c \cdot r^2}{3}$$

I<sub>f</sub> =  $0.024 \text{kg m}^2$

I<sub>c</sub> =  $7.125 \times 10^{-3} \text{kg m}^2$

### Moment of Inertia of Additional Masses

$$I = \int r^2 dm$$

$$M := 0.25 \text{ kg}$$

$$d_1 := 0.2 \text{ m} \quad d_2 := 0.3 \text{ m} \quad d_3 := -0.2 \text{ m}$$

$$I_1 := I_h + I_c \quad I_1 = 0.028 \text{ kg m}^2$$

$$I_2 := I_h + I_f \quad I_2 = 0.045 \text{ kg m}^2$$

$$I_3 := I_2 + 3 \cdot M \cdot d_1^2 \quad I_3 = 0.075 \text{ kg m}^2$$

$$I_4 := I_2 + 2 \cdot M \cdot d_2^2 \quad I_4 = 0.09 \text{ kg m}^2$$

$$I_5 := I_2 + 3 \cdot M \cdot d_2^2 \quad I_5 = 0.113 \text{ kg m}^2$$

$$I_6 := I_2 + 3 \cdot M \cdot d_1^2 + 3 \cdot M \cdot d_3^2 \quad I_6 = 0.105 \text{ kg m}^2$$

### Torque Applied by Additional Masses

$$T = F \cdot d$$

$$F = m \cdot g$$

$$T_3 := 3 \cdot M \cdot g \cdot d_1 \quad T_3 = 1.471 \text{ N} \cdot \text{m}$$

$$T_4 := 2 \cdot M \cdot g \cdot d_2 \quad T_4 = 1.471 \text{ N} \cdot \text{m}$$

$$T_5 := 3 \cdot M \cdot g \cdot d_2 \quad T_5 = 2.206 \text{ N} \cdot \text{m}$$

$$T_6 := 3 \cdot M \cdot g \cdot d_1 + 3 \cdot M \cdot g \cdot d_3 \quad T_6 = 0 \text{ N} \cdot \text{m}$$

## **Appendix B: Data Processing Algorithms**

### **B.1 Low Pass Filter**

## B.1 Low Pass Filter (20)

$$\text{ncLPFkaiser}(\Delta t, f_{\text{pb}}, f_{\text{sb}}, \delta) :=$$

$$f_{\text{samp}} \leftarrow \frac{1}{\Delta t}$$

$$\omega_{\text{pb}} \leftarrow (2\pi \Delta t) f_{\text{pb}}$$

$$\omega_{\text{sb}} \leftarrow (2\pi \Delta t) f_{\text{sb}}$$

$$\omega_{\text{co}} \leftarrow \frac{\omega_{\text{pb}} + \omega_{\text{sb}}}{2}$$

$$\omega_{\text{trans}} \leftarrow \omega_{\text{sb}} - \omega_{\text{pb}}$$

$$A \leftarrow -20 \log(\delta)$$

$$M_{\text{min}} \leftarrow \frac{A - 8}{2.285 \omega_{\text{trans}}}$$

$$M \leftarrow \text{floor}(M_{\text{min}} + 1)$$

$$\text{rmdr} \leftarrow \text{mod}(M, 2)$$

$$M \leftarrow (M + 1) \text{ if } |\text{rmdr}| < 0.001$$

$$\beta \leftarrow 0.1102(A - 8.7) \text{ if } A > 50$$

$$\beta \leftarrow 0.5842(A - 21)^{0.4} + 0.07886(A - 21) \text{ if } (A \geq 21) \wedge (A \leq 50)$$

$$\beta \leftarrow 0.0 \text{ if } A < 21$$

$$\text{for } m \in 1.. \frac{M - 1}{2}$$

$$\text{numArg} \leftarrow \beta \cdot \left[ 1 - \left( \frac{2 \cdot m}{M - 1} \right)^2 \right]^{\frac{1}{2}}$$

$$w_{\text{num}} \leftarrow \text{I0}(\text{numArg})$$

$$w_{\text{den}} \leftarrow \text{I0}(\beta)$$

$$h_{\text{kaiser}_m} \leftarrow \frac{w_{\text{num}} \sin(m \cdot \omega_{\text{co}})}{w_{\text{den}} \cdot \pi m}$$

$$h_{\text{kaiser}_0} \leftarrow \frac{\omega_{\text{co}}}{\pi}$$

$$h_{\text{kaiser}}$$

## **Appendix C: Equipment Specification Sheets**

**C.1 ADIS16350**

**C.2 Optotrak 3020**

## C.1 ADIS16350

ADIS16350

## SPECIFICATIONS

$T_A = -40^{\circ}\text{C}$  to  $+85^{\circ}\text{C}$ ,  $V_{CC} = 5.0\text{ V}$ , angular rate =  $0^{\circ}/\text{s}$ , dynamic range  $300^{\circ}/\text{sec}$ ,  $\pm 1\text{ g}$ , unless otherwise noted.  
Table 1.

Parameter	Conditions	Min	Typ	Max	Unit	
GYROSCOPE SENSITIVITY	Each axis					
	Initial	25°C, dynamic range = $\pm 300^{\circ}/\text{s}$	0.0725	0.07326	0.0740	$^{\circ}/\text{s}/\text{LSB}$
		25°C, dynamic range = $\pm 150^{\circ}/\text{s}$		0.03663		$^{\circ}/\text{s}/\text{LSB}$
		25°C, dynamic range = $\pm 75^{\circ}/\text{s}$		0.01832		$^{\circ}/\text{s}/\text{LSB}$
	Temperature Coefficient	See Figure 5		600		ppm/ $^{\circ}\text{C}$
	Gyro Axis Nonorthogonality	25°C, difference from $90^{\circ}$ ideal		$\pm 0.05$		Degree
Gyro Axis Misalignment	25°C, relative to base -plate and guide pins		$\pm 0.5$		Degree	
Nonlinearity	Best fit straight line		0.1		% of FS	
GYROSCOPE BIAS	In Run Bias Stability	25°C, $1\sigma$		0.015		$^{\circ}/\text{s}$
	Angular Random Walk	25°C		4.2		$^{\circ}/\sqrt{\text{hr}}$
	Temperature Coefficient	See Figure 6		0.1		$^{\circ}/\text{s}/^{\circ}\text{C}$
	Linear Acceleration Effect	Any axis, $1\sigma$ , (linear acceleration bias compensation enabled)		0.05		$^{\circ}/\text{s}/\text{g}$
	Voltage Sensitivity	$V_{CC} = 4.75\text{ V}$ to $5.25\text{ V}$		0.25		$^{\circ}/\text{s}/\text{V}$
GYROSCOPE NOISE PERFORMANCE	Output Noise	25°C, $\pm 300^{\circ}/\text{s}$ range, no filtering		0.60		$^{\circ}/\text{s rms}$
		25°C, $\pm 150^{\circ}/\text{s}$ range, 4-tap filter setting		0.35		$^{\circ}/\text{s rms}$
		25°C, $\pm 75^{\circ}/\text{s}$ range, 16-tap filter setting		0.17		$^{\circ}/\text{s rms}$
	Rate Noise Density	25°C, $f = 25\text{ Hz}$ , $\pm 300^{\circ}/\text{s}$ , no filtering		0.05		$^{\circ}/\text{s}/\sqrt{\text{Hz rms}}$
GYROSCOPE FREQUENCY RESPONSE	3 dB Bandwidth		350		Hz	
	Sensor Resonant Frequency		14		kHz	
GYROSCOPE SELF-TEST STATE	Change for Positive Stimulus	$\pm 300^{\circ}/\text{s}$ range setting	432	723	1105	LSB
	Change for Negative Stimulus	$\pm 300^{\circ}/\text{s}$ range setting	-432	-723	-1105	LSB
	Internal Self-Test Cycle Time			25		ms
ACCELEROMETER SENSITIVITY	Each axis					
	Dynamic Range		$\pm 8$	$\pm 10$		g
	Initial	25°C	2.471	2.522	2.572	mg/LSB
	Temperature Coefficient			100		ppm/ $^{\circ}\text{C}$
	Axis Nonorthogonality	25°C, difference from $90^{\circ}$ ideal		$\pm 0.25$		Degree
	Axis Misalignment	25°C, relative to base-plate and guide pins		$\pm 0.5$		Degree
Nonlinearity	Best fit straight line		$\pm 0.2$		% of FS	
ACCELEROMETER BIAS	In-Run Bias Stability	25°C, $1\sigma$		0.7		mg
	Velocity Random Walk	25°C		2.0		m/s/ $\sqrt{\text{hr}}$
	Temperature Coefficient			4		mg/ $^{\circ}\text{C}$
ACCELEROMETER NOISE PERFORMANCE	Output Noise	25°C, no filtering		35		mg rms
	Noise Density	25°C, no filtering		1.85		mg/ $\sqrt{\text{Hz rms}}$
ACCELEROMETER FREQUENCY RESPONSE	3 dB Bandwidth		350		Hz	
	Sensor Resonant Frequency		10		kHz	
ACCELEROMETER SELF-TEST STATE	Output Change When Active		73	146	219	LSB
	TEMPERATURE SENSOR					
Output at 25°C			0		LSB	
Scale Factor			6.88		LSB/ $^{\circ}\text{C}$	

<b>ADIS16350</b>
------------------

Parameter	Conditions	Min	Typ	Max	Unit
<b>ADC INPUT</b>					
Resolution			12		Bits
Integral Nonlinearity			±2		LSB
Differential Nonlinearity			±1		LSB
Offset Error			±4		LSB
Gain Error			±2		LSB
Input Range		0		2.5	V
Input Capacitance	During acquisition		20		pF
<b>DAC OUTPUT</b>					
	5 kΩ/100 pF to GND				
Resolution			12		Bits
Relative Accuracy	For Code 101 to Code 4095		±4		LSB
Differential Nonlinearity			±1		LSB
Offset Error			±5		mV
Gain Error			±0.5		%
Output Range			0 to 2.5		V
Output Impedance			2		Ω
Output Settling Time			10		μs
<b>LOGIC INPUTS</b>					
Input High Voltage, $V_{IH}$		2.0			V
Input Low Voltage, $V_{IL}$				0.8	V
	For $\overline{CS}$ signal when used to wake up from sleep mode			0.55	V
Logic 1 Input Current, $I_{IH}$	$V_{IH} = 3.3\text{ V}$		±0.2	±10	μA
Logic 0 Input Current, $I_{IL}$	$V_{IL} = 0\text{ V}$				
All except $\overline{RST}$			-40	-60	μA
$\overline{RST}$			-1		mA
Input Capacitance, $C_{IN}$				10	pF
<b>DIGITAL OUTPUTS</b>					
Output High Voltage, $V_{OH}$	$I_{SOURCE} = 1.6\text{ mA}$	2.4			V
Output Low Voltage, $V_{OL}$	$I_{SNK} = 1.6\text{ mA}$			0.4	V
<b>SLEEP TIMER</b>					
Timeout Period <sup>1</sup>		0.5		128	Sec
<b>FLASH MEMORY</b>					
Endurance <sup>2</sup>		10,000			Cycles
Data Retention <sup>3</sup>	$T_J = 85^\circ\text{C}$	20			Years
<b>CONVERSION RATE</b>					
Maximum Sample Rate	SMPL_PRD = 0x01		819.2		SPS
Minimum Sample Rate	SPML_PRD = 0xFF		0.413		SPS
<b>START-UP TIME<sup>4</sup></b>					
Initial Power Up			150		ms
Sleep Mode Recovery			3		ms
<b>POWER SUPPLY</b>					
Operating Voltage Range, $V_{CC}$		4.75	5.0	5.25	V
Power Supply Current	Normal mode at 25°C		33		mA
	Fast mode at 25°C		57		mA
	Sleep mode at 25°C		500		μA

<sup>1</sup> Guaranteed by design

<sup>2</sup> Endurance is qualified as per JEDEC Standard 22 Method A117 and measured at -40°C, +25°C, +85°C, and +125°C.

<sup>3</sup> Retention lifetime equivalent at junction temperature ( $T_J$ ) 85°C as per JEDEC Standard 22 Method A117. Retention lifetime decreases with junction temperature.

<sup>4</sup> This is defined as the time from wake-up to the first conversion. This time does not include sensor settling time, which is dependent on the filter settings



## C.2 Optotrak 3020

### Optotrak<sup>®</sup> Technical Specifications

The Optotrak 3020 is a retired product. Visit the [products page](#) for information on our current product line.

<b>3020 Position Sensor</b>	
Dimensions	1110 mm x 315 mm x 215 mm
Weight	40 kg
Bracket Weight	5 kg
Power Requirements	100/120 VAC, 60 Hz or 220/240 VAC, 50 Hz
Maximum Marker Rate	3500 Hz
Frame Rate	(raw) 750 Hz <sup>1</sup> (3D) 450 Hz <sup>1</sup> (3D with optional hardware) 750 Hz <sup>1</sup> (6D with optional hardware) 145 Hz <sup>1</sup>
RMS Accuracy at 2.25 m distance	0.1 mm for x, y coordinates 0.15 mm for z coordinate
3D Resolution at 2.25 m distance	0.01 mm
Sensor Resolution:	1:200,000
<b>System Control Unit</b>	
Dimensions	483 mm x 373 mm x 138 mm
Weight	11 kg
Power Requirements	100/120 VAC, 60 Hz or 220/240 VAC, 50 Hz
<b>Supported Platforms</b>	
Pentium Class PC:	MS Windows 95/98/NT/2000 <sup>®</sup>
SGI (requires SCSI):	Irix 5.x or higher (o32-bit), Irix 6.x (n32-bit, n64-bit)
HP (requires SCSI):	HP-UX 9.x or higher
SUN (requires SCSI):	Solaris 2.x or higher
Linux support also available for linux 2.x or higher.	

<sup>1</sup> Rates assume 3 markers.

## **Appendix D: Raw Statistical Data**

### **D. 1 Pitch**

### **D. 2 Yaw**

### **D. 2 Yaw**

### **D.4 Z-Direction**

All of the statistic except for the mean are presented as standard deviations for the position and root mean square for the velocity and acceleration.

### D. 1 Pitch

Head Pitch Walk							
		1	2	6	3	4	5
Subject 2	Mean (°)	2.5	11.3	6.2	7.5	7.3	13.6
	MAV (°)	1.3	0.8	0.6	0.4	0.4	0.7
	Pos (°)	1.6	1.0	1.0	0.8	0.8	0.9
	Vel (°/s)	8.3	7.5	9.8	6.8	7.7	7.7
Subject 4	Mean (°)	-10.5	-10.4	7.3	0.2	-3	-1.4
	MAV (°)	1.9	1.5	1.2	1.3	1.3	1.2
	Pos (°)	2.2	1.8	1.5	1.3	1.3	1.2
	Vel (°/s)	19	12.8	12.6	11.5	11.7	11.8
Subject 5	Mean (°)	9.8	5.5	7.6	5.9	9	7.8
	MAV (°)	0.7	0.5	0.4	0.8	0.7	0.7
	Pos (°)	1.3	0.9	0.6	1.2	0.6	0.9
	Vel (°/s)	8.8	7.9	4.8	5.8	5.3	6.3
Subject 6	Mean (°)	-7.1	-4.9	-3.5	-12.3		
	MAV (°)	1.0	1.2	1.2	2.1		
	Pos (°)	1.0	1.2	1.2	1.8		
	Vel (°/s)	14.2	12	11.6	10.9		
Subject 7	Mean (°)	-6.6	1.8	8.2	7.9	3.5	7.2
	MAV (°)	2.7	1.3	2.4	2.1	1.3	2.5
	Pos (°)	1.7	0.9	1.5	1.7	1.3	1.6
	Vel (°/s)	8.8	6.4	6.9	8.1	8	8

Head Pitch Run							
		1	2	6	3	4	5
Subject 2	Mean (°)	9.0	11.5	6.2	8.4	9.9	15
	MAV (°)	2.0	0.9	1.3	1.0	0.9	1.2
	Pos (°)	2.5	1.8	2.2	1.6	1.6	1.7
	Vel (°/s)	15	17.8	22.2	19.1	17.4	20.3
Subject 4	Mean (°)	-9.8	-14	0.3	0.3	-6.1	-7.4
	MAV (°)	1.9	1.1	3.8	2.3	2.8	2.2
	Pos (°)	2.5	2.6	3	3.3	3.6	4.3
	Vel (°/s)	21	21.9	27.8	43.1	42.1	51
Subject 5	Mean (°)	7.7	5.5	6.5	4.5	8.3	6.7
	MAV (°)	1.1	0.9	1.6	0.7	0.9	1.3
	Pos (°)	1.3	1.3	1.9	2.1	2.0	2.1
	Vel (°/s)	19.9	9.2	19.1	22.2	20.3	26.6
Subject 6	Mean (°)	-10.1	-6.5	-2	-11.7		
	MAV (°)	1.4	1.6	1.9	1.4		
	Pos (°)	2.9	2.5	2.5	2.4		
	Vel (°/s)	36.7	17	17.5	30.3		
Subject 7	Mean (°)	-6.3	-1.7	5.9	6.3	2.0	4.2
	MAV (°)	2.1	1.6	1.7	1.5	2.3	1.3
	Pos (°)	2.2	1.9	2.1	2.5	2.2	2.2
	Vel (°/s)	19.1	14.8	16.7	26.8	21.8	23.6

Trunk Pitch Walk							
		1	2	6	3	4	5
Subject 2	Mean (°)	-2.0	-11.6	-14.2	-8.7	-12.1	-11.2
	MAV (°)	0.6	0.6	0.7	0.5	0.5	0.7
	Pos (°)	1.3	1.6	1.6	1.3	1.7	2.1
	Vel (°/s)	8.9	11.3	13.2	12	11.9	11.9
Subject 4	Mean (°)	-7.0	-14.0	-4.5	-5.1	-6.4	-8.8
	MAV (°)	0.8	0.7	0.5	0.8	0.6	0.6
	Pos (°)	1.7	1.3	1.3	1.4	1.2	1.2
	Vel (°/s)	9.9	11.4	11.3	12	11.8	11.7
Subject 5	Mean (°)	1.1	-4.5	0.5	-0.8	-9.7	-4.1
	MAV (°)	0.5	0.6	0.5	0.4	0.6	0.6
	Pos (°)	1.5	1.3	1.2	1.3	1.2	1.3
	Vel (°/s)	12.5	11.9	11.9	11.3	11.4	12.8
Subject 6	Mean (°)	-3.2	-10.5	-8.3	-6.8		
	MAV (°)	1.2	0.9	1.1	1.0		
	Pos (°)	1.2	0.9	1.1	1.9		
	Vel (°/s)	19.6	19.8	17.7	16		
Subject 7	Mean (°)	-0.4	-13.8	-14.6	-14.4	-5.9	-18.6
	MAV (°)	1.6	0.9	2.0	1.2	3.0	2.8
	Pos (°)	2.2	1.7	1.5	1.6	3.6	1.8
	Vel (°/s)	8.7	13.5	10.8	12	12.1	12.3

Trunk Pitch Run							
		1	2	6	3	4	5
Subject 2	Mean (°)	11.5	1.7	-6.0	2.4	2.3	2.3
	MAV (°)	1.7	1.5	1.2	1.3	1.5	1.4
	Pos (°)	6.3	6.1	4.6	4.0	5.8	4.5
	Vel (°/s)	15.9	16.9	17.4	16.5	16.7	19.3
Subject 4	Mean (°)	-4	-12.3	1.2	0.1	3.6	-5.9
	MAV (°)	1.5	1.5	1.2	1.3	1.2	1.8
	Pos (°)	7.2	6.2	2.5	2.2	2.9	6.5
	Vel (°/s)			20.8	23.8	26	23.9
Subject 5	Mean (°)	5.6	-3.9	2.8	3.3	0.0	1.1
	MAV (°)	1.0	1.1	1.3	1.2	0.9	1.1
	Pos (°)	4.9	6.5	3.6	5.2	4.4	4.4
	Vel (°/s)	27.1	24.4	24.1	21.7	21.6	19.8
Subject 6	Mean (°)	-3.2	-9.7	-8.1	-7.6		
	MAV (°)	1.2	1.3	1.4	0.8		
	Pos (°)	2.6	2.8	2.6	2.4		
	Vel (°/s)	24.4	30.7	25.3	31.4		
Subject 7	Mean (°)	-0.4	-7.8	-8.4	-10.8	-1.0	-10
	MAV (°)	1.1	1.2	0.9	1.7	2.1	1.0
	Pos (°)	2.0	1.8	1.6	1.9	2.0	1.6
	Vel (°/s)	26.2	20.1	22.3	24.8	23.6	24.2

**D. 2 Yaw**

Head Yaw Walk							
		1	2	6	3	4	5
Subject 2	Pos (°)	2.3	1.8	1.4	1.3	1.3	1.6
	Vel (°/s)	10.7	7.8	7.0	6.7	6.1	6.8
Subject 4	Pos (°)	2.7	2.0	1.8	1.6	2.4	2.6
	Vel (°/s)	14.0	8.9	7.3	7.7	8.4	9.4
Subject 5	Pos (°)	1.5	1.7	1.3	1.2	1.3	1.2
	Vel (°/s)	8.2	8.3	6.2	6.3	6.7	6.4
Subject 6	Pos (°)	2.4	2.1	2.1	2.3		
	Vel (°/s)	12.5	10.2	9.9	8.3		
Subject 7	Pos (°)	1.4	1.5	1.4	1.4	1.8	2.0
	Vel (°/s)	5.0	6.6	7.3	8.2	9.7	8.1

Head Yaw Run							
		1	2	6	3	4	5
Subject 2	Pos (°)	2.8	2.7	2.6	2.2	2.5	2.8
	Vel (°/s)	20.9	19.7	16.6	14.7	16.1	19.2
Subject 4	Pos (°)	3.6	2.7	2.7	2.6	2.9	4.2
	Vel (°/s)	26.0	14.8	15.3	13.3	15.0	16.6
Subject 5	Pos (°)	2.0	1.6	2.0	1.9	1.9	1.9
	Vel (°/s)	14.4	9.2	11.5	12.1	10.5	11.5
Subject 6	Pos (°)	2.5	3.8	3.1	2.5		
	Vel (°/s)	17.3	27.6	16.9	11.3		
Subject 7	Pos (°)	2.6	3.7	3.0	2.9	3.4	2.8
	Vel (°/s)	18.3	27.8	23.4	21.1	24.7	19.3

Trunk Yaw Walk							
		1	2	6	3	4	5
Subject 2	Pos (°)	2.3	2.9	2.6	2.6	2.8	2.7
	Vel (°/s)	11.6	14.3	11.6	12.3	12.9	12.7
Subject 4	Pos (°)	3.3	3.0	2.0	2.3	2.7	2.8
	Vel (°/s)	22.5	19	15.8	18.4	19.6	18.5
Subject 5	Pos (°)	3.0	2.7	2.0	2.0	2.1	2.1
	Vel (°/s)	15.1	16.1	11.4	11.7	12	12.3
Subject 6	Pos (°)	3.3	2.6	2.7	2.7		
	Vel (°/s)	18.6	14.7	15	14.5		
Subject 7	Pos (°)	1.6	2.3	1.4	1.7	2.6	2.2
	Vel (°/s)	8.5	10.8	7.6	7.4	10.6	7.9

Trunk Yaw Run							
		1	2	6	3	4	5
Subject 2	Pos (°)	10.4	10.5	11.6	9.7	10.7	9.9
	Vel (°/s)	61.4	62.5	69.9	61.5	65.3	60.9
Subject 4	Pos (°)	11	10	8.4	8.5	10.1	9.9
	Vel (°/s)			61.7	62.7	67.6	66.7
Subject 5	Pos (°)	9.7	11.9	8.8	9.7	9.3	9
	Vel (°/s)	54.2	47.7	46.4	46.6	47.1	46.7
Subject 6	Pos (°)	7.4	8.5	7.6	6.8		
	Vel (°/s)	63.2	63.1	58.9	55.9		
Subject 7	Pos (°)	5.0	5.5	4.1	4.3	4.3	3.8
	Vel (°/s)	30.8	31.1	24.6	22.4	26.7	24.2



**D. 3 Roll**

Head Roll Walk							
		1	2	6	3	4	5
Subject 2	Pos (°)	1.1	1.3	1.5	1.3	0.9	1.2
	Vel (°/s)	5.1	7.5	5.9	5.3	5.5	5.9
Subject 4	Pos (°)	1.9	1.5	1.6	1.4	1.4	1.2
	Vel (°/s)	16.6	12.3	9.1	11.7	10.7	9.6
Subject 5	Pos (°)	1.4	1.2	1.0	1.5	1.1	1.2
	Vel (°/s)	7.5	7.2	7.1	7.6	6.7	7.2
Subject 6	Pos (°)	1.4	1.5	1.6	1.0		
	Vel (°/s)	8.5	7.5	8.1	6		
Subject 7	Pos (°)	1.4	1.0	1.4	1.3	1.3	1.2
	Vel (°/s)	5.4	5.9	5.7	5.6	5.9	5.5

Head Roll Run							
		1	2	6	3	4	5
Subject 2	Pos (°)	1.3	1.8	2.0	1.4	2.0	1.6
	Vel (°/s)	9.8	11	12.9	10.4	11.1	12.2
Subject 4	Pos (°)	2.7	2.3	1.6	1.8	2.1	2.5
	Vel (°/s)			16.5	13.3	18.6	18.9
Subject 5	Pos (°)	1.3	1.1	1.1	1.8	1.9	1.7
	Vel (°/s)	9.8	8.3	9.5	8.9	8.5	7.7
Subject 6	Pos (°)	2.6	2.1	1.7	2.0		
	Vel (°/s)	20.7	18.1	18.6	14.8		
Subject 7	Pos (°)	1.7	2.0	1.5	2.2	1.9	1.9
	Vel (°/s)	13.7	14.1	12.3	14.2	12.6	14.8

Trunk Roll Walk							
		1	2	6	3	4	5
Subject 2	Pos (°)	0.9	1.8	1.4	1.1	1.3	1.5
	Vel (°/s)	4.5	6.5	6.5	6.1	7.1	6.6
Subject 4	Pos (°)	1.4	1.7	1.3	1.4	1.1	1.3
	Vel (°/s)		7.8	7.6	7.9	7.5	7.1
Subject 5	Pos (°)	1.9	2.1	1.4	1.7	1.4	1.6
	Vel (°/s)	12.4	11.9	9.3	10.5	9.4	10.3
Subject 6	Pos (°)	1.0	1.1	1.1	1.0		
	Vel (°/s)	7.4	6.6	5.9	5.6		
Subject 7	Pos (°)	1.8	1.3	1.4	1.8	1.4	2.5
	Vel (°/s)	7.7	6.3	6.1	6.4	5.8	5.5

Trunk Roll Run							
		1	2	6	3	4	5
Subject 2	Pos (°)	2.7	6.9	8.0	4.5	5.7	6.0
	Vel (°/s)	17.6	18.0	23.4	18.9	20.8	18.7
Subject 4	Pos (°)	5.1	5.5	3.1	2.9	3.4	4.1
	Vel (°/s)			22.7	19.7	21.3	19.5
Subject 5	Pos (°)	5.1	7.5	4.8	5.5	4.3	4.5
	Vel (°/s)	34.6	32.5	29.2	30.6	29.8	28.4
Subject 6	Pos (°)	2.0	2.7	3.5	2.7		
	Vel (°/s)	13.2	12.7	13.2	9.3		
Subject 7	Pos (°)	3.4	5.0	3.4	4.5	4.6	4.9
	Vel (°/s)	17.8	18.4	13.4	12.3	16.4	12.5

**D.4 Z-Direction**

Head Z Walk							
		1	2	6	3	4	5
Subject 2	Pos (m)	0.011	0.016	0.016	0.016	0.016	0.017
	Accel (m/s <sup>2</sup> )	1.22	1.89	1.88	1.85	1.92	1.92
Subject 4	Pos (m)	0.016	0.017	0.016	0.014	0.015	0.014
	Accel (m/s <sup>2</sup> )	2.11	2.08	1.89	1.91	2.10	2.03
Subject 5	Pos (m)	0.018	0.020	0.018	0.020	0.019	0.018
	Accel (m/s <sup>2</sup> )	2.18	2.37	2.20	2.42	2.37	2.34
Subject 6	Pos (m)	0.009	0.009	0.009	0.008		
	Accel (m/s <sup>2</sup> )	1.28	1.30	1.26	1.19		
Subject 7	Pos (m)	0.015	0.015	0.015	0.015	0.015	0.014
	Accel (m/s <sup>2</sup> )	1.64	1.63	1.64	1.62	1.69	1.54

Head Z Run							
		1	2	6	3	4	5
Subject 2	Pos (m)	0.023	0.026	0.027	0.025	0.026	0.027
	Accel (m/s <sup>2</sup> )	5.41	5.98	6.15	6.06	5.95	6.29
Subject 4	Pos (m)	0.036	0.035	0.034	0.029	0.032	0.033
	Accel (m/s <sup>2</sup> )	8.04	8.45	9.12	7.44	8.20	7.93
Subject 5	Pos (m)	0.037	0.036	0.034	0.034	0.035	0.032
	Accel (m/s <sup>2</sup> )	7.99	8.01	7.63	7.72	7.77	7.53
Subject 6	Pos (m)	0.026	0.028	0.021	0.020		
	Accel (m/s <sup>2</sup> )	6.83	7.75	6.56	5.94		
Subject 7	Pos (m)	0.027	0.032	0.028	0.028	0.031	0.029
	Accel (m/s <sup>2</sup> )	5.88	7.34	6.61	6.69	7.15	6.87

Trunk Z Walk							
		1	2	6	3	4	5
Subject 2	Pos (m)	0.012	0.017	0.019	0.018	0.019	0.019
	Accel ( $m/s^2$ )	1.46	2.25	2.29	2.16	2.32	2.25
Subject 4	Pos (m)	0.018	0.017	0.017	0.016	0.017	0.016
	Accel ( $m/s^2$ )	2.67	2.72	2.59	2.62	2.78	2.68
Subject 5	Pos (m)	0.022	0.025	0.021	0.024	0.023	0.022
	Accel ( $m/s^2$ )	2.45	2.62	2.33	2.65	2.58	2.50
Subject 6	Pos (m)	0.010	0.011	0.010	0.009		
	Accel ( $m/s^2$ )	1.91	1.91	1.83	1.76		
Subject 7	Pos (m)	0.017	0.016	0.017	0.016	0.017	0.015
	Accel ( $m/s^2$ )	1.97	2.00	1.84	1.80	1.88	1.71

Trunk Z Run							
		1	2	6	3	4	5
Subject 2	Pos (m)	0.030	0.033	0.037	0.033	0.033	0.033
	Accel ( $m/s^2$ )	7.14	7.28	8.32	7.78	7.72	7.73
Subject 4	Pos (m)	0.045	0.042	0.043	0.037	0.039	0.039
	Accel ( $m/s^2$ )			10.38	9.78	10.40	10.52
Subject 5	Pos (m)	0.049	0.048	0.043	0.044	0.045	0.043
	Accel ( $m/s^2$ )	10.36	9.75	9.40	9.58	9.79	9.42
Subject 6	Pos (m)	0.030	0.031	0.024	0.023		
	Accel ( $m/s^2$ )	8.90	9.28	7.71	7.61		
Subject 7	Pos (m)	0.030	0.035	0.030	0.030	0.033	0.032
	Accel ( $m/s^2$ )	7.28	8.12	7.11	7.08	7.59	7.34

